The TFTR Advanced Performance Project:

A Proposal to Extend the Deuterium-Tritium Phase of TFTR Operation

Prepared for submission to the

U.S. Department of Energy

by

Princeton Plasma Physics Laboratory,
James Forrestal Campus
P.O. Box 451
Princeton N.J. 08543-0451

July 1995

Table of Contents (cont.)

The TFTR Advanced Performance Project

1. Introduction and Executive Summary

The TFTR Advanced Performance (TFTR-AP) project is a proposal to extend the operational phase of TFTR for a period of three years to develop and exploit its unique capabilities to investigate highly reactive deuterium-tritium (D-T) plasmas in a variety of regimes. This proposal seeks to reap the maximum possible benefit from TFTR both by continuing to build a sound physics and technology basis for an ignition device, such as the International Thermonuclear Experimental Reactor (ITER) [1], and by investigating and developing some exciting possibilities for improving the tokamak reactor concept.

1.1 Physics mission and program elements of TFTR-AP

The TFTR-AP Project will advance the tokamak towards a reactor concept by investigating issues in four major areas which will be important in the core of an ignited D-T tokamak. These areas, illustrated schematically in Fig. 1.1, are 1) achieving high reactivity and MHD stability, 2) the behavior of energetic D-T fusion alpha-particles in reactor-like conditions, 3) the heating and thermal transport of the plasma, and 4) core fueling and power handling. The primary physics mission will be to develop and use techniques for controlling the current and pressure profile to produce plasma regimes with increased D-T fusion performance, thereby allowing a thorough investigation of alpha-particle physics in these advanced regimes at reactor relevant parameters. Additional objectives will be to develop our understanding of enhanced confinement regimes, the underlying plasma transport mechanisms and methods for modifying them, the MHD stability limits of these regimes, the interaction of alpha particles with plasma waves as possible means of controlling their thermalization and transport, and to develop fueling and helium-ash removal techniques applicable to reactors.

A set of program elements for TFTR-AP is proposed to accomplish these investigations. These elements include both equipment modifications, designed to achieve the necessary plasma conditions, and specific experiments. The experiments will extend the substantial body of research results from TFTR, built up over 10 years of operation with deuterium plasmas followed by almost two years of reliable and extremely productive operation with plasmas containing high concentrations of tritium. A significant and unique advantage of the TFTR-AP project is that it would validate the planned physics research and technology development *in D-T plasmas.* For the foreseeable future, the TFTR-AP project is expected to remain the only tokamak within the worldwide fusion effort with a substantial, on-going program of D-T experiments. In addition to addressing vital physics issues for ITER and the potential benefits in improving the tokamak concept, the experience to be gained from continuing to operate a large tokamak in the D-T environment will be invaluable in planning for the next generation of devices

Transport and
Heating

Alpha Physics

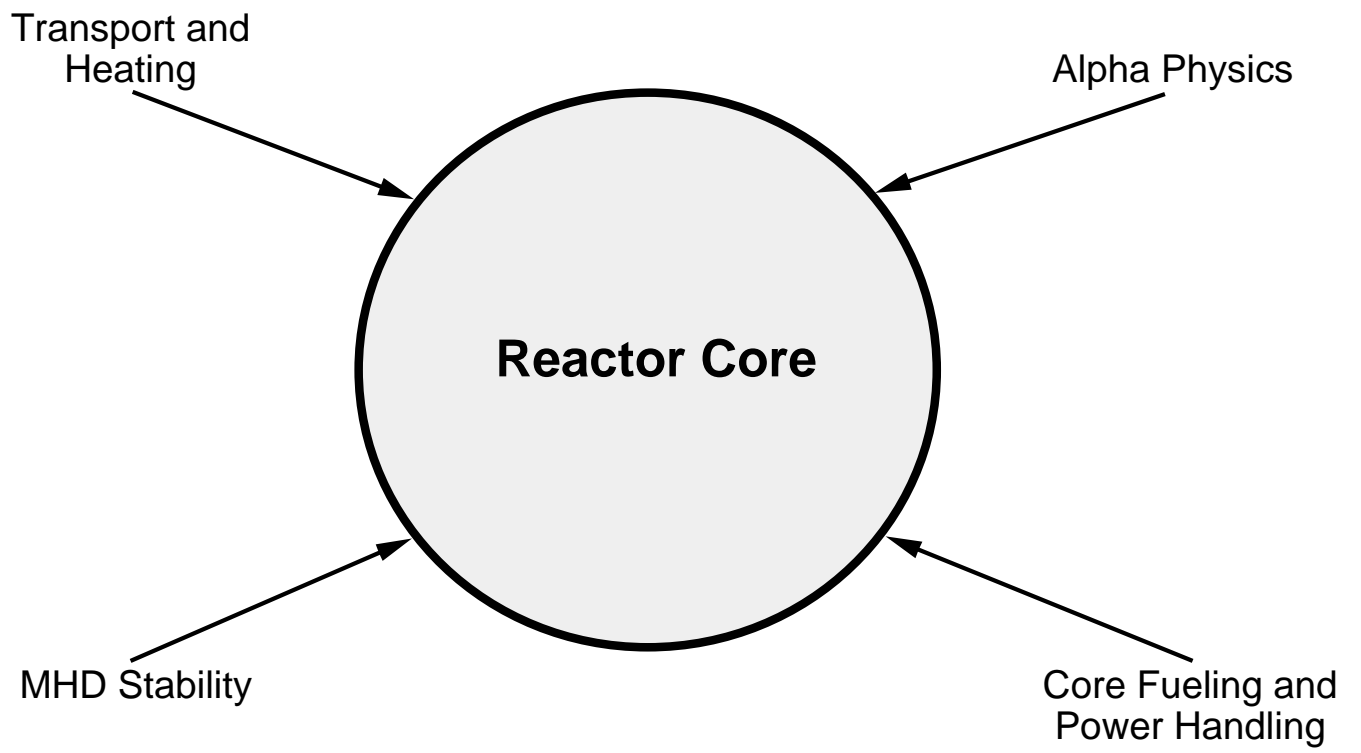**Reactor Core**

MHD Stability

Core Fueling and
Power Handling

Fig. 1.1

designed to produce burning plasmas. The TFTR program has already contributed significantly to fusion technology and will continue to do so, especially in the areas of tritium processing and heating and current drive by waves in the ion-cyclotron range of frequencies (ICRF).

The TFTR-AP project at the Princeton Plasma Physics Laboratory (PPPL) is proposed in the context of the three-year delay in construction of the Tokamak Physics Experiment (TPX). The TPX has been designed both to exploit some established techniques and to investigate more speculative possibilities for improving tokamak performance, and to study these techniques when applied on long timescales. These goals for TPX have been widely discussed in the fusion community and achieved a national consensus. While the TFTR-AP project would not address the issues of long-pulse tokamak operation at high performance, some important elements of the TPX program will be studied in the TFTR-AP. It is proposed to investigate in TFTR-AP fundamental questions of whether alternative routes to ignition in a tokamak exist and, if so, what capabilities and features would be required in the next generation of experiments to exploit these schemes in steady state. In particular, TFTR-AP will extend promising techniques for transport control, such as current profile modification and flow shear control by RF waves, to plasmas in reactor-like conditions.

The new interim design for ITER has decreased the margins with respect to several important limits to tokamak performance, notably the -limit, the confinement enhancement factor and the density limit. The TFTR-AP project addresses several key issues in support of ITER. Among these are the alpha-particle heating and transport in the presence of normal MHD activity, including sawteeth, the mechanism of the high-beta disruption in high-temperature plasmas, the effects of predisruptive phenomena on alpha-particle losses, the use of plasma waves to control alpha-particle transport, the possibility of using a hot-ion plasma core to initiate a thermonuclear burning plasma, the use of a radiating mantle to control heat fluxes through the plasma edge and the issues of density limits and fueling. In addition to the importance of D-T-plasma operation for some of these topics, all of these investigations will be carried out in plasmas with *absolute* values of the central temperature, density, magnetic field, fusion power density and edge power fluxes the most relevant to reactor of any existing tokamak. The outcome from these investigations could have a major impact on the cost and size of ITER and future ignition devices.

Within the world fusion program, the operation of each of the three large tokamaks, JET, JT-60 and TFTR, has been extended to support the research and development needs for ITER and eventual power-producing reactors. All of these devices have undergone significant upgrades to perform key research elements. In particular, JET has installed one new divertor and is in the process of installing a second, and the JT-60U upgrade involved a new vacuum vessel and poloidal field coils and a current drive system. TFTR has been modified for tritium operation to study alpha-particle physics.

It has been argued that research and development for ITER should be carried out in tokamaks with cross-section shaping similar to ITER itself. Indeed, there are several important issues for ITER that must be studied in tokamaks, such as JET, JT-60U, Alcator C-MOD ASDEX-U or DIII-D with elongated, divertor plasmas. The importance of the issues associated with divertor operation is demonstrated by the decision taken by the JET project to concentrate its resources on studying divertor physics during the period 1997 – 1999 following an abbreviated D-T operation phase planned to last only about four months at the end of 1996. However, while JET and other divertor tokamaks concentrate on the outer regions of the plasma most affected by the cross-section shaping, it is vital that complementary research concentrating on the high-reactivity plasma core be carried out in conditions prototypical of an ignited D-T plasma. With its specialized capability of routine operation with D-T fuel and an achieved central fusion power density of $\sim 2.5\,\mathrm{MWm^{-3}}$, TFTR provides the most relevant conditions amongst all current tokamaks for studying the phenomena likely to affect the core of a burning plasma and for developing methods to control these phenomena.

1.2 Equipment modifications proposed for TFTR-AP

In order to produce the plasma conditions desired for several of the experiments planned for TFTR-AP, a set of upgrades and modifications to the ancillary systems of TFTR is proposed, as follows.

1) Installation of a Lower Hybrid Current Drive system to assist in controlling plasma current profiles in order to increase plasma stability and modify the transport. The proposed system comprises a 4.6 GHz source (currently installed on PBX-M) and a launcher with full phase control, capable of injecting 1.3 MW into the plasma for a 3 s pulse. This system could be upgraded to 2.6 MW by adding a second power unit.

2) Modifying some of the neutral beam injectors for 5 s NBI pulse capability at full acceleration voltage (120 kV). This would increase their capability to modify the plasma current profile. In the recent experiments which successfully developed "reversed-shear" plasma equilibria in TFTR, the present 2 s pulse length, at a reduced voltage of 95 kV, was a significant limitation.

3) Installation of an antenna to launch ion Bernstein waves (IBW) for control of the density profile by producing a transport barrier through generation of a sheared-flow layer in the plasma. This antenna would be fed by two of the existing RF sources and operate in the frequency range 30 – 50 MHz at power levels up to 3 MW.

4) Installation of two modified 4-strap antennas for heating and current drive with IBW mode-converted from the fast wave. The antennas would be capable of launching toroidally-directed waves with toroidal mode numbers in the range of 10 – 50, appropriate for mode conversion to an IBW both for current drive and for studying the possibility of "channeling" alpha-particle energy to the fuel ions in D-T plasmas. Four strap antennas are also expected to reduce the impurity influx which often occurs with two-strap antennas operating in current drive phasing.

5) Re-aiming six (of the twelve) neutral beams to inject at larger tangency radii. This modification will broaden the beam power deposition profile and the resulting plasma pressure profile to increase the -limit and, therefore, the D-T fusion yield.

6) Adding a fifth neutral beam box to accommodate a re-configuration of the existing neutral beam injectors from the present 6 co- : 6 counter- injecting to a 9 co- : 3 counter- injecting configuration to modify the plasma rotation and the profile of the beam-driven current at full injected power. This modification would be undertaken after completing planned reversed-shear experiments with the existing configuration.

7) Upgrades to some diagnostic and control systems. In particular, a measurement for poloidal plasma rotation will be installed for the experiments to investigate advanced confinement regimes. The control system will be upgraded to provide an improved system for disruption avoidance and real-time feedback control of additional plasma parameters, including control of the q profile.

In addition, two systems will be installed to develop technology suitable for use on ITER. Both of these systems will be developed in collaboration with Oak Ridge National Laboratory.

8) Installation of a tritium pellet injector (TPI) for studying this approach to fueling of ITER. A simplification of the original TPI has resulted from the experience gained in D-T on TFTR.

9) Installation of a folded waveguide (FWG) antenna for ICRF waves to develop this technology for possible use in ITER. The antenna will be a modification of the one designed for PBX-M.

1.3 Timetable

The full TFTR-AP project would be carried out over a period of three years, starting in October 1995. A timetable for the project, including the major modifications and experiments is shown in Fig. 1.2. It can be seen that the program builds logically on the existing capabilities and is designed to make the most effective use of the available experimental time. The proposed TFTR-AP project encompasses many important experiments for the development of a viable tokamak reactor and involves upgrades for which adequate lead time for scoping experiments, design, construction and installation is required.

1.4 Overview of this proposal

Sections 2 – 5 of this proposal describe in detail the research plans for the TFTR-AP Project. Upgrades to the control system and diagnostics of TFTR to facilitate the proposed experiments are described in Sec. 6. Section 7 then describes the experience already gained in the tritium operation environment and the implications for continued D-T experiments in TFTR. Estimates of the costs of the major equipment changes are presented in Sec. 8. Section 9 discusses plans for collaboration with other institutions during the TFTR-AP project. Section 10 is a brief summary of the proposal.

• IBW

• Poloidal Rotation Diag.   • LHCD (1.3MW)

• FWG   • TPI   • (NB Reconfiguration)

• ICRF Antenna Mods.   • (NB Reaiming)   • LHCD (2.6MW)

◄——————— **1996** ———————►◄——————— **1997** ———————►◄——————— **1998** ———————►

• Reverse Shear   • CH mode   • LHCD   • Current Profile Control

• Radiative Mantle   • Velocity Shear   • T Pellet Fueling   • Alpha Ash Control

• D Pellet Fueling   • IBW Interactions With Alphas   • ~ 20 MW

                       • Ext. Driven TAE
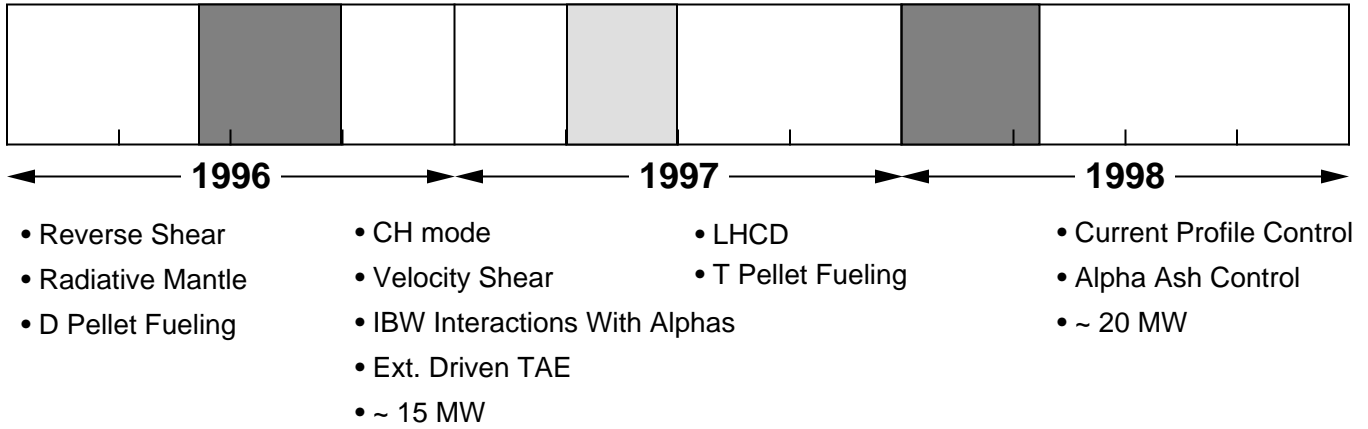
                       • ~ 15 MW

Fig. 1.2   Plan for modifications and experiments to be carried out in each fiscal year of the TFTR-AP
           project. Vacuum vessel openings are indicated with heavy shading. The installation of the LH
           coupler in FY'97 does not require a full vacuum opening since it will be inserted through a valve.
           New capabilities are indicated.

2. Enhancement of Plasma Stability and Fusion Performance

2.1 Experience in maximizing the fusion reactivity in TFTR

Since December 1993, TFTR has been operated routinely with mixed deuterium-tritium plasmas. To date, more than 400 plasmas have been heated and fuelled by neutral beam injection with at least one neutral beam source injecting pure tritium. In the first year of D-T operation, the peak fusion power was increased from 6.2 to 10.7 MW, meeting goals set for TFTR by the Department of Energy prior to the D-T experiments. Apart from the favorable recognition created for fusion research by these significant results, which represent the practical culmination of more than 40 years of effort worldwide, the campaigns to increase the fusion power have produced new insights into the physics of plasmas in reactor-like conditions. Initial studies of alpha-particle physics, plasma stability and plasma transport have been carried out. Further progress in increasing the fusion power is possible by optimizing and combining techniques for enhancing plasma performance in TFTR. Such increases in fusion power would allow a more thorough investigation of the physics of fusion alpha particles and of the phenomena to be expected in the core of a reactor, and would justly qualify TFTR for the description "advanced performance" tokamak.

In experiments on all the large tokamaks, TFTR [2], JT-60U [3] and JET [4], the highest fusion performance has been obtained from hot-ion plasmas in which $T_i > T_e$. With the further characteristic of peaked density profiles, the hot-ion regime becomes the "supershot" regime on TFTR [5]. The highest fusion rates in TFTR for both DT and D-only plasmas have been obtained in supershots heated by high-power tritium and deuterium neutral-beam injection (NBI) [6–9]. Supershot plasmas are characterized by very high central ion temperatures, $T_i(0) = 20 – 45 \text{keV} >> T_e(0) = 10 – 15 \text{ keV}$, high central densities, $n_e(0)$ up to $1.0 \times 10^{20} \text{ m}^{-3}$, highly peaked profiles of the density and ion temperature, a broad electron temperature profile, and good energy confinement, with enhancements of the global energy confinement time over the ITER-89P scaling [10] by factors up to 3. In addition to excellent confinement, supershots have the favorable characteristics that $W_i > W_e$, *i.e.* a large fraction of the plasma energy is in the fuel, and that, as a result of the peaked density profile, the bootstrap current profile is more aligned with the ohmic profile than achieved in H-modes. The unfavorable aspect is that hot-ion plasmas depend on a method for preferentially heating the ions. However, for future devices, driven supershot or hot-ion operation could produce substantial fusion power which may be extremely useful in crossing the H-mode threshold and reaching ignition.

For a reactor, the volume-average fusion power density is an important figure of merit. In the expected temperature range for D-T fuel, it is given approximately by:

$$\left\langle P_{fus} \right\rangle \ \sim \ \left\langle n_{DT}^2 T_i^2 \right\rangle \ = \ C_{fus}\beta^2 B^4 \tag{1}$$

where <> indicates a volume average, n_{DT} is the local fuel ion density, T_i the local ion temperature, B the magnetic field, β the average total beta and C_{fus} is a coefficient which depends on several factors, including the pressure profile shape, the ratio of the fuel-ion to the electron temperature and the fuel dilution by impurities. Figure 2.1 shows the average fusion power density obtained in TFTR D-T plasmas *vs*. $\beta^2 B^4$ and compares the results with those from the JET Preliminary Tritium Experiment [11], extrapolated to a 50:50 D:T fuel mixture, and the design values for ITER [1] and other reactor concepts [12]. From this data, it is clear that TFTR has already achieved very high levels of fusion performance in D-T plasmas compared to the ITER design. Furthermore, the various reactor studies indicate the need to develop methods for reaching significantly higher fusion power densities than are planned for ITER or are currently achieved in TFTR. To investigate the advanced operating regime which would make the tokamak an attractive reactor, however, requires increasing the plasma pressure at maximum toroidal field while maintaining the reactivity advantage of existing supershots. The goal of increasing the sustainable plasma pressure at full field is a major focus of the TFTR-AP project.

We can also express Eq. 1 in terms of the Troyon-normalized- [13], β_N ($=10^8 \cdot 2\mu_0 <p>a/BI$ where $<p>$ is the volume-average pressure a the plasma minor radius and I the plasma current) as follows

$$\left\langle P_{fus} \right\rangle \quad C_{fus}\beta_N^2 \ q_e^{-2}\varepsilon^2\kappa^2 B^4 \tag{2}$$

where q_e ($= 2\pi\kappa a^2 B/\mu_0 RI$) is an effective safety factor, ε the inverse aspect ratio and κ the elongation for an elliptical plasma cross-section. TFTR has a higher value ($10.4\ T^2$) of the product $\varepsilon\kappa B^2$ of device-dependent parameters than either JET ($7.2\ T^2$) or JT-60U ($9.2\ T^2$). Equation 2 shows that in a tokamak with given plasma geometry, the highest fusion power density will be obtained by operating at the highest magnetic field and at the highest ratio β_N/q_e compatible with plasma stability *and with simultaneously achieving a high value of C_{fus}*. Supershots with high values of C_{fus} were originally produced only at quite high values of q_e, typically 6– 10. However, as experience with this regime has developed in TFTR, the value of q_e at which supershot characteristics are obtained has been steadily decreased. The plasma which produced 10.7 MW of fusion power was run with a toroidal magnetic field of 5.5 T and a plasma current of 2.7 MA for a q_e of 3.1, corresponding to an MHD-q of 3.9.

Supershots are produced with NBI heating when the edge influxes of hydrogenic species and carbon are reduced so that the plasma core is fuelled predominantly by the injected neutrals. In addition to the enhanced confinement, this provides the advantage for D-T experiments that the central fuel-ion mix can be varied by changing the fraction of sources injecting tritium. In TFTR, the edge influxes of hydrogenic species and carbon have been controlled through the injection of solid lithium pellets (1 – 4 pellets each containing typically 4×10^{20} atoms) into the ohmic phase of the discharge, 1.5 – 0.5 s prior to NBI [14]. The use of lithium conditioning has increased the plasma current at which the

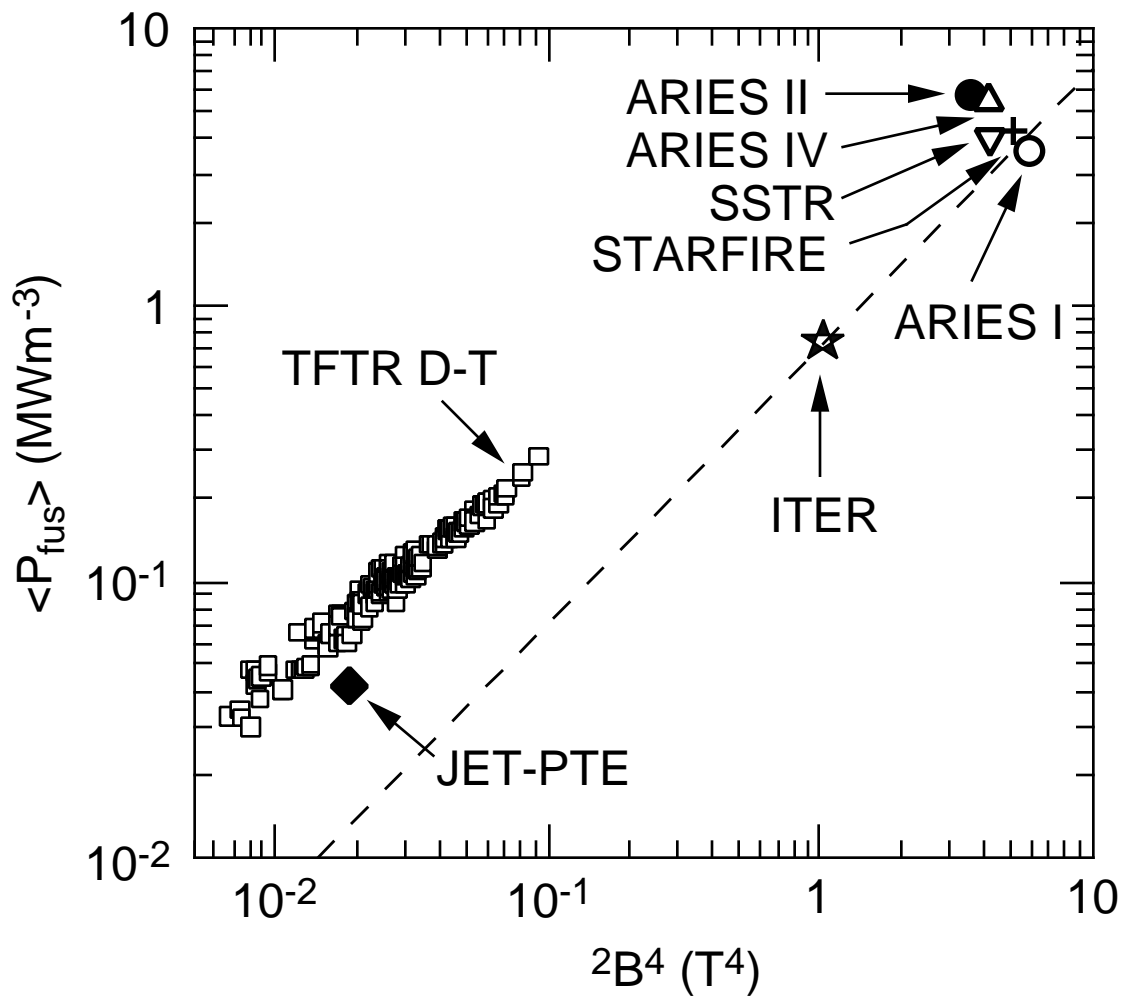Fig. 2.1 Average D-T fusion power density *vs.* the square of the average plasma energy density for existing D-T experiments and at the planned operating points for several reactor designs. The TFTR data are restricted to those with nearly optimal D:T mix (175 discharges). The point labelled JET-PTE is taken from the extrapolation of the results of the JET Preliminary Tritium Experiment to a 50:50 D:T fuel mix.

supershot characteristics are obtained [15] and increased the highest energy confinement time to 0.33 s in a plasma with 17 MW of T-only NBI; this confinement time is approximately 2.4 times the prediction of ITER-89P scaling [10], based on an average ion mass of 2.7. This plasma achieved a world-record "fusion triple product", $n_i(0) \cdot T_i(0) \cdot \tau^*$ (where τ^* is simply defined as W_{tot}/P_{tot}) of 8.3×10^{20} m$^{-3} \cdot$keV$\cdot$s, which represents an increase by a *factor of 64* over an L-mode plasma with similar size, current, magnetic field and heating power. Figure 2.2 shows the peak fusion power as a function of total heating power for the subset of plasmas heated by a nearly optimal mixture of D- and T- NBI. The improvement in fusion performance generated by increased lithium injection is evident. In the D-T supershots, the total NBI power has reached 39.5 MW using 7 T and 5 D sources. The NBI pulse has been typically 0.7 to 2.0 s in duration.

As expected from Eq. 2, a strong dependence of the peak fusion rate on the total plasma energy, or equivalently β_N, is observed in both D-T and D-only supershots [8,16]. A considerable effort has been undertaken in the past year to increase the maximum toroidal field (TF) in TFTR above the original coil rating to exploit the improved confinement of supershots at the full NBI power available in DT operation. After extensive analysis and review of the coil structure and rearrangement of the power supplies, it has proved possible to increase the TF coil current by 16%. This capability has recently (June 2, 1995) been demonstrated in test shots although, so far, an increase of only 8% has been actually used in D-T experiments.

Figure 2.3 shows the peak D-T fusion power produced in TFTR as a function of β_N for the three series of experiments conducted from December 1993 through October 1994 to maximize the fusion power production in TFTR. It can be seen that for each series, in which the plasmas were run at the same plasma size, current and magnetic field, the fusion power increased approximately as $\beta_N^{1.8}$ up to the highest values which were at, or close to, the β-limit. It should be noted that because the pressure profiles are highly peaked in supershots, the parameter of relevance for fusion performance, β_N^* ($=10^8 \cdot 2\mu_0 \langle p^2 \rangle a/BI$, where $\langle p^2 \rangle$ is the root-mean-square plasma pressure) has reached 2.8 at a edge MHD-q of 3.9 ($q_e = 3.1$); this is comparable to the expected β-limit for plasmas with broad pressure profiles where β_N is closer to β_N^*.

Since the last campaign to push the fusion power, new developments in the techniques for lithium pellet conditioning have increased confinement times even further, so that it would be possible to reach the apparent supershot β-limit even at the highest magnetic field and plasma current now available. If the shape of the pressure profile could be preserved and, by current profile modification, the β-limit increased to $\beta_N = 2.5$ for a plasma current of 2.7 MA and a magnetic field of 5.9 T, a peak D-T fusion power above 20 MW should be possible. Furthermore, at lower fusion power, a greater stability margin would be achieved, potentially allowing the alpha particles to accumulate for more than a slowing down time and reach an equilibrium distribution. Modifying the current profile transiently, by ramping down the total current, has already been shown to produce a significant improvement in the β-limit in
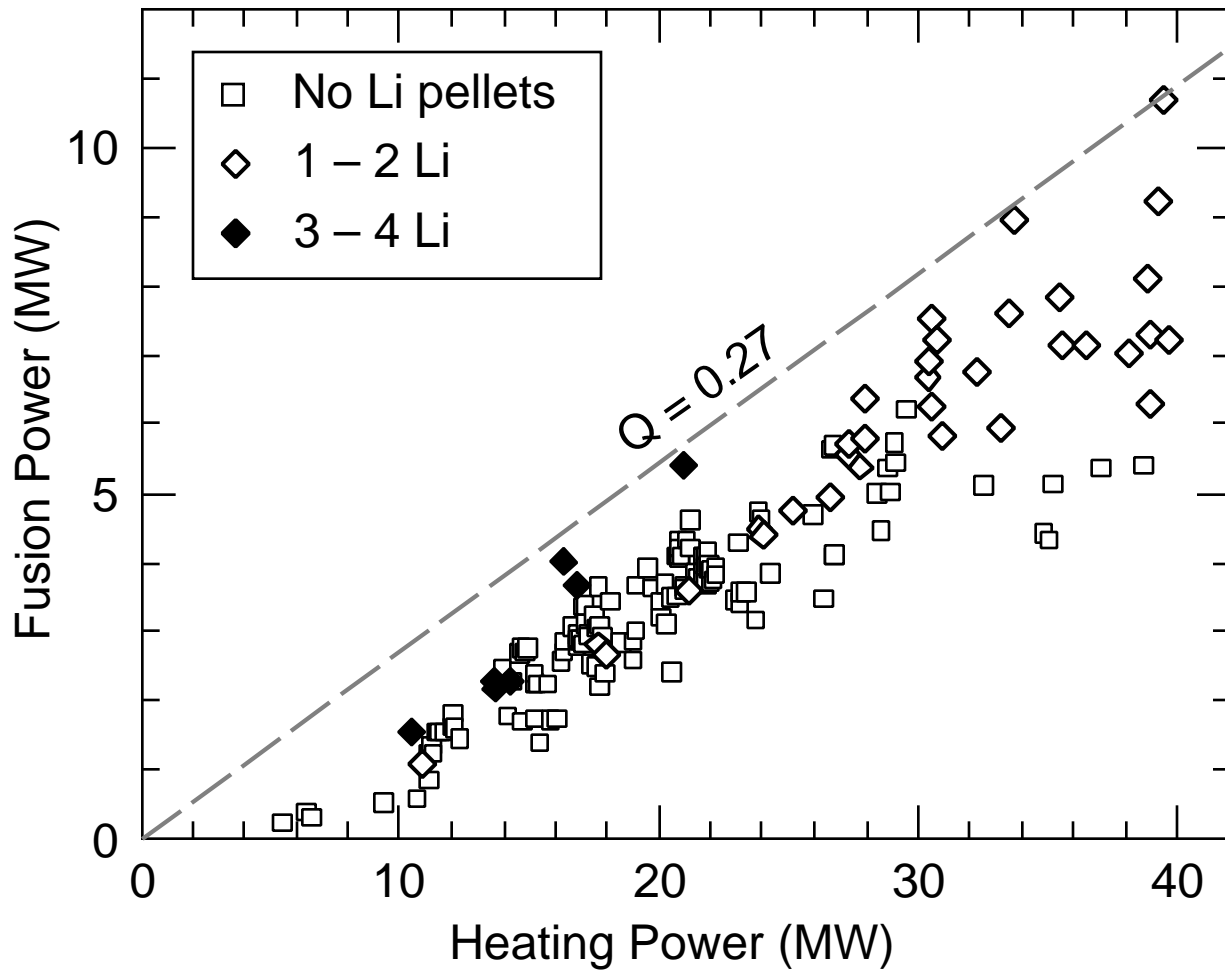
Fig. 2.2 Dependence of the peak DT fusion power output on the total heating power (NBI plus ohmic). The data are for NBI heated supershots with at least one source injecting tritium. Shots with nearly optimal tritium fraction, $0.4 < P_{T\text{-}NBI}/P_{NBI} < 0.8$, are distinguished. For a given heating power, increased fusion output is made possible through conditioning the limiter by injecting multiple lithium pellets before the NBI pulse.
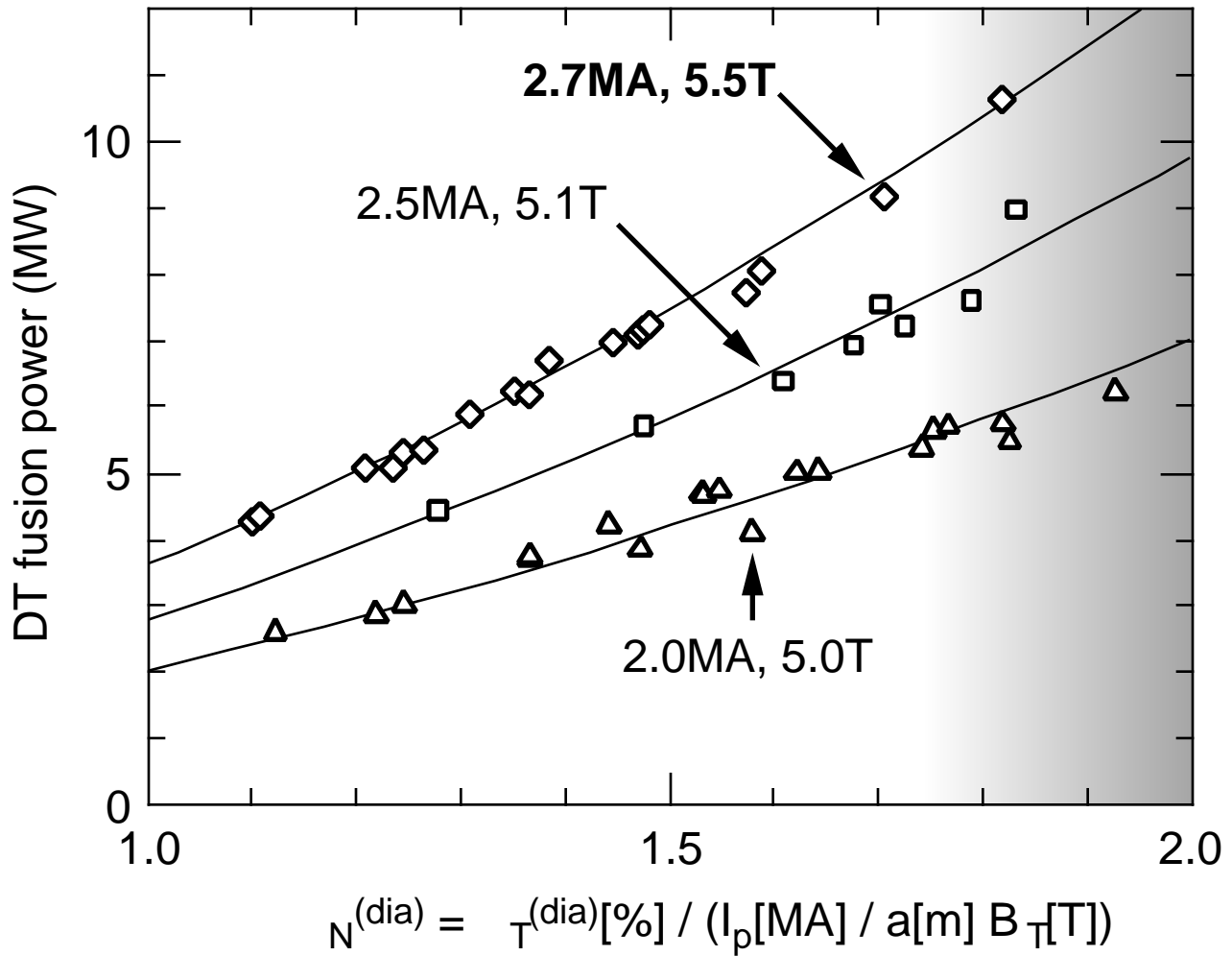
Fig. 2.3 Variation of the peak DT fusion power with the Troyon-normalized-in TFTR
D-T supershots heated by NBI. The three series of plasmas at progressively
higher machine parameters were run in December 1993, May 1994 and Octobe
1994 as part of the campaign to maximize the fusion power output from TFTR
The lines of best fit for each series vary as $_N{}^{1.8}$. The shaded area to the right
represents the region of increasing probability of a disruption for high-
performance, constant-current TFTR supershots.

TFTR: in such plasmas, a fusion power of 6.7 MW has already been produced at $\beta_N = 3.0$ and $\beta_N = 4.2$ [17]. Calculations of current profiles with improved stability, and means of producing them in TFTR, will be discussed in Sec. 2.4.

A maximum global Q, defined as the ratio of the total fusion power to the total heating power, of 0.27 has been achieved in TFTR. As seen in Fig. 2.2, this value has been achieved both at the highest heating power and also at a neutral beam power of only 21 MW in a D-T plasma with exceptionally high confinement, $\tau_E = 0.27$ s, produced by extensive lithium conditioning. These plasmas are calculated to have reached a ratio of the local fusion power to the heating power density of 0.5 – 0.75 at the center. The central fusion power densities achieved in the high-performance TFTR supershots, 1.5 – 2.8 MWm^{-3}, are comparable to or greater than those expected in ITER [1]. The hot-ion ($T_i > T_e$) nature of these plasmas does increase the central DT reactivity by a factor 1.5 – 2 compared to that of an isothermal ($T_e = T_i$) plasma with the same total energy and particle densities (including impurities). An additional increase in reactivity by a factor of two at constant β^2, apparent in Fig. 2.1 for TFTR compared to ITER, results from the highly peaked profiles in supershots. It is important to note that, although the NBI provides the dominant heating and fueling, in the core of high-power supershots, the non-Maxwellian ion distribution does *not* increase the DT reactivity compared to that of a plasma having a locally thermalized ion distribution with the same total fuel energy and particle densities.

The central alpha-particle pressure in supershots is determined both by the maximum achievable plasma pressure, which defines the alpha-particle source rate, and by the time for which that source rate can be sustained [18]. The maximum central pressure is limited by the onset of pressure-driven MHD instabilities which, in extreme cases, cause rapid plasma disruptions [19]. Also, in general, there appears to be a roughly reciprocal relationship between the central plasma pressure and the sustainable pulse length. After reaching a maximum value, typically after 0.4 – 0.6 s of neutral beam heating, the plasma pressure often declines because either plasma instabilities develop, typically MHD activity with low mode numbers, or there are increasing influxes of deuterium or impurities, particularly carbon, from the limiter. Both of these phenomena reduce the central pressure and degrade the plasma confinement. An important part of the TFTR-AP program will be to resolve both of these limitations to D-T performance in TFTR.

2.2 Investigating a hot-ion route to ignition in a D-T plasma

It is interesting to examine the implications of TFTR supershot for the performance of future toka-maks, such as ITER. Recent changes in the design parameters for ITER [1], in particular the reduction in the plasma current to 21 MA (from 24 MA) and the assumption of broader profiles for H-mode plasmas, require operating much closer to accepted stability boundaries and with more optimistic assumptions about confinement. For ITER to obtain its design goal of 1500 MW of fusion power at the beta limit assuming TFTR supershot-like conditions, *i.e.* the same value of C_{fus} and β_N as the

shotproducing 10.7 MW of D-T power, only 14 MA of current would be required and the stored energy in the plasma would be half that required in the planned H-modes at an optimum density. Alternatively, the MHD stability could be improved by operating at maximum current to reduce the value of β_N. The recommendations concerning the ITER design contained in the recent draft report on Fusion Research issued by the President's Committee of Advisors on Science and Technology reinforce the need to reduce the projected cost of ITER, which may entail further improvements in the physics performance.

Another outstanding question on ITER is what power is required to induce an L to H-mode transition. With 100 MW of auxiliary power and operation at a density of $3 \times 10^{19}\,\text{m}^{-3}$, some present scalings for the threshold transition power suggest that it may not be possible to obtain an H-mode in ITER. Operation in a driven mode to enhance the plasma reactivity and increase the power flow through the plasma boundary from 100 MW to 200 MW could be valuable in this regard. This more modest goal of producing 500 MW of fusion power from a supershot-like plasma would, according to the discussion above, require only 30% of the stored energy in the plasma at the planned operating point.

These estimates are simplistic and do not address the critical issue of whether the characteristics of a supershot can be achieved in a reactor or in ITER and how much auxiliary power would be required to achieve these benefits. To assess more realistically the benefits of the hot-ion regime and density peaking, a series of simulations was performed for ITER. A fixed volume-average plasma density of $3 \times 10^{19}\,\text{m}^{-3}$ was taken, classical alpha slowing-down was assumed, T_i and T_e were made equal and the auxiliary heating was applied to the ion channel. The resulting fusion power is shown versus the confinement time enhancement factor, $\tau_E/\tau_E^{\text{ITER-89P}}$, in Fig. 2.4. (For reference, the present ITER operating point for ignition corresponds to $\tau_E/\tau_E^{\text{ITER-89P}} = 2.6$ at a density of $1.2 \times 10^{20}\,\text{m}^{-3}$.) By operating in the hot-ion mode, a large gain in fusion power can be obtained, although, at ignition, the gain is less than in present devices due to the relatively stronger electron-ion coupling compared with transport. A significant improvement also results from the peaked density profiles. Furthermore, it must be pointed out that in these simulations, the confinement was taken to be independent of the density profile, whereas in supershots, confinement is observed to improve with density peaking. These results point out the motivation for achieving peaked density profiles as well as ion heating.

In these simulations, the largest improvements occur with ion heating. This implies use of low energy neutral beams, which preferentially heat the ions, or ICRF (ion-cyclotron range of frequencies) heating in modes which couple to the ions. Both techniques have been demonstrated to work in D-T plasmas in TFTR. Good ion heating with neutral beams restricts the beam voltage to $<200\,\text{kV}$ with D-beams and $<300\,\text{kV}$ with T-beams. However, if the beam deposition profile had to be similar in ITER to that in TFTR, then the required beam voltage would actually need to be about 500 kV for D-NBI and 750 kV for T-NBI with tangential NBI geometry. While a perfect match may not, therefore, be possible, it may be acceptable to have a somewhat broader heating profile in order to maintain prefer-

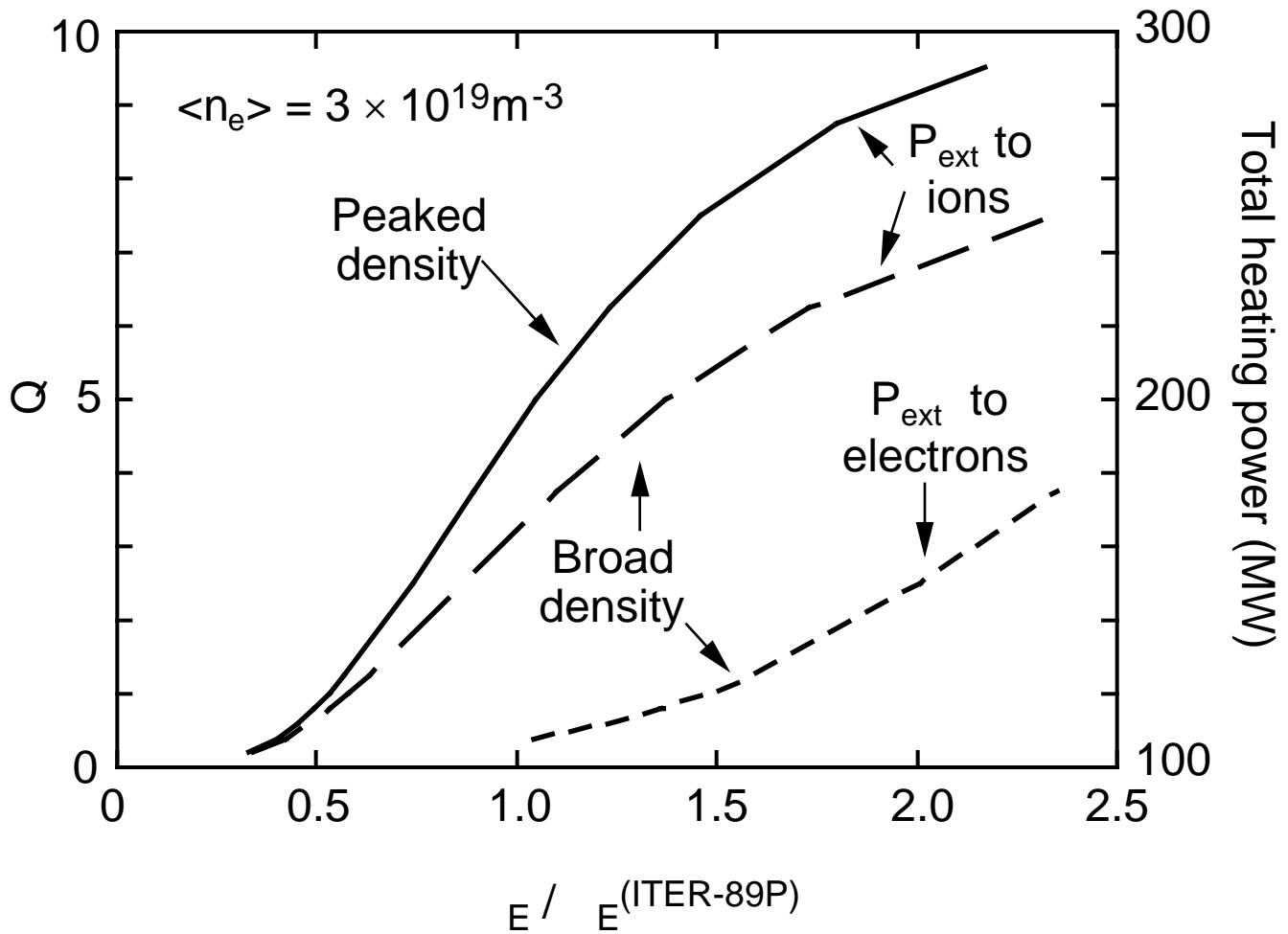Fig. 2.4 Variation of the fusion power gain Q P_{fus}/P_{ext} with the enhancement of the globa confinement time relative to ITER-89P scaling for various assumptions about the densi profile shape and the target of the external heating. A fixed volume-average density o $\times 10^{19} m^{-3}$ and ITER parameters were taken. The total plasma heating power is indicat for an external heating power of 100MW.

ential ion heating. ICRF heating, on the other hand, has the advantage that the power would be centrally deposited and preferentially coupled to the ions: about 50 – 75 % of the ICRF power could be coupled to the bulk ions. Thus, preferential ion heating appears possible. Furthermore, in supershots, the ion heat transport in the core is less than that of the electrons. This may allow the ion stored energy to increase relative to the electrons more than in the simulations for Fig. 2.4, which assumed $\chi_i = \chi_e$. The benefit of auxiliary heating of the ions is greatest for Q < 5 because alpha-particle heating, which flows preferentially to the electrons, will result in a smaller difference between the electron and ion stored energies. With its high-power neutral beam and ICRF heating systems, TFTR-AP will continue to study ion heating schemes in regimes of interest to the startup of future ignition tokamaks.

Several techniques exist to produce peaked density profiles. The most established is using relatively deeply penetrating neutral beams coupled with control of the recycling at the edge. In recent TFTR experiments with extensive lithium wall conditioning, density peakedness ratios $n_e(0)/<n_e>$ up to 4 have been achieved with NBI. However, beam fueling does not appear to scale well to ignition because the fueling decreases with increasing acceleration voltage resulting in modest values of Q. In most plasma regimes, the particle diffusivity is found to be comparable to the electron and ion thermal diffusivities. The ITER-89P scaling for the energy confinement would then imply a favorable scaling of the particle diffusivity with plasma size and elongation. In a full-size ITER plasma with the beam energy increased to provide the same deposition profile as in TFTR, this reduced diffusivity would compensate somewhat for the increased plasma volume, but the central density would only be about 70% of that in TFTR for the same beam current.

A different approach to fueling a supershot in ITER with neutral beams would be to start with a small minor radius plasma to allow good penetration of ~100 keV neutral beams from positive-ion sources, similar to those now in use. If the diffusivity scaling implied by the ITER-89P confinement scaling is valid, then there should not be a problem in fueling a supershot in ITER on the inside wall with R = 6.8 m, a = 1.5 m, and $P_b \approx 20$ MW. The main goal would be to obtain high Q in this small plasma and then to grow the plasma to the full ITER size. If the plasma can be maintained near ignition conditions while the plasma is grown, then only particle fueling will be required with little external heating. To explore this possibility, we have performed simulations based on the TFTR supershot produced with lithium conditioning, which achieved a triple product of $n_i(0) \cdot T_i(0) \cdot \tau^* = 8.3 \times 10^{20}$ m^{-3}·keV·s with only 17 MW of neutral beam power. To project from this supershot to ITER, we will assume that the central values and profile shapes for density and temperature are the same as in TFTR, but that the global confinement time can be described as a multiple of ITER-89P L-mode scaling. Based on results from TFTR, JET [4] and JT-60U [3], we take $\tau_E \approx 2.7 \tau_E^{ITER-89P}$. For an elongation of 1.6 and $q_a = 3.6$, the reduced-size plasma in ITER can support a current of 5.6 MA. With 13.5 MW of NBI heating, the ITER supershot is projected to have $\tau_E \approx 4.6$ s and a Q of approximately 17. Starting from this

high-Q condition, the plasma size and current would slowly be increased to achieve ignition in the full size ITER plasma.

A peaked profile can be sustained with modest central fueling if the central particle confinement time is sufficiently long. As discussed above, in most plasma regimes, $D \sim \chi_i \sim \chi_e$ so this is not normally possible. Recently, however, experiments on TFTR with reversed-shear configurations have produced plasmas in which the density profile became very peaked with $n_e(0)/\langle n_e \rangle$ up to 4.2 [20]. This appears to be due to a reduction in transport in the core with $D << \chi_e$ and $\chi_i < \chi_e$; a reduction in the core particle diffusivity by a factor up to 50 has been inferred for these plasmas. Thus in this configuration, neutral beam fueling of the core may be feasible, especially if higher aspect ratio plasmas are used. Experiments to explore fully this intriguing new regime of operation are a significant element of this proposal, described more fully in Sec. 2.3.

Another approach would be to use ion Bernstein wave (IBW) heating to create a particle transport barrier. Experiments on PLT, Alcator-C, JIPPT-2 and PBX-M have demonstrated density profile peaking during the application of IBW. Recent analysis of the PBX-M experiments indicates that a transport barrier, *i.e.* a region of reduced D, is formed near the resonant layer. Though further work is required to establish the physics of the transport barrier and demonstrate this technique in reactor-grade plasmas, estimates of the IBW power required to establish a transport barrier in ITER are relatively modest, 10 – 20 MW. Plans for studying this technique in TFTR will be discussed in Sec. 2.4.

Many experiments on a variety of tokamaks, including TFTR, have demonstrated that it is also possible to peak the density profile using pellet injection. Though experiments on TFTR indicate that the improvement in global confinement time is less in a pellet fueled discharge than in a beam-heated discharge with the same density profile shape, the improvement in performance is still considerable relative to a broad profile L-mode discharge. A dramatic improvement in D-D fusion reactivity, by a factor of 3, at roughly constant plasma energy, was observed in JET in the PEP ("pellet enhanced performance") mode [21] as well as in TFTR and, more recently, Alcator C-MOD. Fuel pellets injected at conventional velocities will not penetrate to the center of the plasma in ITER. However, the experiments in TFTR have shown that even with quite shallow pellet penetration it is possible to produce a moderately peaked density profile. It remains, however, to optimize the pellet injection for high fusion reactivity and extended pulses. The possibility of studying pellet fueling for ITER in TFTR-AP will be discussed further in Sec. 5.1.

In this discussion, we have seen that by means of ion heating and density profile peaking, it would be possible to increase the fusion power substantially in ITER, or any tokamak planned to reach ignition, without increasing the plasma energy. This gain in reactivity could be exploited to produce high Q at modest power or to facilitate achieving an H-mode transition en route to ignition. TFTR-AP will have

the capability to explore the optimization of these plasma scenarios and will provide valuable data on these possibilities in its planned experimental program.

2.3 Current profile modification

Calculations with the PEST code [22] have shown that, by perturbing the current profile in the central region of the plasma, significant increases can be achieved in the critical   for destabilizing the modes thought to be responsible for the disruptions which ultimately limit fusion performance in TFTR. An example of the current profile for the supershot which produced 10.7 MW of D-T fusion power and a modified profile which is calculated to have a substantially higher   -limit are shown in Fig. 2.5. Analyses such as these, together with the experimental evidence gained from TFTR [17] and other tokamaks [23,24] in improving the   -limit through modifications of the current profile, have prompted an intensive search for methods to control the current profile in supershots in TFTR.

In a low-collisionality tokamak with moderately low aspect-ratio such as TFTR (R/a typically 2.7 – 3.1) with centrally aimed neutral beam injection, there is a close coupling between the pressure profile and the NBI driven and the bootstrap components of the current profile. Thus, there would appear to be few options for controlling the equilibrium current profile in TFTR during auxiliary heating. It should be noted in this regard that in future reactors operating near the   -limit with high bootstrap fractions, very similar conditions will apply. However, despite these apparent limitations, remarkable success has recently been achieved in modifying the current profile in TFTR through a combination of ramping the plasma current inductively and applying carefully tailored NBI heating pulses. With these techniques, three different classes of q-profiles have been created transiently: 1) monotonic q profiles with high central q, q(0) up to 2.5 with an edge q of 6, 2) profiles with reversed shear (dq/d   < 0) for r/a   0.5 [20] and 3) profiles with increased shear in the edge region, r/a > 0.6 [17]. Examples of the q profiles measured by the motional Stark-effect (MSE) diagnostic, together with the calculated total pressure profiles, are shown in Fig. 2.6. Each of these regimes has shown interesting stability and transport properties in preliminary experiments but their full potential to improve performance in D-T plasmas has not yet been explored.

In reversed-shear plasmas, substantial improvements in confinement have been observed in the region where the shear is negative [20]. With ~20 MW of balanced co- and counter- deuterium NBI, reversed-shear plasmas are observed to undergo an abrupt transition marked by the formation of an extremely peaked density profile: a central electron density up to 1.2×10^{20} m^{-3} and a peakedness parameter $n_e(0)/<n_e>$ up to 4.2 have been achieved with only 25 MW of NBI at $B_T = 4.8$ T, and $I_p = 1.6$ MA. As seen in Fig. 2.7 the central density increases by a factor of 2.7 in 0.35 s following the transition. Even with these high densities, the central temperatures remain high, with $T_i(0)$ 20 keV and $T_e(0)$ 8 keV (Fig. 2.8). The measured toroidal rotation velocity is relatively low, peaking near the minimum-q surface at about -150 km/s. The pressure peaking factor is ~8 and the calculated

Current density (MAm^{-2})

4

q(0) = 0.9,
$_{N,max}$ = 2.0

I_p = 2.7MA
B_T = 5.5T

3

q(0) = 1.4,
$_{N,max}$ = 2.7

2

1

0
0   0.2   0.4   0.6   0.8
Minor radius (m)
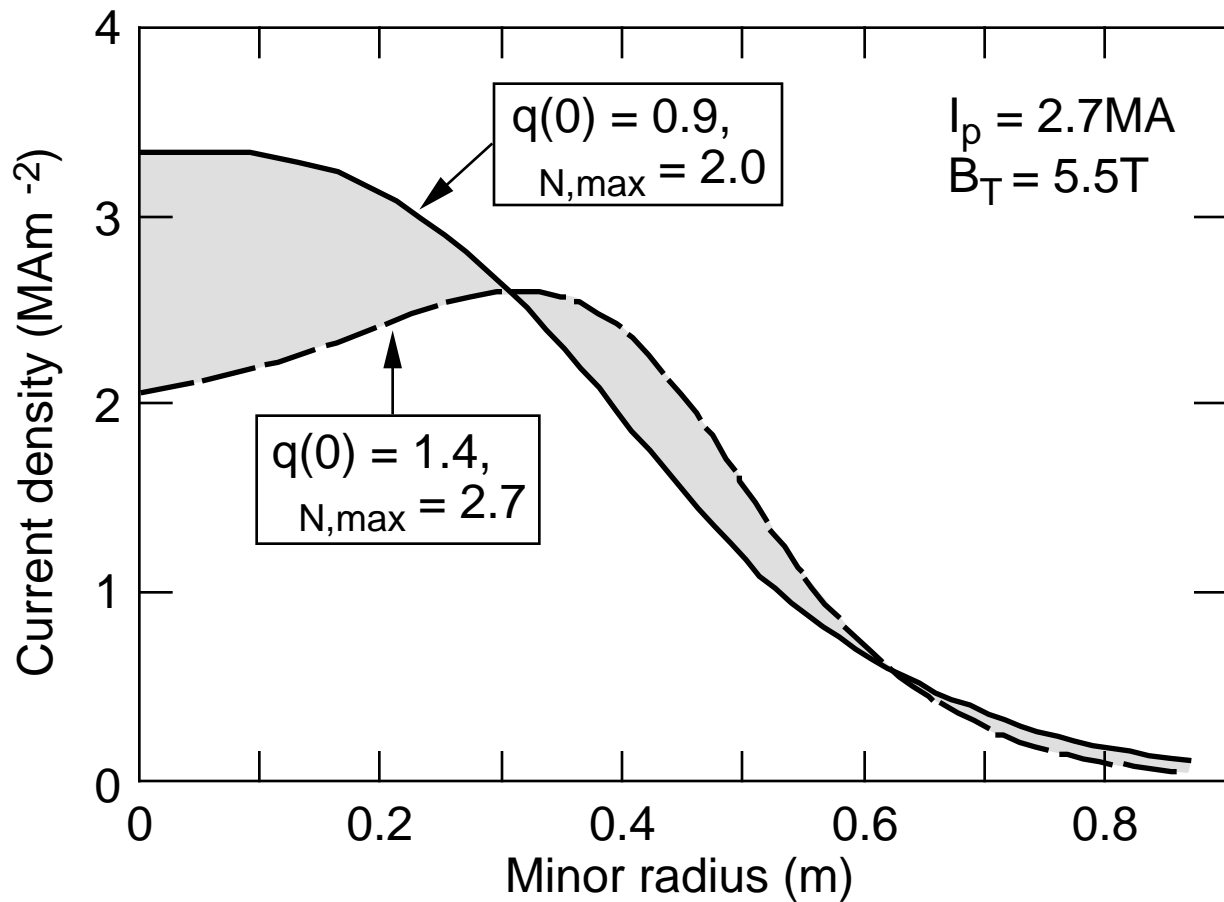
Fig. 2.5 Current profiles for shot 80539 (solid curve, 2.65MA, 5.5T, B_T=10.7MW), which
suffered a minor disruption at $_N$ 1.9, compared with that for a plasma (dashed curve
with the same total current but mildly reversed shear which is calculated to have
normalized- limit of 2.7. The difference between the profiles (shaded regions) wou
require current drive of only 0.4MA. Extrapolating on the basis of existing D-T plasma
in TFTR, such a plasma should be capable of producing 20MW of D-T fusion power at
toroidal field of 6T.
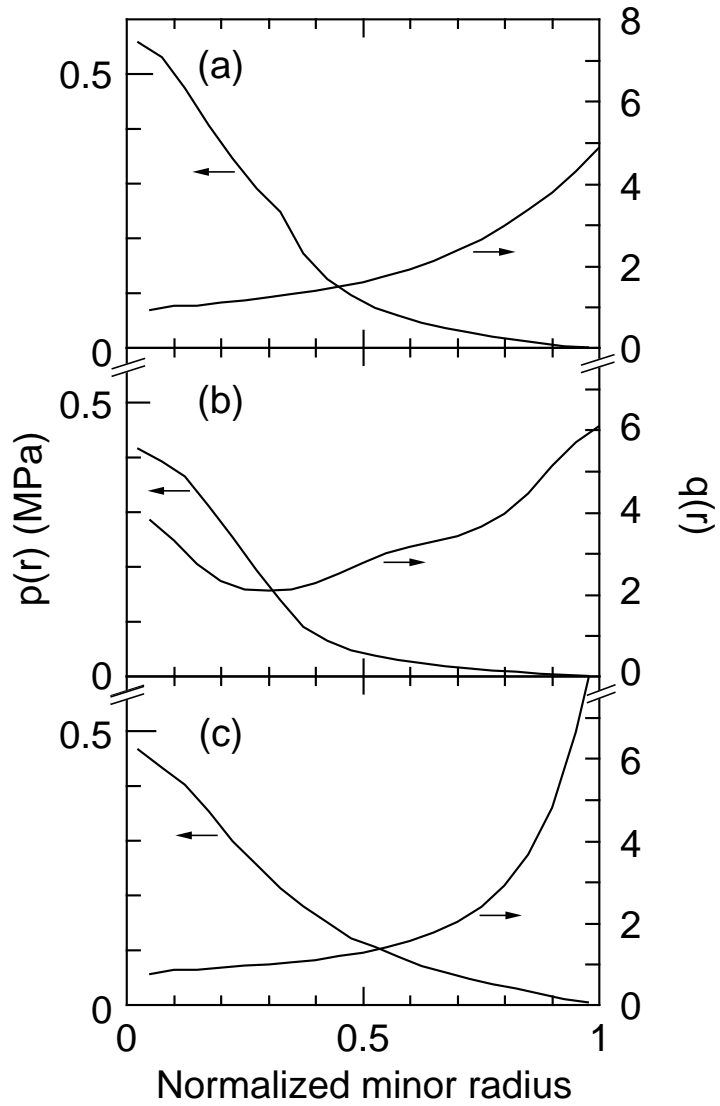
Fig. 2.6 Examples of the profiles of the total plasma pressure and q for advanced tokamak regimes in TFTR. (a) Supershot (77309), 2.1MA, 21MW DT-NBI; (b) Reversed-shear plasma (84011), 1.6MA, 21MW D-NBI; (c) High edge-shear (rampdown) plasma (78185), 1.5MA, 31MW DT-NBI.
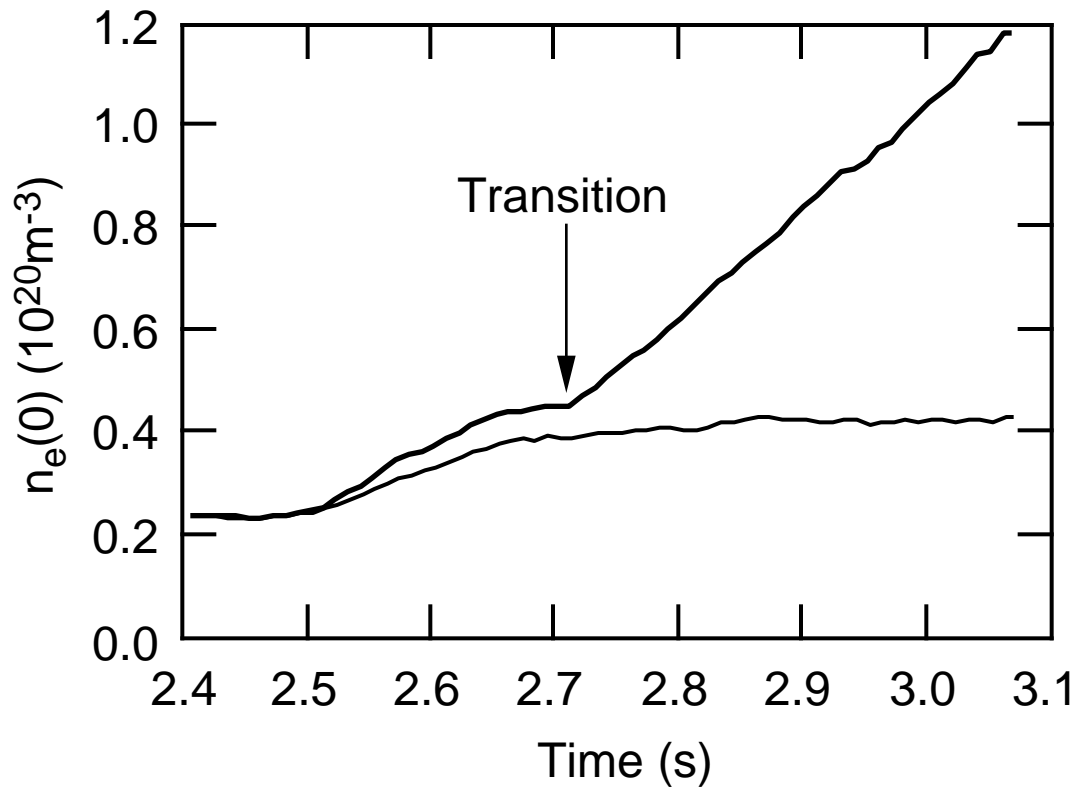
Fig. 2.7   Evolution of the central electron density in two neighboring reversed-shear shots without and with a transition to improved central confinement during the high-power NBI phase.
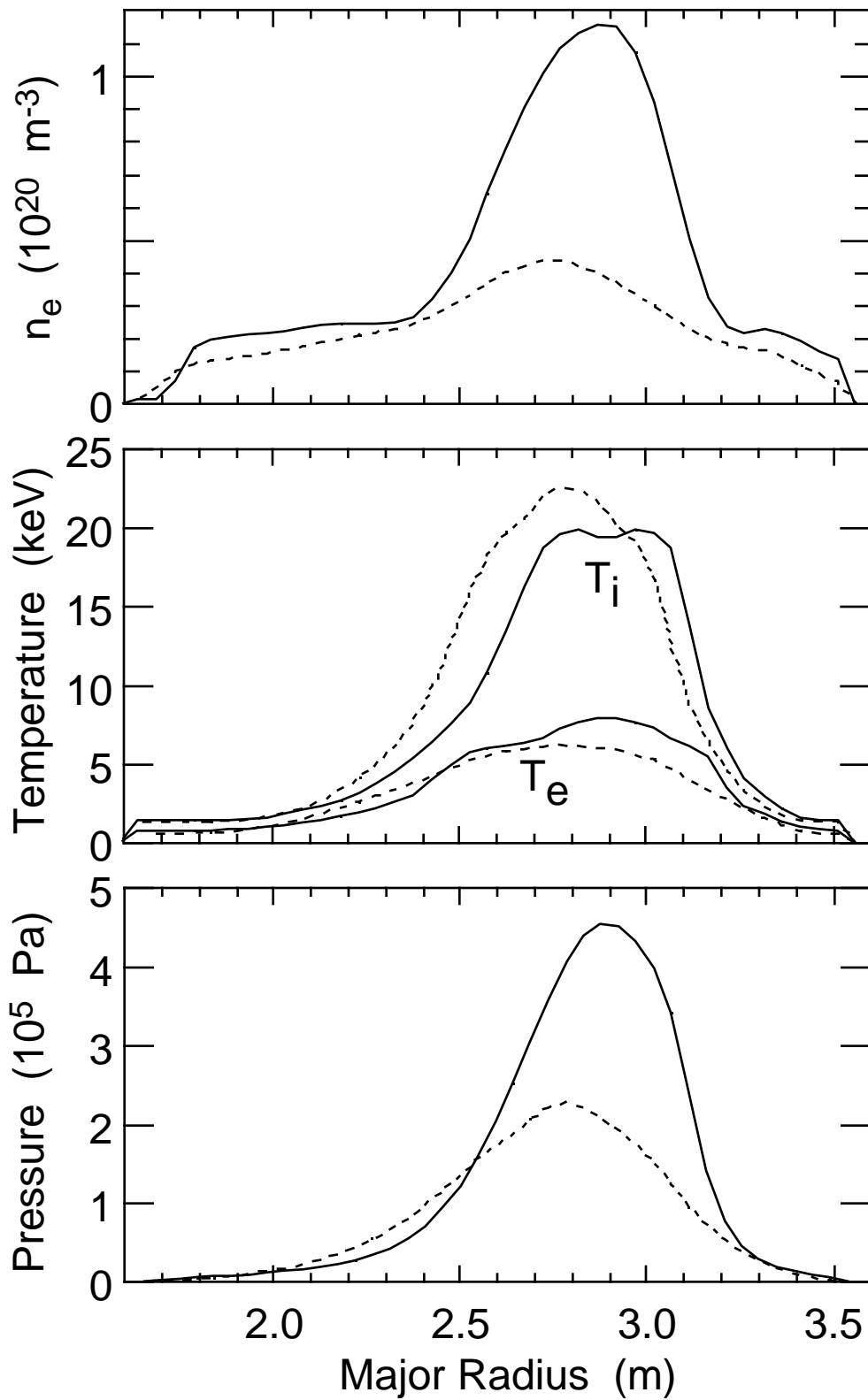
Fig. 2.8 Profiles of the electron density, electron and ion temperatures and the kinetic pressure before (dashed) and after (solid) the transition to improved central confinement in a reversed-shear plasma in TFTR.

bootstrap current reaches ~2/3 of the total plasma current. Transport analysis of these plasmas indicates that the electron particle diffusivity has decreased by a factor up to 50 and is in approximate agreement with the neoclassical value, as shown in Fig. 2.9. Assuming the classical ion-electron energy exchange, the inferred ion thermal loss in the core is substantially lower than predicted by neoclassical theory. The electron thermal loss is not changed significantly, and the inferred χ_e is much larger than χ_i or D_e. Initial measurements by the correlation reflectometer indicate that the amplitude of density fluctuations is substantially reduced with reversed shear. Furthermore, during the reversed-shear phase, there is a complete absence of coherent MHD activity from the core of the plasma. The extreme peaking of the pressure profile has resulted in a maximum β_N of 3.1 in these plasmas, compared to the upper limit of ~2.8 in normal supershots. So far, these plasmas have only been studied in deuterium. Simple projections, including TRANSP code simulations, indicate that similar plasmas would produce between 4 and 6 MW of fusion power with D-T NBI, depending on assumptions.

As shown in Fig. 2.10, q_{min} continuously declines in the reversed shear plasmas produced so far, due to the inductive penetration of the current and the absence of significant off-axis current drive. As q_{min} decays, r_{min} also decreases. In the high-performance reversed shear plasmas, the plasmas disrupted as q_{min} approached 2, with an $n = 1$ ideal-like mode observed outside the reversal radius (far outside the peak of the pressure gradient). At the time of disruption, the plasmas are far from transport equilibrium in the reversed and low shear regions. Most of the core heating and fueling is balanced by the continuing increase in the plasma parameters, not by radial losses. Ideal stability analysis indicates that at the disruption these plasmas are near the $n = 1$ stability boundary for infernal modes [25] (which is more restrictive than high-n modes) in the region where a mode is observed experimentally. Furthermore, theoretical analysis of these plasmas indicates that by optimizing and controlling the evolution of the current profile during the main NBI heating pulse, the β-limit for these plasmas should be at least doubled by dropping q_{min} to ~1.3 and q_{edge} into the range 4 – 5, as seen in Fig. 2.11. This increased limit would be expected to quadruple the fusion power to roughly 20 MW. Increasing the reversal radius beyond r/a ≈ 0.3 is also predicted to increase the β-limit and may broaden the volume of reduced transport. Finally, increasing B_T beyond 4.8 T at fixed q_{edge} and β could further increase the stored energy by ~45% and fusion power by roughly an additional factor of two. Clearly, if these plasma configurations can be developed, they would present a substantial increase in the performance of TFTR and a radically different core-plasma regime for future reactors. The relationship between stability, transport and heating in this new regime has not yet been established and remains to be explored in the proposed extension.

The reversed-shear plasmas are produced by ramping up the plasma current during neutral beam injection. The most successful strategy has been to apply a small amount of neutral beam power, typically 5 – 8 MW very early in the discharge, starting as early as 0.6 s after initiating the plasma, and then apply the main heating pulse, up to 25 MW, at about 2.5 s at the end of the current ramp-up. The typical
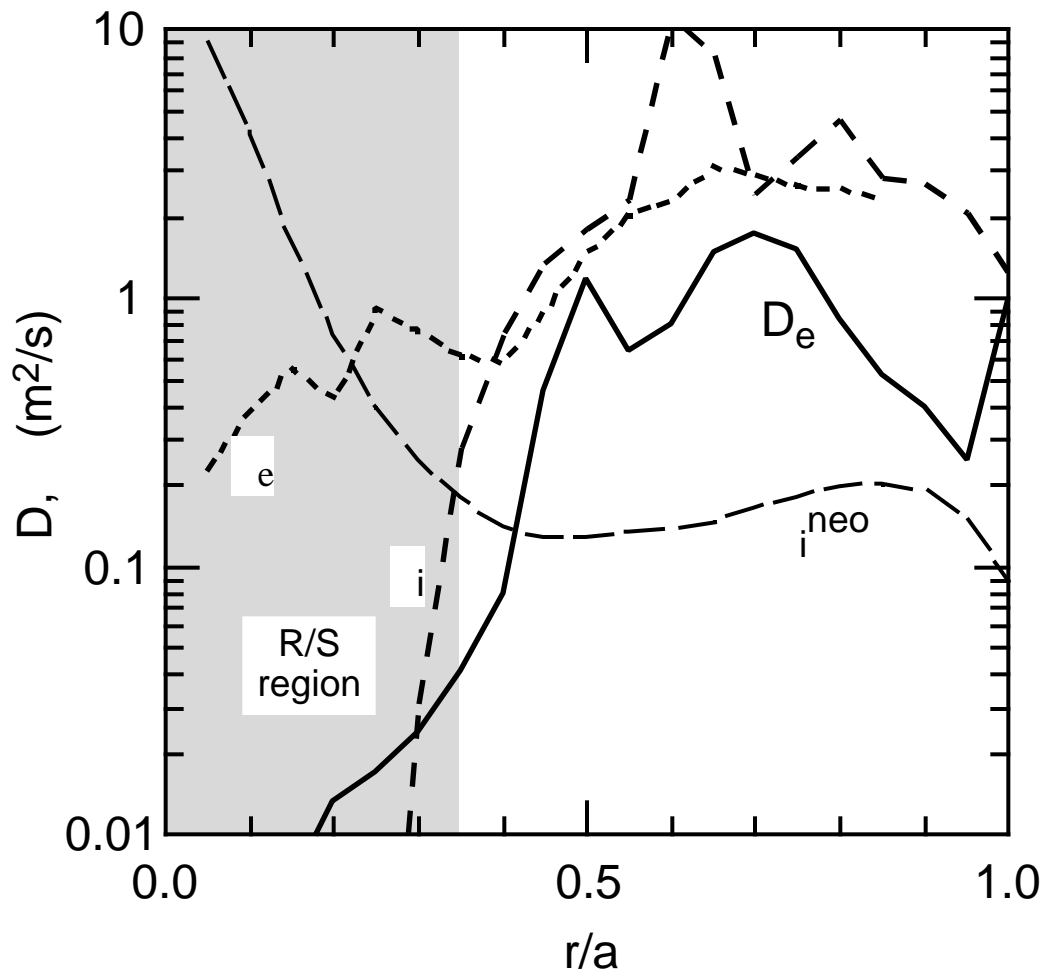
Fig. 2.9   Profiles of the particle and thermal diffusivities during a reversed-shear phase. The neoclassical ion thermal diffusivity is also shown. Within the region of reversed-shear (shaded), there is a substantial reduction in the particle and the ion thermal transport. The data was analyzed by TRANSP.
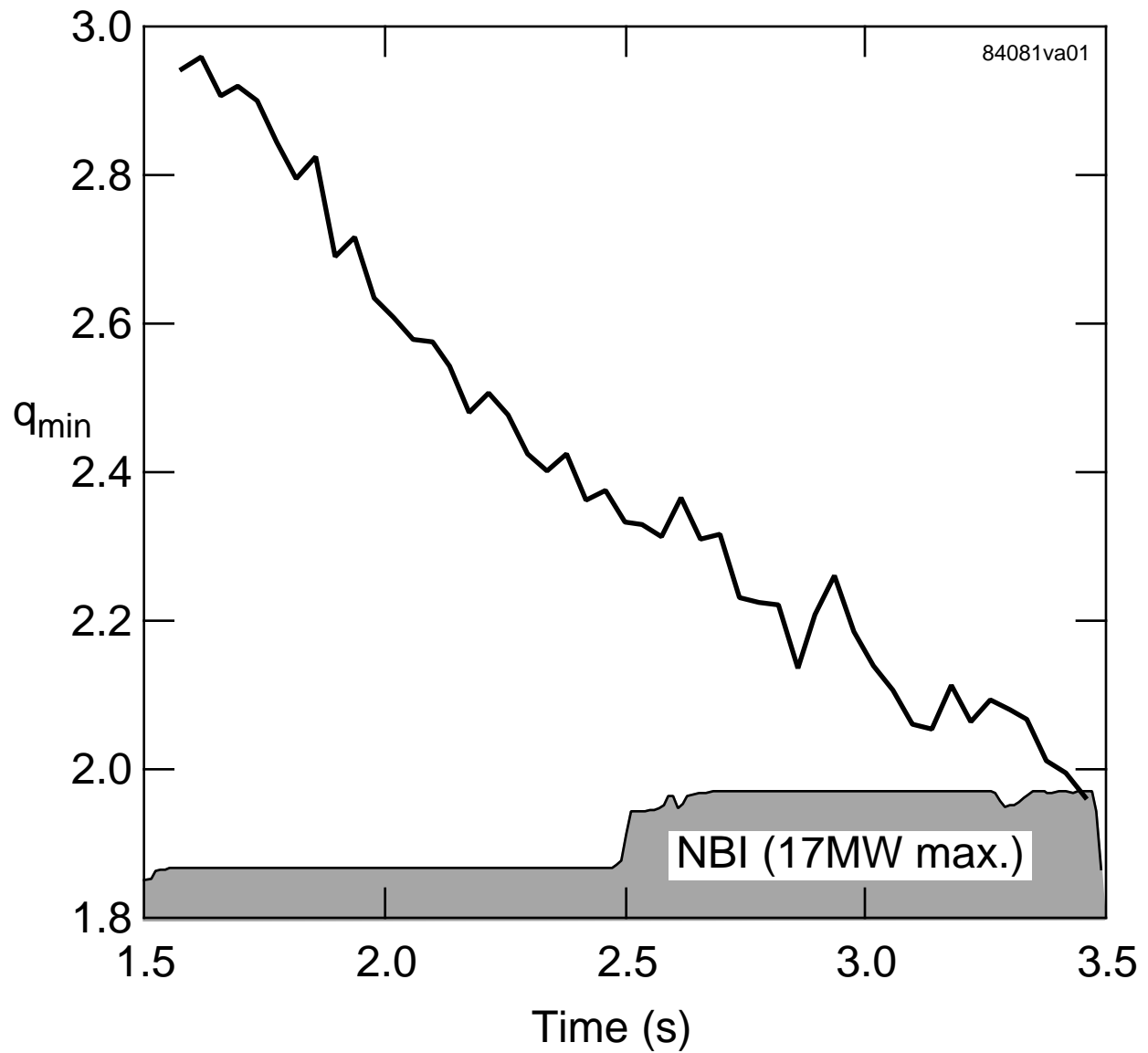
Fig. 2.10 Evolution of the the minimum q in the profile of a reversed-shear plasma. The
q profile is measured by the MSE diagnostic during the time when NBI
source 5b is injecting. The overall NBI pulse extends from 0.7s to 3.5s. The
time evolution is consistent with TRANSP calculations based on neoclassical
resistivity including the bootstrap and NBI-driven currents.
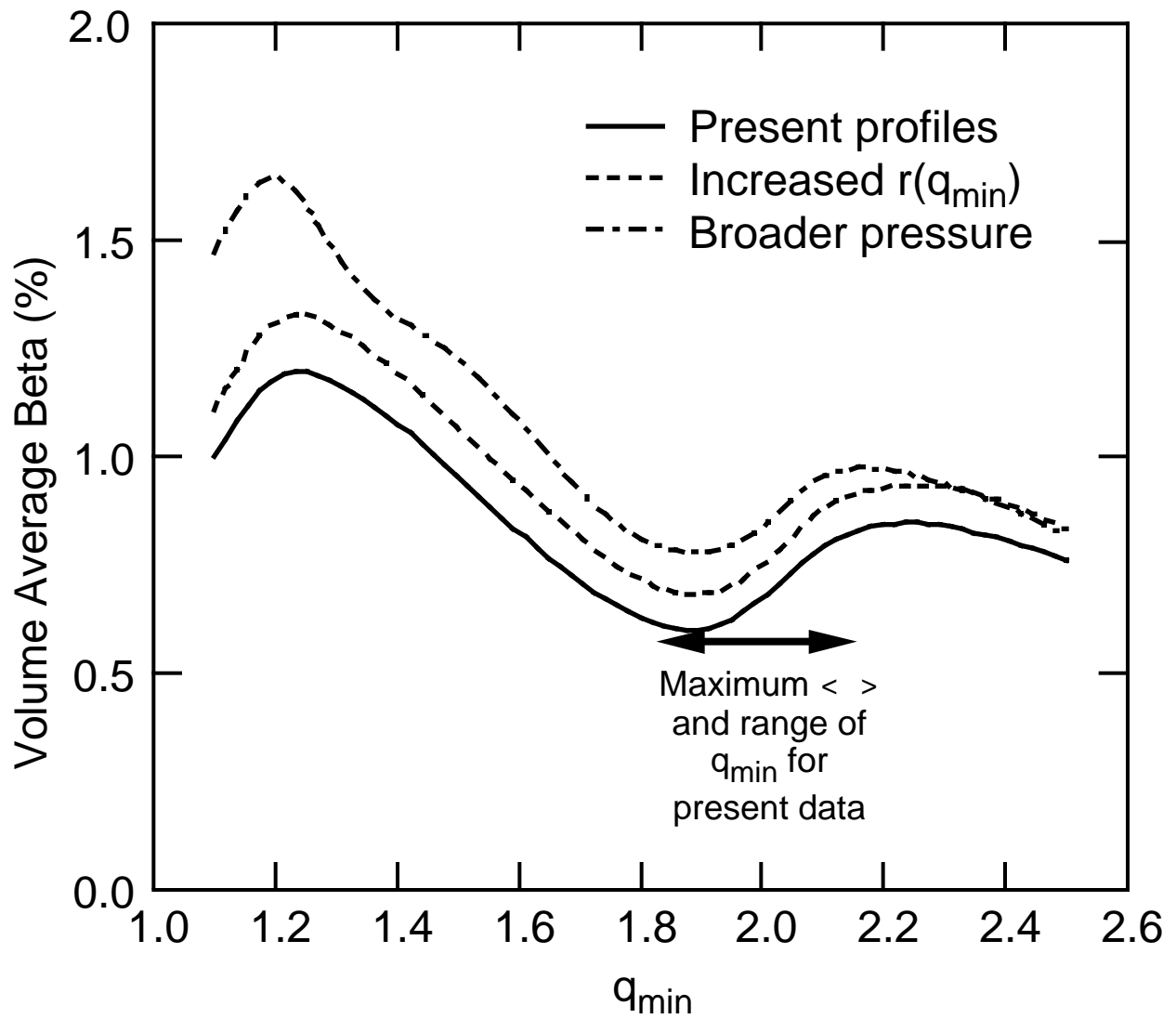
Fig. 2.11 Calculated limiting value of < > *vs.* minimum q in reversed-shear plasmas for different profile shape assumptions.

waveforms are shown in Fig. 2.12. Off-axis current drive is needed to stabilize the time-decay of q_{min}, since this decay can cause the plasma to cross the stability boundary producing disruptions, and to separately control r_{min}, since increasing r_{min} is predicted to increase the   limit and may likely increase the volume of enhanced confinement. Two strategies are presently envisioned for producing plasmas with $q_{min} \sim 1.3$. The easiest is to let q_{min} continue to decline and to time the high-power injection to obtain the desired q_{min}. Unfortunately, r_{min} will also decrease, reducing the volume of the reversed shear region. The other strategy is to continue to ramp the plasma current to higher values, perhaps at a higher rate, to concentrate the current off-axis further. This technique may also need significant off-axis current drive in order to drop q_{min} enough.

Since individual NBI sources can presently inject for a maximum of 2 s at 95 keV, the long overall NBI pulse has been produced by sequentially firing sources. This has limited the number of sources available for the high-power heating phase when the reversed-shear profile has been established. An upgrade of one neutral beamline is proposed for TFTR-AP to allow a 5 s NBI pulse for three sources. This involves modulating the magnetic field which deflects the unneutralized beam to sweep it across the beam dump, thereby reducing the surface temperature which limits the pulse length. Power supplies for this purpose already exist. This inexpensive modification would significantly improve our capabilities for studying reversed-shear plasmas.

Experience with plasmas having strong magnetic field shear near the plasma edge comes from experiments conducted at high poloidal-beta on TFTR. These experiments have sought to investigate the effects of equilibrium profile modification on plasma stability and to determine optimized configurations. The current profile has been modified both by altering the co- /counter- NBI balance and by rapidly ramping the plasma current to produce profiles with increased internal inductance, l_i. The pressure profile in these plasmas has been modified by deuterium and lithium pellet injection.

Increasing l_i in this manner produces a magnetic field geometry with increased edge magnetic field shear. TFTR experiments at high β_p have demonstrated that by operating at high l_i the total plasma current may be reduced without sacrificing plasma stability and energy confinement. The ability to operate at reduced current is of great importance to next-generation devices such as ITER, where minimizing the plasma current is desirable for reducing the impact of disruptions. During the D-T phase of TFTR operation, high β_p plasmas at moderate plasma current (0.85 I_p (MA)   1.5) have been produced with energy confinement enhancement factors, H as large as 4.5 during the ELM-free phase of a limiter H-mode configuration. Stable operation at $\beta_N = 3.2$ has also been produced in these plasmas. A maximum DT fusion power of 6.7 MW has been reached with $I_p = 1.5$ MA and 31 MW of heating power. We have found that characteristics of ELMs, precursor MHD activity to β collapses, and disruptions are generally similar in D-T and D plasmas. However, the most recent experiments have revealed that a coupling of strong ELM and fishbone behavior in these plasmas may lead to a reduction of the β_N limit. We have begun to investigate methods of decoupling the ELMs and
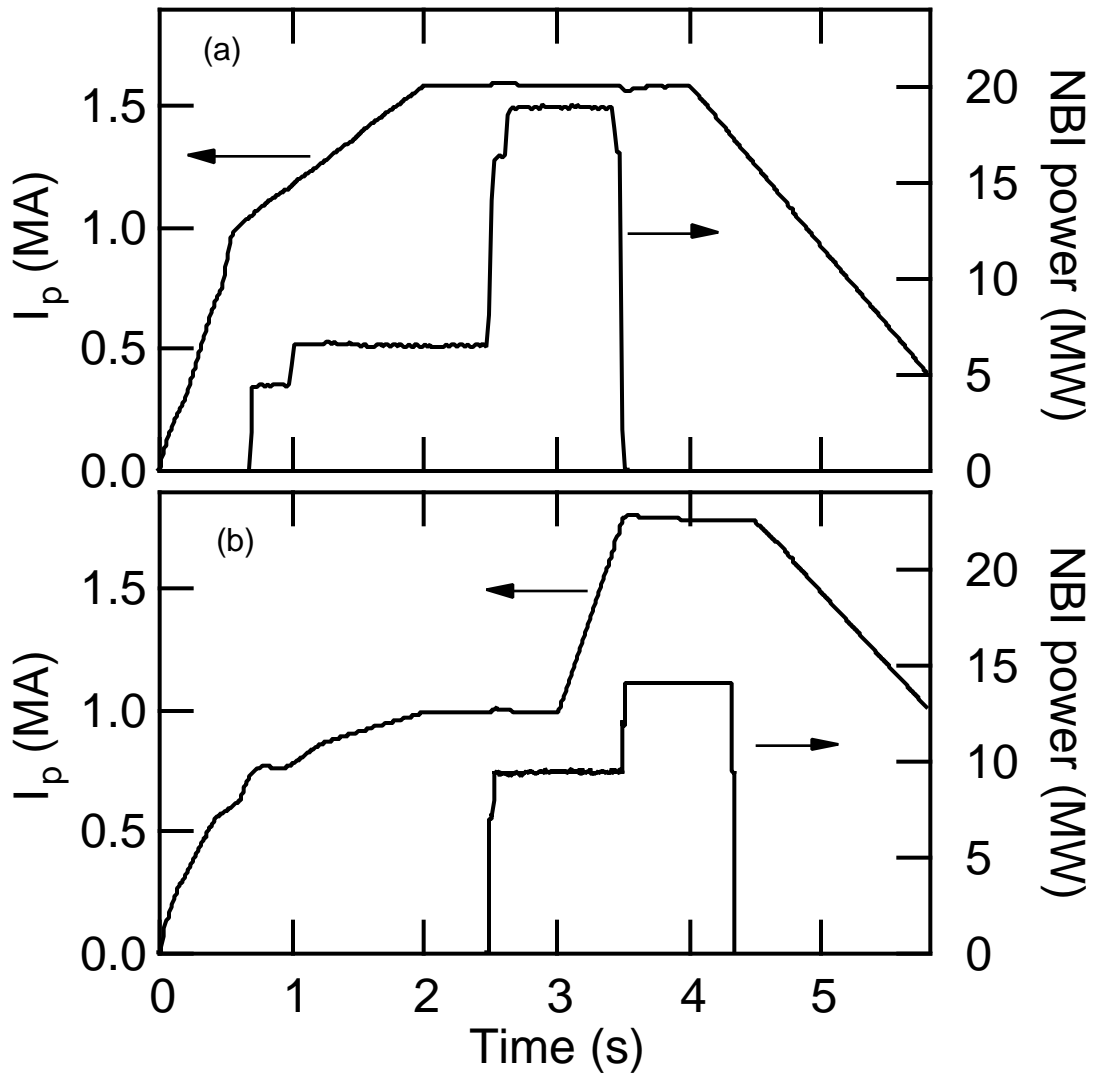
Fig. 2.12 Schemes for producing reversed-shear plasmas in TFTR: (a) non-grown (*i.e.* constant major and minor radius) startup with standard current ramp rate and early NBI; (b) standard "grown" startup to low initial current followed by rapid current ramp-up during low-power NBI.

fishbones and of reducing the impact of the fishbones by altering the central q profile, which may be a key to achieving peak performance in these plasmas.

An examination of the effects of increasing q_0 in high l_i plasmas has been continued and expanded from low (0.5 MA) to higher (1.0 MA) current operation. These experiments complement the reversed-shear experiments described above. An important result is that high q_0, magnetic shear reversal in the plasma core, and increased magnetic shear near the plasma edge are compatible. Furthermore, the favorable effects of increased edge magnetic shear and reversed central shear may have a synergistic effect on plasma stability. In particular, plasmas with high q_0 and either reduced or reversed magnetic field shear in the core are robustly stable to high-n ballooning modes, therefore the so called "second stability region" is always attainable. Experimentally produced plasmas with $q_0 \quad 3$ have been computed to be stable to high-n modes for up to 75% of the plasma minor radius.

It is also found that the modes responsible for the disruptive beta limit in these plasmas are low-n modes. Modelling of experimental equilibria yields ideal MHD stability limits which match the observed β_N limit, the mode localization, and toroidal and dominant poloidal mode numbers of the external kink/ballooning mode precursors to the disruption. In general, plasmas with higher l_i yield larger β_N limits. This result has been observed both experimentally and theoretically, and research performed so far shows a roughly linear increase of the maximum attainable β_N with l_i. In addition, the modelled instabilities at higher β_N and l_i show a stronger coupling out toward the plasma edge, which make them more amenable to wall stabilization.

These studies can be continued and further developed by introducing the enhanced capabilities of TFTR-AP. Use of non-inductive current drive in TFTR-AP may allow investigation of high l_i plasmas over longer timescales. These plasmas currently exist only on the resistive timescale of the edge plasma. Increasing l_i by adding positive current drive in the plasma core (rather than reducing the edge current density ohmically) may yield to further optimization of the current profile with respect to core localized instabilities. Eliminating or impeding the time evolution of the current profile in these plasmas will also greatly aid in the understanding of the parameters which are most important in affecting the stability (q_0, q_{min}, l_i, central or edge magnetic field shear, *etc.*).

The TFTR-AP project seeks to develop these regimes of modified stability and transport fully through additional, dedicated experimental time and by providing additional methods for controlling current profile. These methods, which include the addition of a Lower Hybrid Current Drive (LHCD) system, a modification of the ICRF antennas to improve their capability for current drive and a reconfiguration of the neutral beam injectors, will be described in detail in the subsequent sections of this proposal.

2.3.1 Lower hybrid current drive system

The LHCD system proposed for TFTR-AP initially comprises a 4.6 GHz, 2 MW power unit, consisting of 8 0.25 MW klystrons, and a launcher with full phase control. This system is capable of coupling 1.3 MW to the plasma. The pulse length of 3 s is limited by the power supplies. The power unit is presently installed on PBX-M [26] and is operational. Following initial experiments with this system, the coupled power could be doubled by adding a second power unit and associated transmission lines to the coupler. A second power unit is presently at MIT but would require some refurbishing before installation on TFTR. The complete system is shown schematically in Fig. 2.13.

The launcher system, shown schematically in Fig. 2.14, consists of a stack of 4 grills, each with 32 waveguides. Tentatively the dimensions of each waveguide are 58 mm × 6 mm. Since each waveguide is independently phased, the spectrum can be varied over a wide range, $-4.5 \leq n_{||} \leq +4.5$. The launcher is arranged in two independent halves so that it is also possible to launch a compound spectrum which has been shown to be effective in increasing the current drive efficiency [27]. The launcher is being designed to be inserted through a valve to be installed on Bay-K of the TFTR vacuum vessel. During the fabrication of the LHCD components in FY'96 and the first half of FY'97, this port would be used for testing the prototype folded waveguide ICRF antenna (see Sec. 7.6).

The goal of adding LHCD to TFTR-AP is to provide a flexible tool for modifying and controlling the current profile, particularly allowing the location of the driven current to be dynamically varied. In the reversed-shear plasmas, increasing the radius of shear reversal r_{min} (where q is a minimum) is predicted to increase the β-limit and should increase the volume of the plasma with reduced transport. The addition of LHCD will allow TFTR-AP to increase r_{min} beyond the range currently obtained using early NBI during the current rise phase. In addition, LHCD will be used to stabilize the time evolution of q_{min}, preventing the inductive decay of q_{min} from causing disruptions, as is presently inferred. The LHCD can also be used to control the magnitude of the reversed shear in the core.

To model the effects of LHCD on the current profile in TFTR plasmas, the TRANSP code has been coupled with the code LSC [28] which calculates the wave spectrum launched by the proposed coupler for a specified phasing of the grill elements, and the wave propagation and damping in the plasma as it evolves self-consistently with transport coefficients deduced from prototypical TFTR plasmas. This combined code has been used successfully to analyze LHCD experiments in PBX-M, JET and Tore-Supra. For TFTR, the code has been used to simulate both the reversed-shear and standard supershot plasmas with LHCD.

Figure 2.15 shows the driven current profiles predicted with 1 MW of LHCD at 90° and 120° phasing angles for the reversed-shear plasma which has achieved the highest performance so far (as discussed above). These plasmas are well suited for LHCD since, despite the high central density, they have low

Fig. 2.13 Schematic diagram of the Lower Hybrid Current Drive system proposed for TFTR-AP.
The system would initially be installed with one power unit (8 klystrons) and would
later be upgraded with a second power unit and transmission equipment.
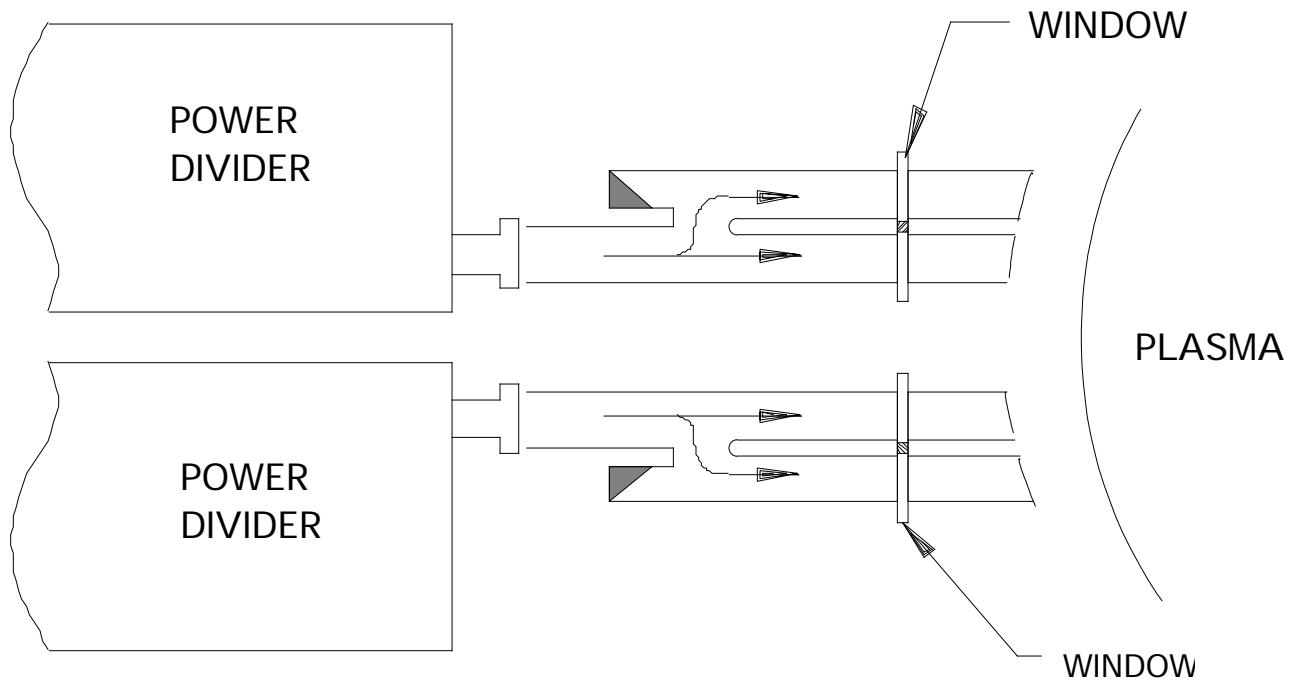
Fig. 2.14 Schematic diagram of the Lower Hybrid Current Drive couplers proposed for TFTR-AF
         Each of the four stacked grills comprises 32 waveguides. The coupler will be insertable
         and retractable through a vacuum isolation valve.
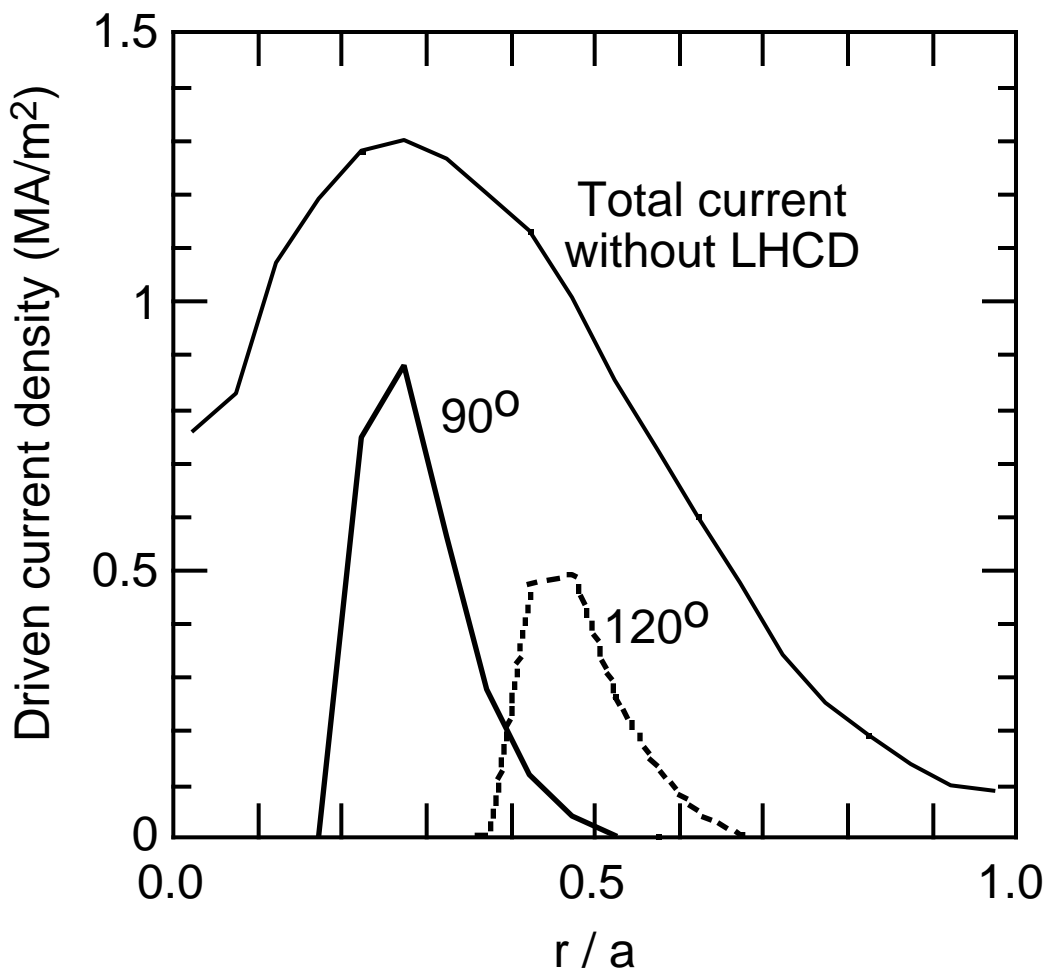
Fig. 2.15 Calculated profile of the current driven by 1MW LHCD at 4.6GHz in the "prelude" phase of a TFTR reversed-shear plasma with two different phasings of the LH coupler. The total current density in the reference shot is also shown

density and quite high electron temperature in the outer region where positive (*i.e.* co-parallel to the conventional current) current drive would be applied. The LHCD profiles are shown at the end of the prelude phase, just before the start of high-power NBI, and illustrate the flexibility in the positioning the LHCD. At earlier times when the density is lower, correspondingly higher current is driven by the LHCD. The 90° LHCD is predicted to decreases q_{min} slightly with the same r_{min}, and increases the negative shear in the core. Applying the LHCD with 120° phasing during the prelude pushes r_{min}/a to ~0.5 from the original 0.35, doubling the volume of the reversed shear region, as shown in Fig. 2.16.

During the high power phase, the high pressure gradients obtained after transition to the improved confinement generate very large core bootstrap currents that tend to reduce r_{min} over time. By adding 3MW of 120° LHCD, which requires the two power units, the LHCD is also able to maintain q_{min} and r_{min}/a 0.5 roughly constant during the main NBI heating, as seen in Figure 2.16. Furthermore, if the region of improved confinement expands with the shear-reversal radius, the region of high bootstrap current will also move outwards, helping to maintain the larger r_{min}.

The effect of the proposed LHCD on more traditional supershots has also been investigated with TRANSP/LSC. For this study, the modelling was based on a 1.8 MA D-T supershot with 24 MW NBI and 5.5 MW ICRF heating. In this case, 3 MW LHCD, launched with $n_{\parallel}$ 2.3, was capable of driving a total of 0.9 MA current with a profile peaked in the region $r/a = 0.15 – 0.25$ during the low-density ohmically heated phase before the auxiliary heating. This driven current could create a q profile with mildly reversed-shear in the region $r/a < 0.3$ after about 1 s of LHCD which was then "frozen in" by the reduced plasma resistivity during the main heating pulse. Analysis of the stability of these plasmas with the PEST code is encouraging: the global -limit is raised significantly in the reversed-shear case.

2.3.2 Mode-conversion current drive

Majeski *et al.* [29] have suggested that an ion Bernstein wave (IBW) excited by mode conversion from a fast wave at the $n_{\parallel}^2 = S$ layer in a multiple ion species plasma, such as D-T, could be used for electron heating or to drive localized electron currents. Experiments using mixed ^{3}He-^{4}He-D plasmas have shown localized electron heating at the calculated radial position of the mode conversion surface. Up to 80% of the power is measured to be deposited on electrons at the mode conversion surface, in good agreement with numerical modelling. Central electron temperatures greater than 10 keV have been produced with 4 MW of RF power, the highest electron temperature achieved in TFTR in a discharge heated by RF alone. (In comparison, the highest electron temperature achieved in the hydrogen minority heating regime was 7.5 keV with over 10 MW of RF power.) Experiments to investigate mode conversion current drive (MCCD) and fast wave current drive (FWCD) as a means of current profile control have begun. Initial results from the FWCD experiments indicate that 70 kA of current has been driven with 2 MW of RF power in a plasma with a central density of 3.3×10^{19} m^{-3}, and a central electron temperature of 5 keV. With mode conversion current drive, up to 120 kA of current has
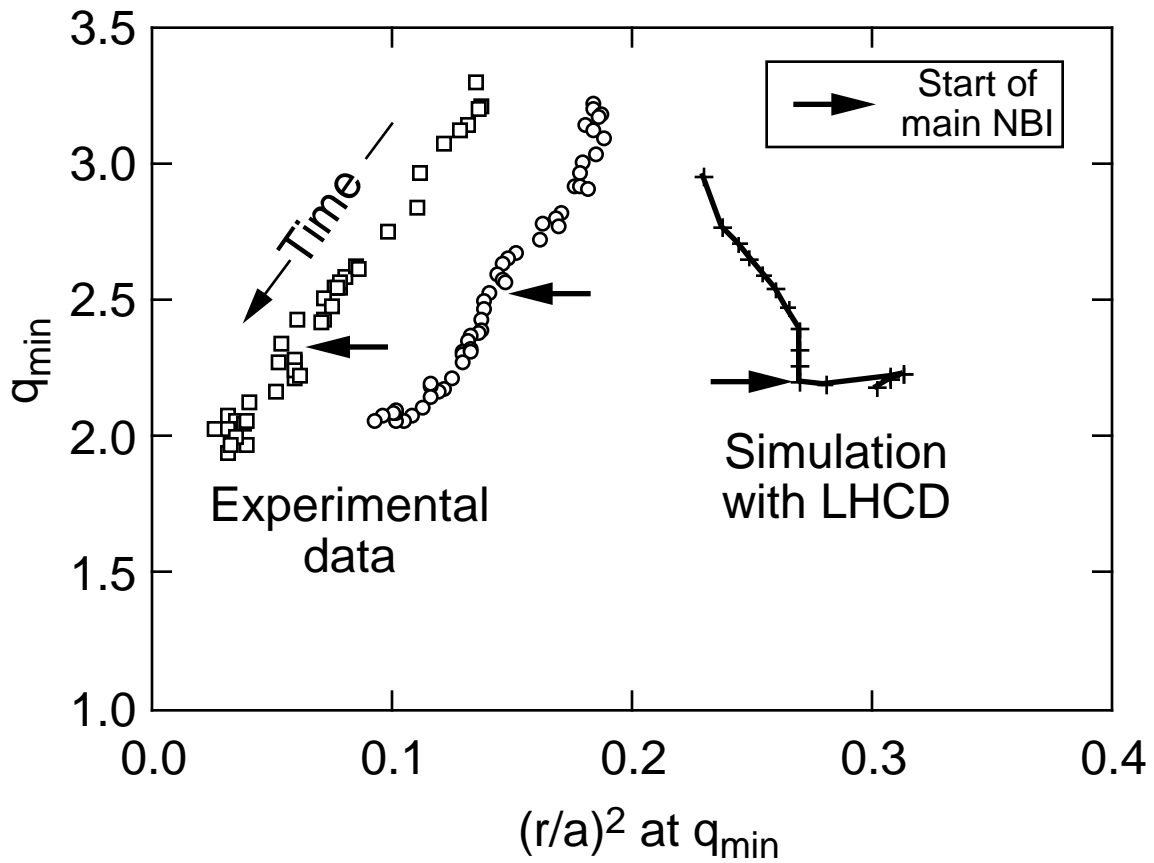
Fig. 2.16 Evolution during the NBI heating pulse of the value of q_{min} and the square of the normalized radius at which q_{min} occurs in reversed-shear shots. The measured data are from two shots with co- (circles) and counter- (squares) dominated "prelude" phases and show the range of behavior obtained so far. The TRANSP/LSC simulation is based on the co-NBI prelude with 1MW LHCD increasing to 3MW during the main NBI pulse. The LHCD maintains q_{min} above 2 and increases significantly the volume of the reversed-shear region.

been driven on-axis in D-^{4}He-^{3}He plasmas with a central density of $4 \times 10^{19}\,\text{m}^{-3}$, and a central electron temperature of 5 keV, for a normalized current drive efficiency of $0.07 \times 10^{20}\,\text{Am}^{-2}\text{W}^{-1}$. Off-axis currents of 100 kA have also been driven at r/a ~ 0.2. In this latter case, the MCCD has produced changes in the q-profile: differences of 50% in the value of q_0 are measured by the Motional Stark Effect (MSE) diagnostic between plasmas with co- and counter- MCCD [30].

For the TFTR-AP program it is proposed to modify two of the ICRF antennas to launch a toroidally directed fast wave at 30 – 33 MHz, which is predicted to undergo efficient mode conversion to an IBW in a D-T plasma at the D-T ion-ion hybrid frequency [31]. The ion cyclotron layers and mode conversion layer for the present D-^{3}He case, and for the proposed D-T case, are shown in Fig. 2.17. With the proper choice of parameters the present D-^{3}He resonance geometry can be duplicated in D-T. The problem of impurity generation with two-strap ICRF antennas operated at other than 180° phasing is well known [32], and is largely alleviated with four strap antennas since the straps are operated in 180° pairs. The proposed antenna and source arrangement is shown schematically in Fig. 2.18.

With a coupled power of 6 MW in the 30 – 33 MHz range, a centrally peaked current of about 0.5 MA could be driven by MCCD in a NBI-heated D-T plasma with a central density of $6 \times 10^{19}\,\text{m}^{-3}$ and typical TFTR profiles. By operating at 35 – 38 MHz, the MCCD would be shifted off-axis to r/a = 0.5 – 0.6, producing a total current of about 0.3 MA at the same power level. The profiles of the MCCD current are shown in Fig. 2.19. These driven currents would be used to help sustain reversed shear-current profiles established during the NBI prelude phase by inductive current ramping, as discussed in Section 2.4. Combining MCCD with the LHCD would provide enhanced capability for controlling both the magnitude and profile of the noninductively driven current.

2.3.3 Neutral-beam reconfiguration

The installation of a fifth neutral beam box, oriented to inject in the direction parallel to the plasma current, is proposed for the later phases of the TFTR-AP project. This fifth beam box, currently used as a neutral beam test stand, would be mounted on a port currently occupied by one of the ICRF antennas. It could be fitted with up to three of the six neutral beam sources now installed in the counter-injecting beam boxes. This scheme is preferred over moving one of the existing beam boxes because it minimizes the facility down-time. This modification would allow us to alter the ratio of co- and counter- directed beam sources from its present "balanced" 6:6 to a co-dominated 9:3 ratio. The principal motivation for such a reconfiguration is to increase the capability for significant beam-driven currents at high heating power. In addition, we expect a modest increase in fusion performance since τ_E appears to be maximized in plasmas with co-dominated (but not co-only) beam heating. The 9:3 beam configuration would also permit present studies of velocity-shear stabilization of transport to be extended to higher heating power, higher density, and higher temperatures.
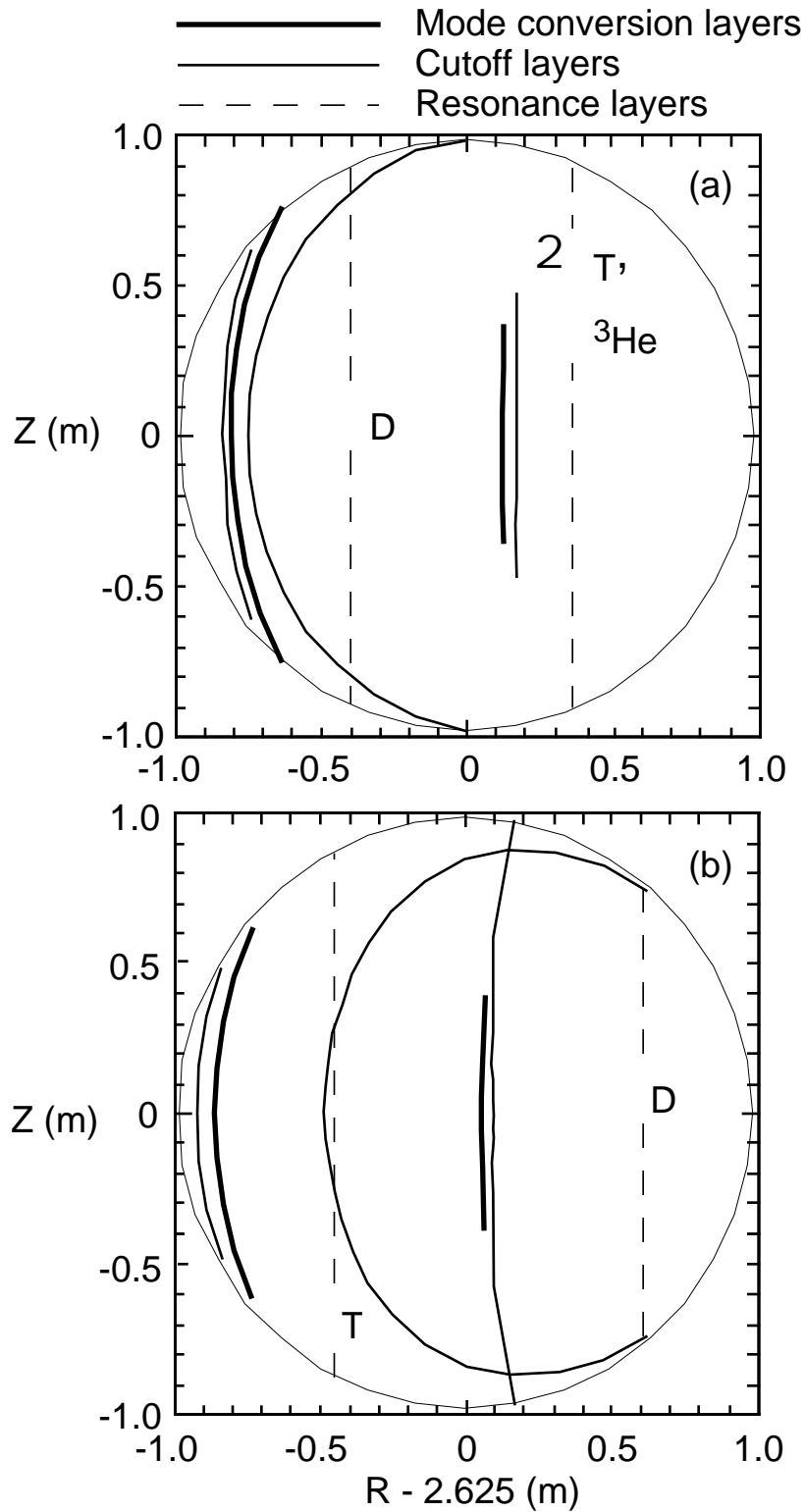
Fig. 2.17 Mode conversion schemes for generating IBW in TFTR.

(a) Scheme presently available in D-^{3}He plasmas with the 43MHz system at 72kA TF current. Due to the low reactivity of these plasmas, the effect of the IBW on the D-D fusion products can be measured only with the lost particle detectors.

(b) Scheme which could be produced in D-T plasmas at 85kA TF current (6T at 2.48m) with the ICRF system modified to operate at 32MHz. In these high-reactivity plasmas, the full range of alpha-particle diagnostics could be used.
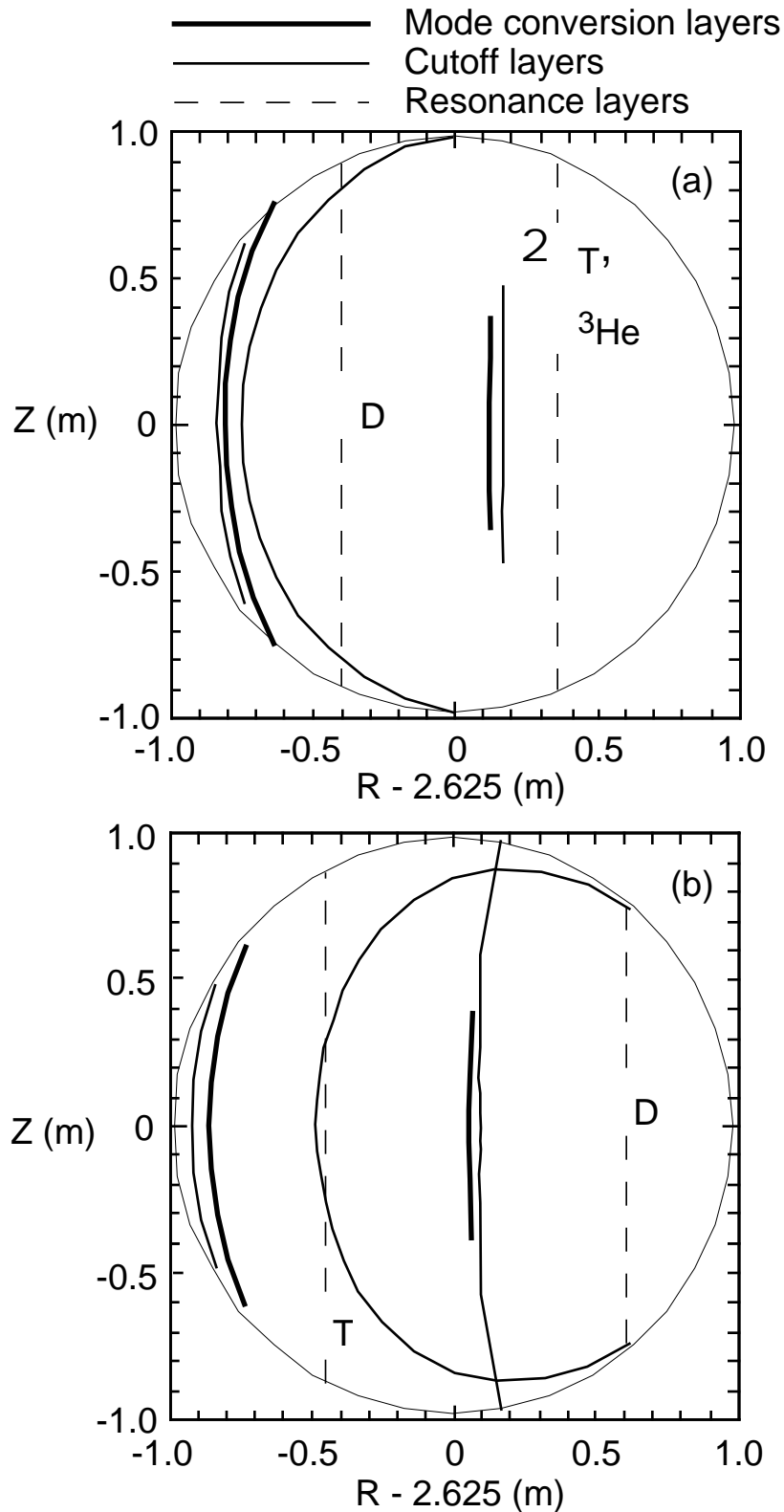
Fig. 4.9 Mode conversion schemes for generating IBW in TFTR.
(a) Scheme presently available in D-^{3}He plasmas with the 43MHz system at 72kA TF current. Due to the low reactivity of these plasmas, the effect of the IBW on the D-D fusion products can be measured only with the lost particle detectors.
(b) Scheme which could be produced in D-T plasmas at 85kA TF current (6T at 2.48m) with the ICRF system modified to operate at 32MHz. In these high-reactivity plasmas, the full range of alpha-particle diagnostics could be used.
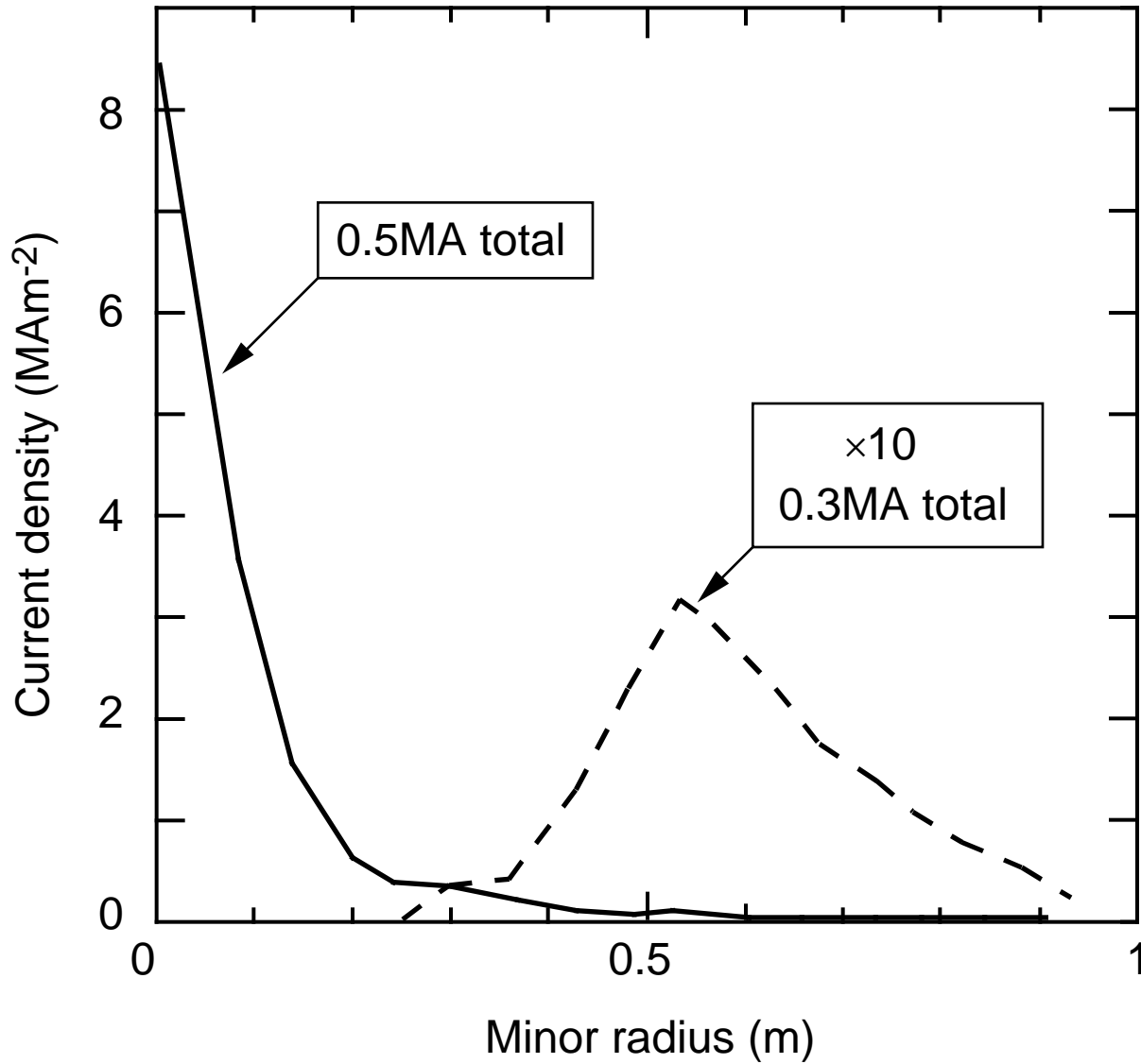
Fig. 2.19 Calculated profiles of the current driven by a mode-converted IBW in TFTR. The calculations are for a coupled power of 6MW in a D-T plasma heated by NBI with a central density of $6 \times 10^{19} m^{-3}$ and profiles typical of TFTR supershots. For central MCCD, the frequency would be in the range 30 – 33 MHz; for off-axis MCCD it would be 35 – 38 MHz.

The interaction of beam penetration and beam-ion thermalization in strongly rotating plasmas causes very significant differences in the beam-driven currents near the plasma center by co- and counter-directed beam sources. In the proposed 9:3 configuration, this difference may provide a new mechanism to control the current density profile near the plasma center, and thereby influence stability. For the toroidal rotation speeds expected in the 9:3 configuration (v = (6 – 10) × 10^5 ms^{-1}), *counter-directed beams provide 5 - 10 times more beam driven current on-axis than co-beams per unit injected power.* This surprising difference is the consequence of effects of the toroidal rotation on both deposition of beam neutrals and thermalization of beam ions in the rotating plasma frame.

Figure 2.20 shows the strong effect of plasma rotation on beam deposition, the energy density of unthermalized beam ions, and the beam-driven current. The illustrative profiles shown were computed by the SNAP transport code assuming 10 MW of beam injection at a tangency radius of ±2.60 m, using the actual measured profiles of density, temperature, and toroidal rotation speed in the beam deposition and thermalization codes. Very similar results are obtained using the actual proposed co/counter beam configuration, for which the co-beams are aimed slightly more tangentially than the counter beams. In the absence of toroidal rotation, the peakedness of the beam power deposition profile h(0) is ~4.6 for both co- and counter-injection. Co-toroidal rotation at v (0) = 6 × 10^5 m/s decreases h(0) for co-injection to 4.2, and increases h(0) for counter-injection to 6.4, due to the change of the beam neutral energy in the rotating plasma frame. Rotation also affects the birth energy of the fast ions in the plasma frame, resulting in longer thermalization times for counter-injected beam ions compared to co-injected beam ions. At the plasma center, the combined effect on beam deposition and thermalization time is striking: beam energy density (per unit injected power) is about six times higher for counter injection and the beam-driven current density is ten times higher. Integrated over the inner 0.3 m, the beam-driven current due to counter-beams is more than three times that due to co-beams.

In previous TFTR experiments, approximately 1.4 MA of beam-driven current was obtained with 15 MW of co-injected power only. Approximately 25 MW of co-power would be available in the 9:3 reconfiguration which should be sufficient to sustain more than 2 MA of beam-driven current.

The difference between the current-drive efficiencies of the co- and counter- injecting beams in strongly co-rotating plasmas can provide substantial control over the total current profile. Figure 2.21 shows the profile of beam-driven current for discharge 83546 computed by SNAP from the actual conditions obtained with a "beam-balance parameter", B_{NB} $(P_{co}-P_{ctr})/(P_{co}+P_{ctr})$, of 0.34 at a total power of 17.2 MW, compared to the projected case assuming tangentially-oriented beams at higher power, 25.2 MW, and the same balance. A second projection is also shown for reduced plasma major radius, which causes additional broadening of the co-deposited power deposition profile. Due to the improved efficiency of counter beam injection, the net beam-driven current is negative on axis, despite there being twice as much beam power injected in the co-direction compared to the counter

Power deposition h(r)

counter-
injection

co-injection

J_{NB} (MAm^{-2})

U_{NB} (MJm^{-3})

I_{NB} (MA)

SS950650

MINOR RADIUS (m)

Fig. 2.20 Profiles of beam ion parameters calculated by the SNAP analysis code for a highly
co-rotating plasma with a central toroidal speed of 6×10^5 m/s. These calculations
were performed for 10MW co (solid) or counter (dashed) D-NBI at 100kV
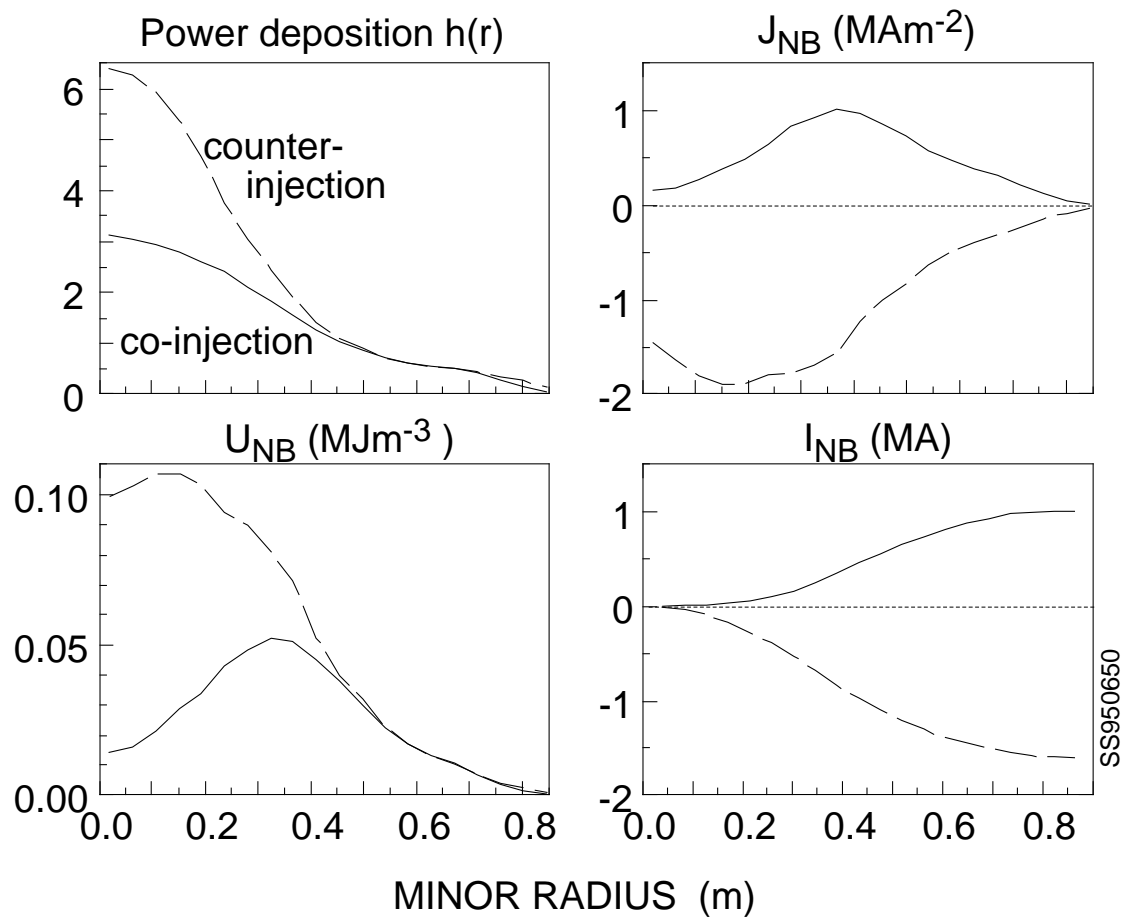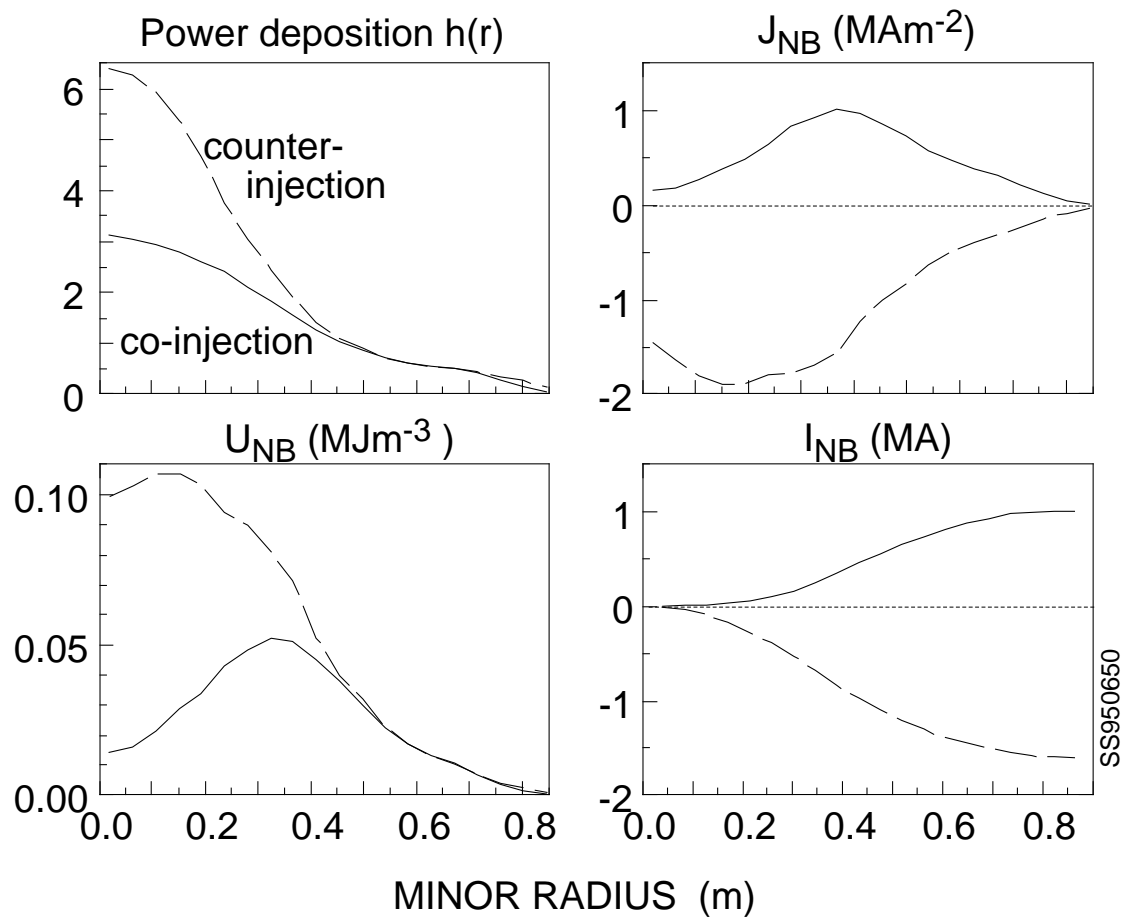accelerating voltage with an average tangency radius of 2.60m.

Fig. 4.4 Profiles of beam ion parameters calculated by the SNAP analysis code for a highly co-rotating plasma with a central toroidal speed of 6×10^5m/s. These calculations were performed for 10MW co (solid) or counter (dashed) D-NBI at 100kV accelerating voltage with an average tangency radius of 2.60m.

direction. For the projection with slightly reduced major radius, the computed beam-driven current increases from -0.9 MA/m^2 at the axis to +1.1 MA/m^2 at r = 0.5 m. The net beam-driven current is +0.8 MA, which represents 35% of the total plasma current. With the 9:3 beam configuration, it should therefore be possible to explore transport in regions of the plasma with significantly reduced magnetic shear.

Figure 2.22 illustrates the dependence of energy confinement time on the direction of beam injection in TFTR at high plasma current. The vertical axis has been scaled to remove dependencies on beam power and limiter conditioning. Maximum performance is obtained at $B_{NB} = 0.4 – 0.5$. Note that B_{NB} = 0.5 is obtained for the 9:3 beam configuration. Also shown in Fig. 2.22 is the range of the beam balance parameter that can be achieved with different numbers of operating beam sources. As expected, there is little variability in B_{NB} when all 12 sources are fired, but flexibility improves when only 11 or 10 sources are used, since one can choose to fire the co or counter sources preferentially. Thus the range of available B_{NB} decreases with increasing power. In the current beam configuration $B_{NB} = 0$ at maximum power (12 sources) which is less than optimum. As shown in the figure, operation with mixed deuterium and tritium beam sources provides slightly better control over B_{NB} than use of only one beam isotope, since the tritium beam sources deliver 25 – 30% more power than deuterium sources. With the present beam configuration (6:6), close to the optimum value of B_{NB} can be reached if the number of beam sources is limited to 10; but at full power, the optimum B_{NB} can be reached only by reconfiguring the beams. An open question is whether the effect of the balance of co and counter injection depends on the momentum or power delivered by the beams. In principal, with mixed D and T NBI, the momentum balance can be changed somewhat more than the power balance with the current 6:6 configuration. Experiments to address this issue are planned and the results from them will be assessed before undertaking the proposed reconfiguration.

Figure 2.23 presents similar analysis at $I_p = 1.5 – 1.6$ and $I_p = 2.5$ MA. Although there is considerable variability, optimum performance is still obtained for significantly co-dominated ($B_{NB} = 0.3 – 0.5$) beam injection. At lower plasma current (~1 MA), the B_{NB} for optimum performance appears to occur at more nearly balanced injection, $B_{NB} = 0 – 0.2$. Prior to 1988, good supershot performance was only obtained at low currents but the beam configuration on TFTR was 9:3. For this reason the beams were reconfigured to their present 6:6 configuration. Since then, however, techniques for producing supershots at high plasma current have been developed. Given the observed confinement dependence on beam direction at higher plasma current (which is necessary for stability against disruption at high heating power), a return to the original 9:3 configuration appears warranted to optimize high-current supershot performance. However, before undertaking such a reconfiguration, a careful assessment would be made of its possible impact on the reversed-shear regime in TFTR. The initial indications are this new, and potentially very important, regime is quite sensitive to the co- and counter- injection mix.

Present beam configuration

Proposed configuration

1.2

10 mixed D or T sources

10 mixed D or T sources

11

11

12

12

R = 2.52 m

I_{TF} = 71-73 kA

I_p = 2.0 MA

P_b = 11 - 31 MW

D^O NBI only

1.1

Normalized W_{tot}

1.0

Legend

▲ 18 ± 2 MW

✕ 20 ± 2 MW

0.9

10 D or T sources

10 D or T sources

11

11

12

12

0.8

-0.5

0.0

0.5

1.0

$B_{NB} = [P_{co} - P_{ctr}] / [P_{co} + P_{ctr}]$

SS950560bw
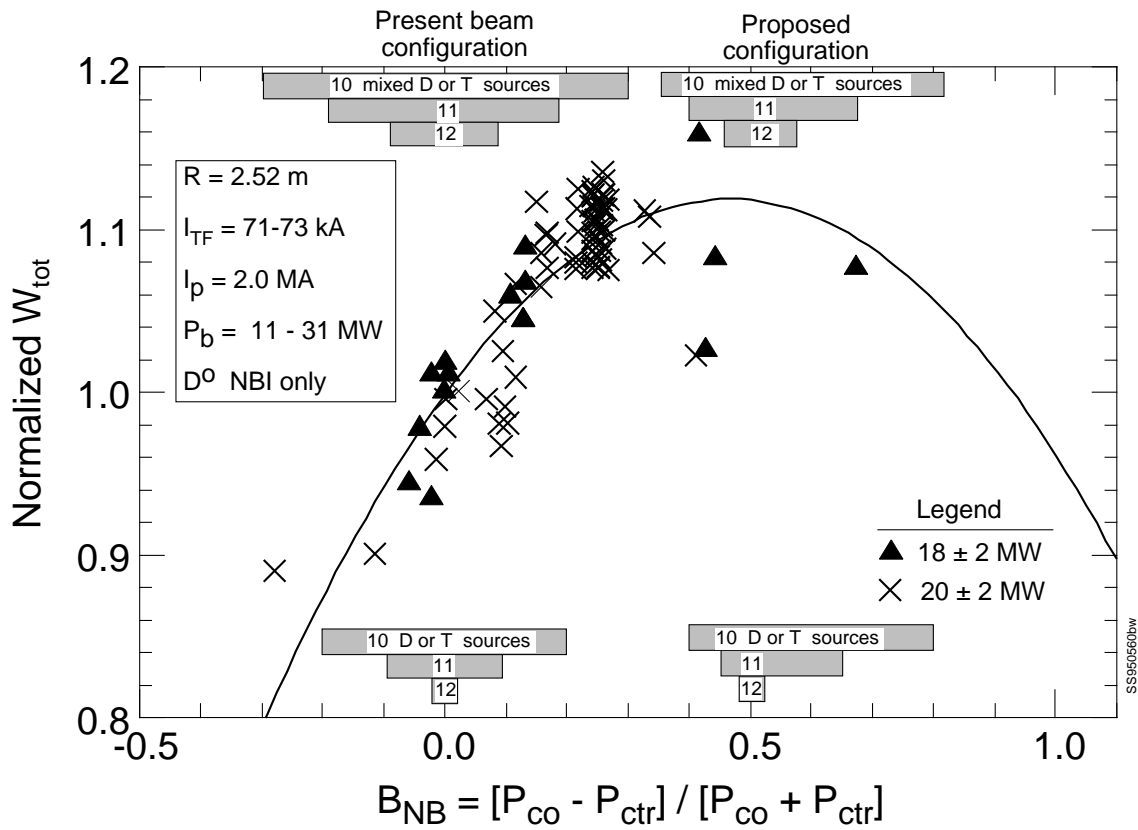
Fig. 2.22 Normalized total stored energy in TFTR supershots as a function of direction of beam injection. The vertical scale is the total stored energy after 0.45s of neutral beam heating, normalized by the observed dependence on beam power and limiter conditioning (W_{tot} $P_b^{0.93} C_{II(tgt)}^{-0.35}$). To most clearly identify the dependence on beam direction, the data shown have been tightly constrained to supershots with good limiter conditioning at fixed plasma size, toroidal field, and plasma current. The quoted range of B_{NB} with "mixed" D and T beams assumes operation with nearly equal numbers of tritium and deuterium beam sources (the difference being less than or equal to 2).

Fig. 4.6   Normalized total stored energy in TFTR supershots as a function of direction of beam injection. The vertical scale is the total stored energy after 0.45s of neutral beam heating, normalized by the observed dependence on beam power and limiter conditioning ($W_{tot} \quad P_b^{0.93} C_{II(tgt)}^{-0.35}$). To most clearly identify the dependence on beam direction, the data shown have been tightly constrained to supershots with good limiter conditioning at fixed plasma size, toroidal field, and plasma current. The quoted range of B_{NB} with "mixed" D and T beams assumes operation with nearly equal numbers of tritium and deuterium beam sources (the difference being less than or equal to 2).

The reasons for this sensitivity will also be explored thoroughly explored before committing to the reconfiguration.

2.4 Pressure profile modification techniques

In the D-T experiments, TFTR has attained the highest central plasma pressure of any tokamak. If this pressure could be extended over a larger region, substantial gains in fusion performance could be achieved. Therefore, two techniques for modifying the pressure profile are proposed as part of the TFTR-AP project. The first involves adding an antenna for direct excitation of ion Bernstein waves in the plasma. These waves have been found to create a particle transport barrier at the resonant absorption surface in experiments in the PBX-M tokamak. Such a barrier in TFTR supershots could significantly improve the central confinement which, for the ions, is determined mainly by convective losses. The second technique is to re-aim some of the neutral beam sources to broaden their heating and fueling profile. With this modification it is calculated that it should be possible to achieve a higher total fusion rate without increasing either the central pressure or its maximum radial gradient, thereby making more effective use of the available plasma volume without exceeding the stability limit.

2.4.1 Pressure profile modification through IBW heating

It is proposed to modify one of the ICRF antennas for direct excitation of ion Bernstein waves (IBW) in TFTR-AP. In PBX-M, IBW heating has been found to create a particle transport barrier in the vicinity of the absorption layer [33]. Similar observations have been made in other tokamaks, including PLT [34] and Alcator-C [35]. The formation of such a barrier in TFTR supershots could significantly improve the central confinement which, for the ions, is determined mainly by convective losses.

To launch the IBW directly, the orientation of the current-carrying straps and Faraday shield in one of the ICRF antennas must be changed. The antenn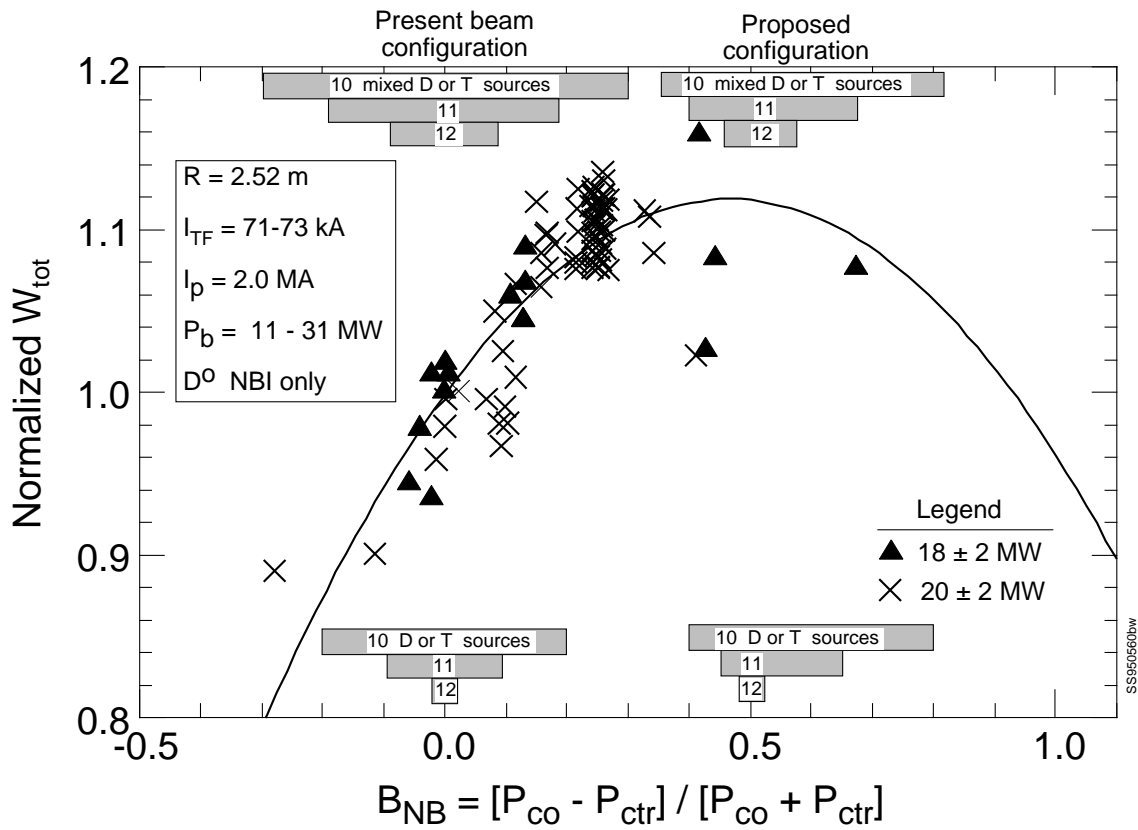a would also be converted to a 4-strap configuration. A schematic of the modified antenna is shown in Fig. 2.24. Each antenna element is energized by the existing feed-through. By changing only external elements of the RF system, the antenna current straps can be fed in-phase ($0°$ phase shift) or out-of-phase ($180°$ shift). Out-of-phase operation is attractive for reducing edge sheath effects. Two independent power sources will be used for the IBW antenna, permitting $90°$ phase shift for launching poloidally unidirectional waves. The IBW antenna straps will be housed in a box which is identical to that of the existing ICRF antenna. The rest of the system, such as the sources, transmission line, matching network and the diagnostic/control system, remains the same. For investigating control of the density profile in D-T plasmas, operation of the IBW system at $50\,$MHz (the second harmonic resonance of tritium at a magnetic field of $5\,$T) would be used. This modification would be made early in the TFTR-AP project.
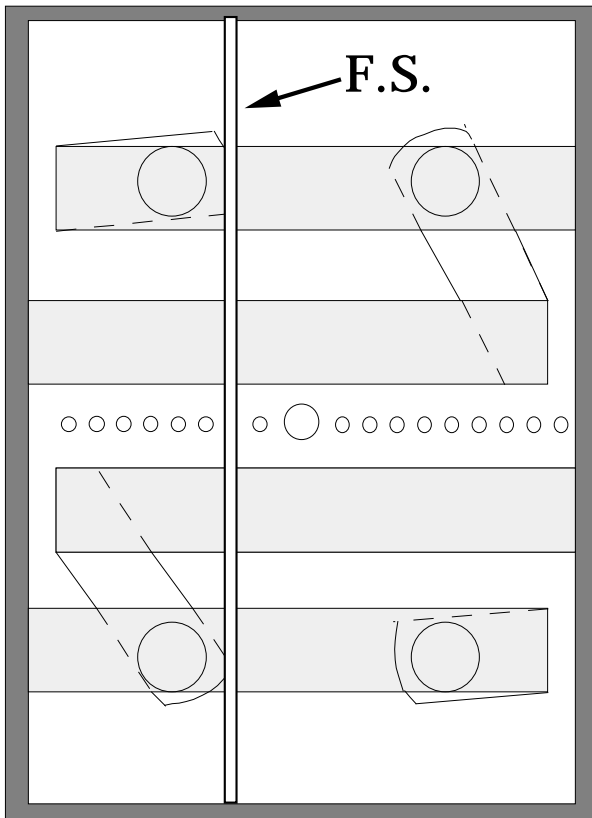
FRONT VIEW

SIDE VIEW

F.S.
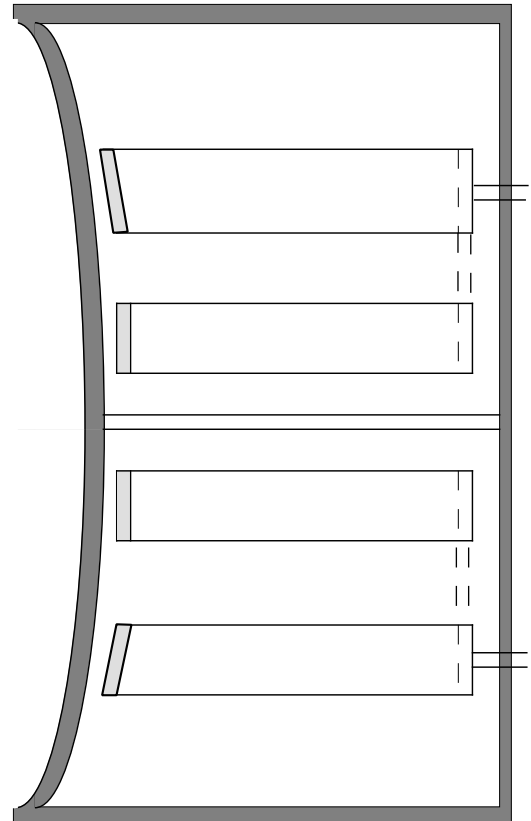
Fig. 2.24 Front (plasma) and side view of IBW antenna. Current-element sections closest to plasma are shown in light gray. One element of the Faraday shield (F.S.) is seen. Assembly box (dark gray) is identical to that of existing ICRF antenna.

In PBX-M, the application of a modest amount of IBW power, ~300 kW, into an H-mode plasma with strong NBI heating (~2 MW) caused significant peaking of the density profile and produced central densities up to 1×10^{20} m^{-3}. This mode of operation has been termed the CH-mode (Core High-confinement Mode) [33,36,37]. Detailed profile measurements indicate the formation of a transport barrier in the region of expected IBW power absorption [38]. The observations have been found to be consistent with a theoretical model based on the formation of RF-induced sheared-flow layer [39]. This model predicts that the IBW can generate, through non-linear effects, strong sheared flow near the absorption layer [40,41]. The IBW is well suited for efficient generation of such a sheared flow for the following reasons:

1. It is a high momentum content wave (short wavelength);

2. The wave electric field intensity is high (electrostatic, short wavelength);

3. There is a strong ion response (ion cyclotron range of frequency);

4. It is absorbed in a single-pass (no radially standing waves for non-zero Reynolds stress).

A comparison of the theory with the experimental data shows good agreement in terms of the required power (200 – 300 kW for PBX-M) and the location of the barrier. Typically, the sheared flow must exceed the turbulence suppression condition [42]

$$\frac{\partial V_p}{\partial r} = \frac{E_r}{B}\bigg|_{critical} \quad \frac{C_s}{L_s} \quad \frac{C_s}{R} \tag{3}$$

Where V_p is the poloidal flow velocity, C_s is the acoustic speed and L_s is the connection length.

To estimate the IBW power requirements for TFTR, a ray tracing analysis was made using TFTR high performance plasma profiles. Various cases were run to optimize the IBW-induced sheared flow location and magnitude. The non-linear equation governing the sheared flow is [38]

$$\frac{dV_p}{dr} = \frac{d}{dr}\left[(\tilde{V}_r \; ik_r) \; \tilde{V}_p \; \mu_{neo}^{-1} \right] = \frac{d}{dr} \; \mu_{neo}^{-1}\bigg|_{rays-j} a_j \; b_j \; \tilde{E}^2_j \; k_{r,j} \; sgn(k_r) \tag{4}$$

$\tilde{V}$	ion oscillation velocity vector
μ_{neo}	neoclassical ion viscosity damping frequency
a_j, b_j	ion response functions
$sgn(k_r)$	+1 for in-going waves, -1 for out-going waves

The ray-tracing code calculates the local wave electric field and the non-linear poloidal momentum drive for each ray, and then sums over all rays for all ion species. The resulting sheared flow is

averaged over the flux surfaces. In Fig. 2.25, the ray trajectories are shown for the proposed mid-plane IBW antenna. The chosen IBW configuration is heating at the $2\Omega_T$ resonance layer (~50 MHz at $B_T \approx 5$ T). The inward propagating waves (rays moving to the left) are damped locally in the vicinity of, but before reaching, the $2\Omega_T$ resonance layer. Most of the power is directly absorbed by the tritium ions. In Fig. 2.25, the calculated poloidal sheared flow profile is also shown. With a modest amount of power (~1 MW), the induced poloidal sheared flow exceeds the value estimated for turbulence suppression as indicated by Eq. 3. The antenna is designed to deliver up to 3 MW of IBW power to allow for possible experimental inefficiencies. It should be noted that if a barrier closer to the plasma edge is desired (*i.e.*, r/a ≈ 0.75), the same antenna can be used at 78 MHz (the upper range of transmitter frequency) to heat at $4\Omega_T$ for a toroidal field on axis of 4.5 T. The estimated power needed for turbulence suppression is still near 1 MW because the lower density and temperature compensate for the larger volume. A diagnostic to measure the poloidal flow velocity is planned for TFTR-AP.

The TRANSP code has been used in a predictive mode to simulate TFTR plasmas with IBW heating. These simulations involve varying the density profiles of existing TFTR supershots run in conditions compatible with additional IBW heating. The modified density profiles were chosen to be consistent with the peaking of the profiles which occurred during IBW heating in PBX-M. Similar peaking has also been seen in JIPPII-U; Alcator-C and PLT also observed increases in the overall particle confinement during IBW heating. Although in PBX-M the core ion-energy confinement was also observed to improve, the core of TFTR supershots already has good ion energy confinement so the temperature profiles were not changed for these simulations. In Fig. 2.26 we show an overlay of the original density profile for a supershot with NBI only and that of the simulated IBW-assisted case: the IBW interaction has induced a transport barrier so that more fuel ions occupy the reactive core region. Figure 2.27 shows the predicted D-T neutron rates for the two conditions together with the measured rate for the prototypical shot. TRANSP reproduces well the time evolution but slightly underestimates (by ~10%) the total neutron rate; this level of agreement is typical. The TRANSP prediction for the IBW-assisted discharge exceeds substantially, by 70%, that of the original supershot.

The ideal-MHD analysis code PEST was used to assess the stability of the IBW-assisted plasma. In both the original supershot and the IBW-assisted case, an internal kink was found to be unstable but other modes, in particular ballooning and external kink modes, were stable. In the original shot, the internal kink was not observed experimentally, however, so it was presumably stabilized by non-ideal, *e.g.* $\omega*$, effects which would be expected to operate in the IBW-assisted case as well.
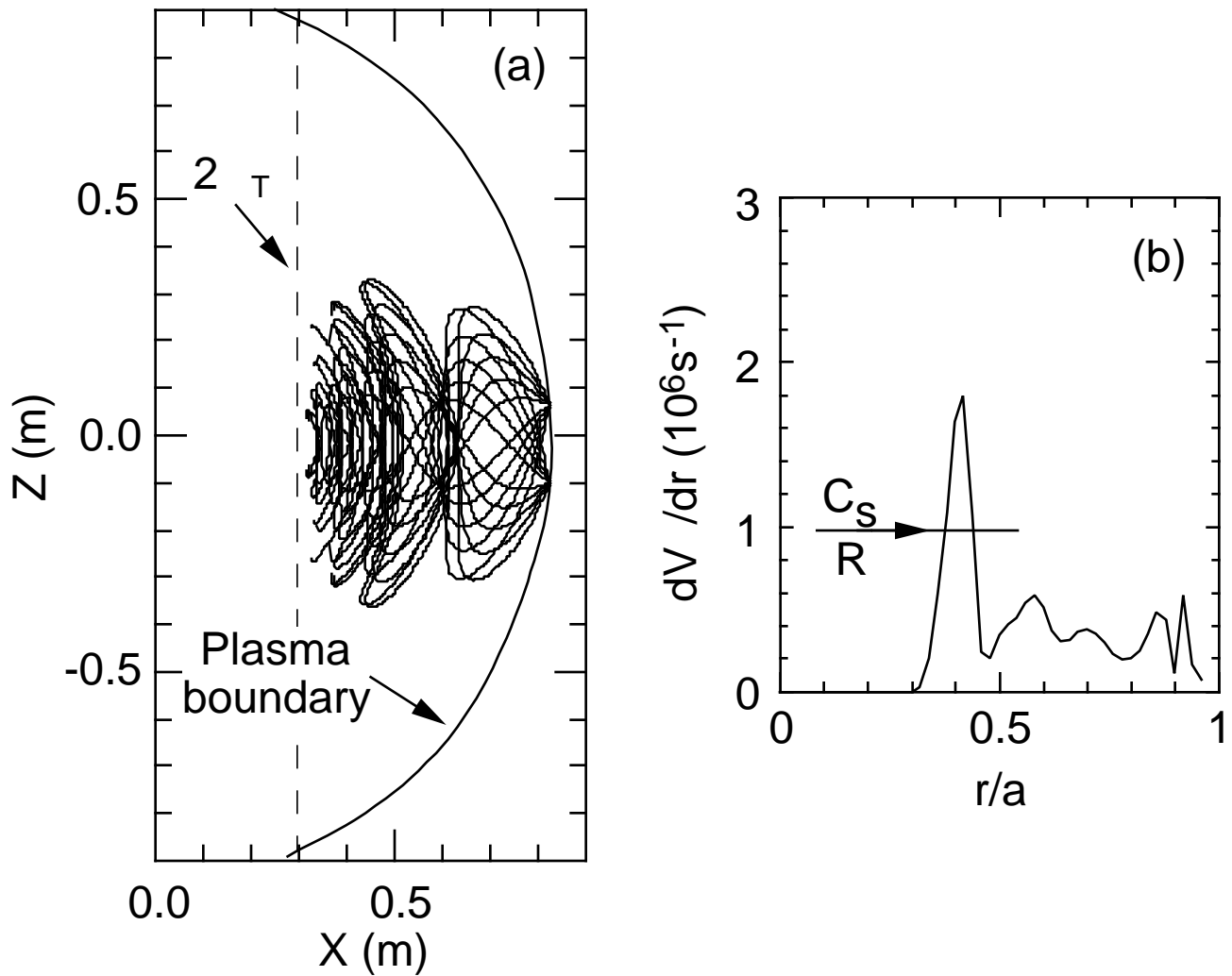
Fig. 2.25 (a) IBW ray tracing for full-bore D-T (50:50) supershot. The origin is the Shafranov
shifted magnetic axis. The IBW is completely damped before reaching the 2_T
resonance layer. Conditions: $B_T = 5.0T$, $f = 43.3MHz$, $n_e(0) = 7.8 \times 10^{19} m^{-3}$,
$T_i(0) = 20keV$, $T_e(0) = 8keV$, $Z_{eff} = 2.5$.

(b) Induced shear in poloidal flow for IBW power of 1 MW. Flow shear exceeds
C_s/R criterion for turbulence suppression., where C_s is the acoustic velocity and R
is the major radius.
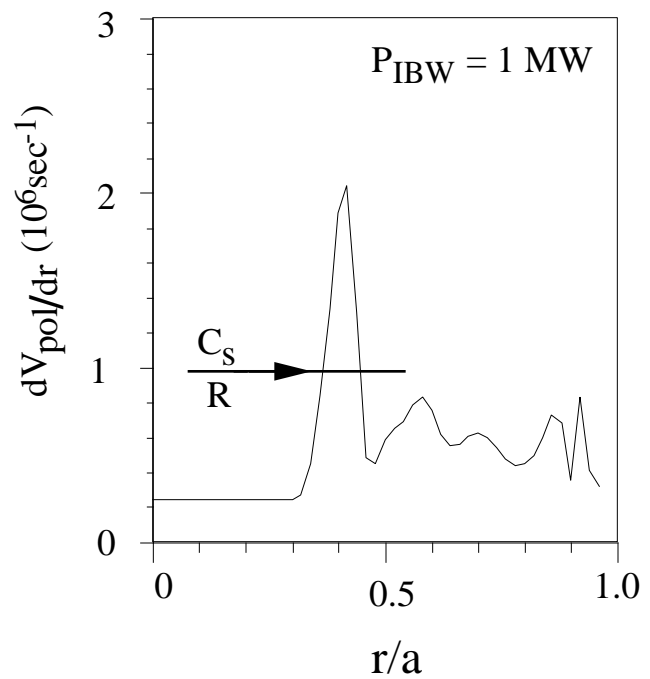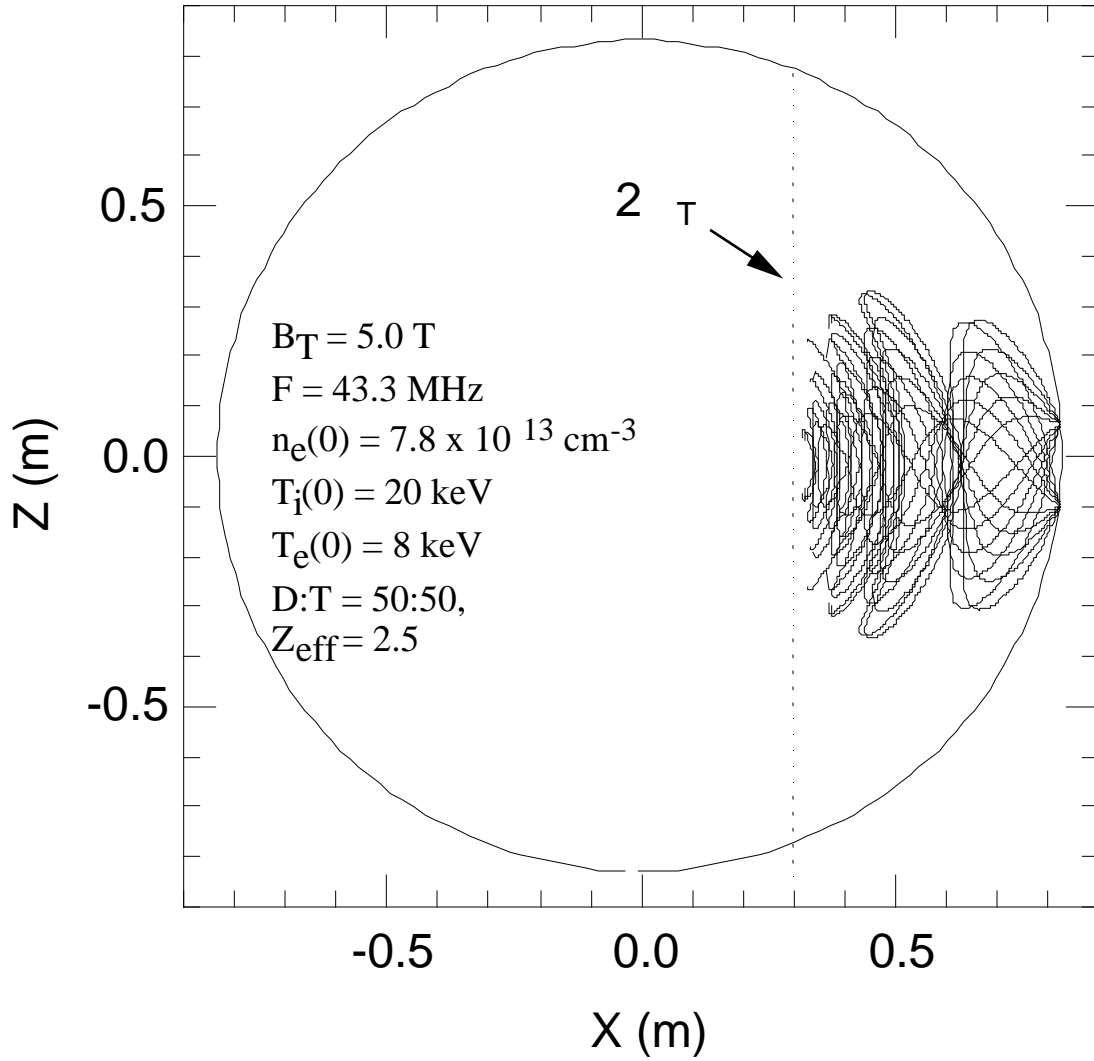
Fig. 2.7 *Top panel:* IBW ray tracing for full-bore supershot. IBW wave is completely damped before reaching $2\Omega_T$ resonance layer. IBW power applied is 1 MW.

Lower panel: Induced sheared poloidal flow exceeds C_S/R criterion for turbulence suppression., where C_S is the acoustic velocity and R is the major radius.

Figure labels (top panel):
$2\Omega_T$

$B_T = 5.0$ T
$F = 43.3$ MHz
$n_e(0) = 7.8 \times 10^{13}$ cm^{-3}
$T_i(0) = 20$ keV
$T_e(0) = 8$ keV
D:T = 50:50,
$Z_{eff} = 2.5$

Z (m)

X (m)

Figure labels (lower panel):
$P_{IBW} = 1$ MW

dV_{pol}/dr $(10^6 sec^{-1})$

$\dfrac{C_S}{R}$

r/a

Fig. 2.27   Simulation of the D-T neutron rate for a D-T supershot with the addition of a transport barrier induced by IBW heating. The simulation is based on full bore shot 74652. The larger number of particles in the core region induces a 70% increase in D-T fusion power.

With the system proposed for TFTR-AP, a clear demonstration of transport modification with IBW heating should be possible. In addition to benefits for TFTR D-T experiments, in terms of increased fusion power production, such a demonstration would have important implications for an advanced tokamak reactor. Once alpha-particle heating becomes dominant in the plasma, we will have very limited control over the heating profile, unless ways of controlling the alpha-particle transport can be developed. Thus, some control over the plasma transport will be required in order to achieve the pressure profiles necessary for maintaining plasma stability.

2.4.2   Re-aiming the neutral beams

Three of the four neutral beam injectors on TFTR are connected to the vacuum vessel through flexible bellows and can be rotated, without opening the vacuum system, to change the tangency radius of the beam axis with respect to the plasma major axis. By increasing the tangency radius of two of these movable beamlines we would achieve greater control of the neutral beam heating and fueling profiles, and therefore the pressure profile, than is currently available. This re-aiming of the neutral beams would be carried out in the second year of the proposed TFTR-AP project after assessing the capability of the IBW system to control the pressure profile.

A characteristic feature of plasmas in the supershot regime is radially peaked profiles of density, temperature, toroidal rotation speed, and pressure. This is a consequence of both centrally peaked neutral beam deposition and better confinement (lower diffusivities) near the plasma center compared to the edge. Ratios of central to volume-average values of 4.1 for n_e, 3.0 for T_e, 4.6 for T_i, 5.4 for v , 10 for total pressure, 11.5 for neutron emission and 4.6 for beam power deposition have been produced simultaneously in the supershot with the highest global confinement time, $\tau_E = 0.325$ s. Correspondingly, a large fraction of the plasma stored energy and neutron emission originate in a fairly small volume near the plasma center. For the best discharge, 75% of both the total and thermal plasma stored energy are confined in the inner 18% of the plasma volume (r/a < 0.42), while 75% of the neutron emission originates from the inner 11% of the plasma volume (r/a < 0.27).

There is evidence that pressure-gradient-driven instabilities are responsible for the disruptions which limit the fusion performance of TFTR supershots. Figure 2.28 shows the occurrence of disruptions in a plot of the Troyon-normalized- , β_N, against the peakedness of the density profile (which correlates with peakedness of the pressure profile). Values of β_N above 2.0 have been achieved in discharges with modest profile peaking, but the disruption limit decreases significantly, down to $\beta_N = 1.0 - 1.2$, in the most highly peaked discharges. However, these highly peaked supershots are precisely the discharges which attain the highest energy confinement time and Q.
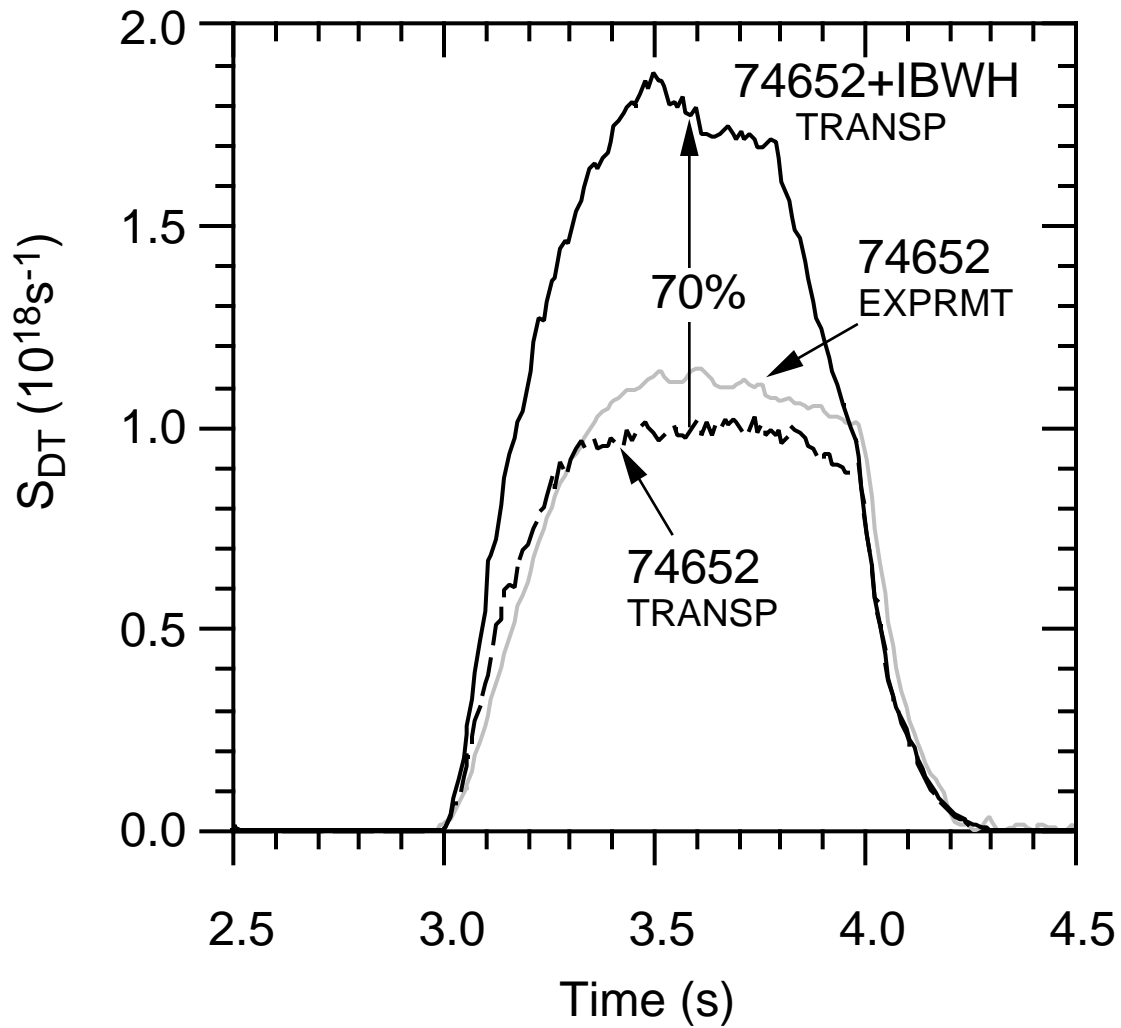
Fig. 2.   Simulation of the D-T neutron rate for a D-T supershot with the addition of a transport barrier induced by IBW heating. The simulation is based on full bore shot 74652. The larger number of particles in the core region induces a 70% increase in D-T fusion power.

These results suggest that it may be possible to significantly increase the total plasma stored energy and DT fusion power in TFTR super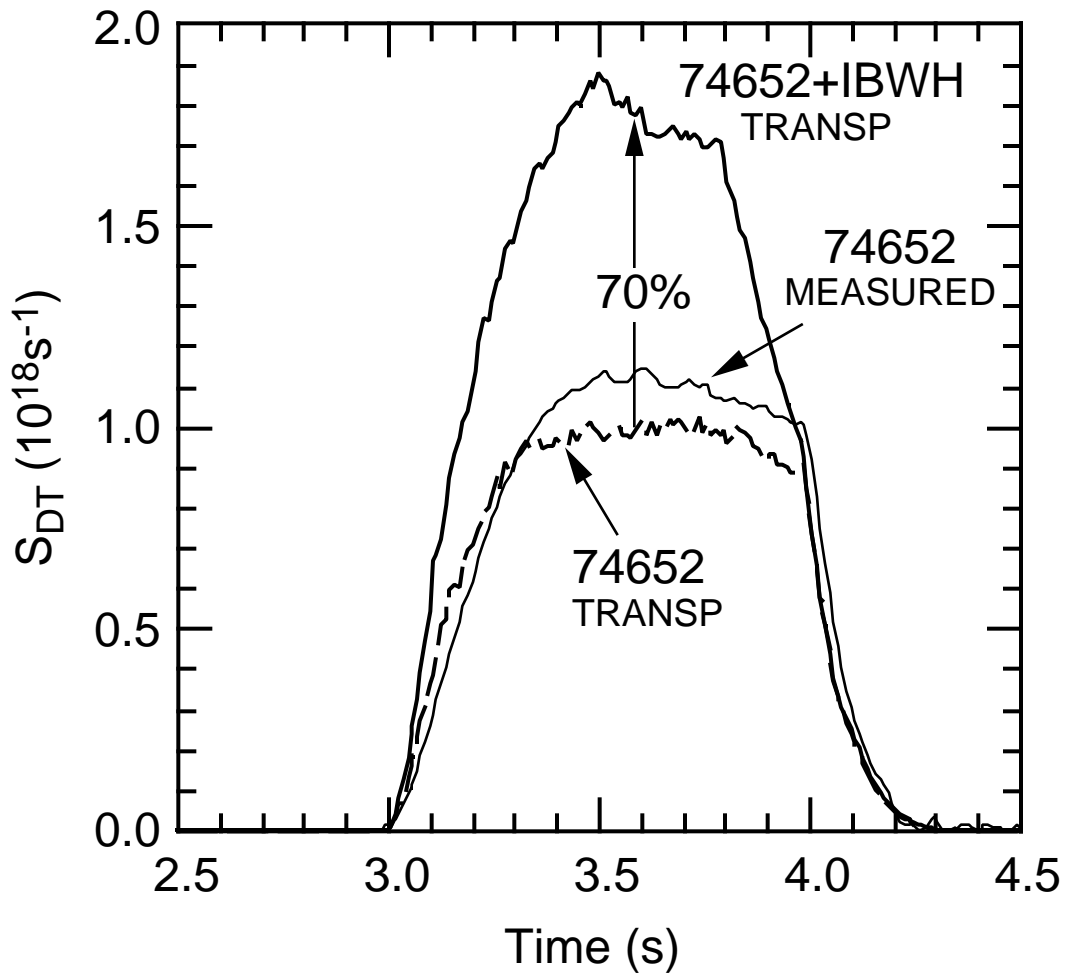shots simply by broadening the beam deposition profile. Effectively, this would increase the volume of the highly-reactive core volume, without increasing the maximum core pressure or maximum pressure gradient anywhere in the plasma. Projections based on measured transport coefficients (D_e, $_e$, $_i$,) in existing supershot plasmas suggest that increases of 30-40%, and possibly more, in the fusion power could be realized *at the same core pressure and same maximum pressure gradient already achieved,* by injecting higher beam power along a more tangential trajectory. These projections assume that the local transport coefficients for particle, momentum, and heat flow remain unchanged, so the global energy confinement decreases slightly as the beam deposition profile is broadened. Essentially, by re-aiming the beams, we hope to trade some confinement for stability against disruptions. At present, stability is the major limitation to fusion performance in TFTR.

Self-consistent calculations of density and temperature have been carried out to assess projected changes in profile shapes and fusion power yield as the beam geometry is changed. These calculations are based on transport coefficients for electron particle transport (D_e), ion and electron heat transport ($_e$, $_i$), and momentum transport ( ) in selected TFTR discharges. These transport coefficients are assumed to remain constant as the beam geometry is varied. Since the projected density and temperature profiles differ slightly from the actual operating experience, this procedure neglects possible dependence of the local transport coefficients on local density, temperature, and their gradients. However, they do represent the first-order effects of broadened density, temperature and pressure profiles as the beams are injected less deeply into the plasma. The objective of these calculations is to estimate how much the fusion power could be increased in TFTR as the volume of the highly-reactive core region of the plasma is increased by broadening the beam power deposition, without exceeding currently-achieved central pressure values or maximum pressure gradients.

Figure 2.29 illustrates a typical projection of fusion performance with more tangentially-oriented beams. The solid lines represent the actual performance of discharge 83546 with 17.2 MW of neutral beams with the current average tangency radius of 2.08 m. The dashed lines show the projected performance using the D_e, $_e$, $_i$, inferred from the original data, assuming that the co-beams are re-aimed to an average tangency radius of 2.61 m, and that the number of sources injecting is increased to raise the heating power by 50% to 25.7 MW. Note that plasma parameters such as the central density and temperature change very little. The profiles are broadened slightly, due to the broadened beam deposition profile. The plasma with tangential beams achieves 21% higher fusion power despite having ~5% less central pressure, and ~10% smaller maximum pressure gradient. This suggests that the fusion power could be increased ~30 – 40% over the reference shot if the assumed heating power
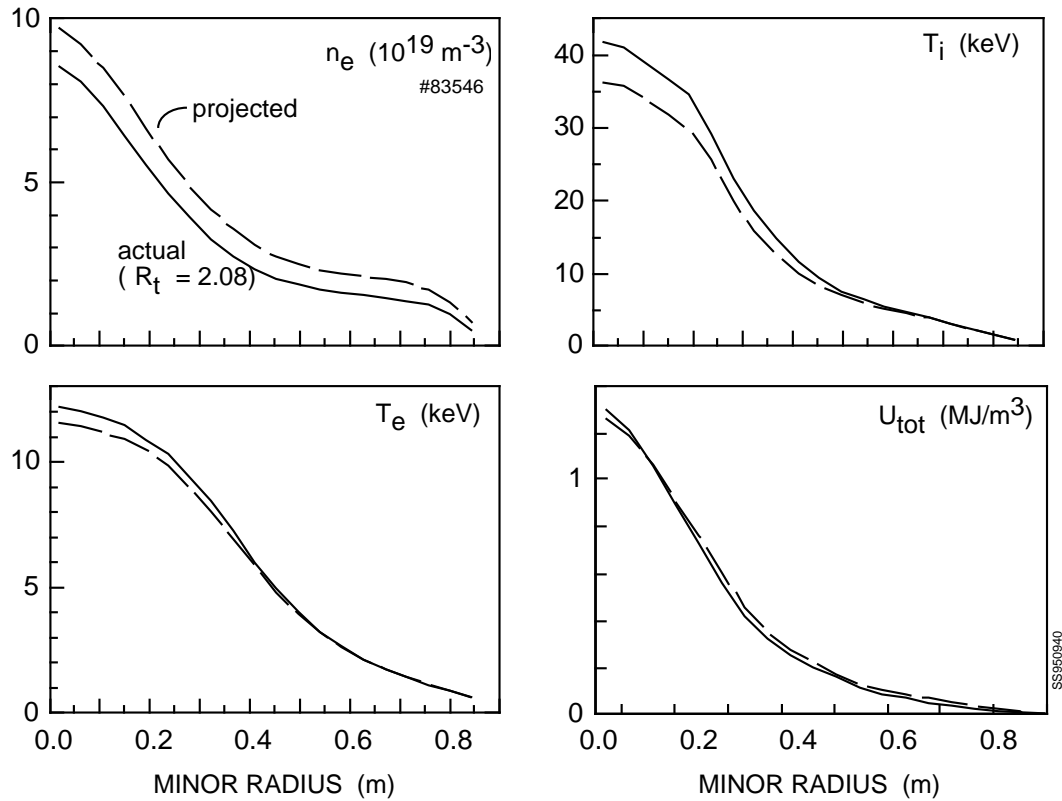
Fig. 2.29 Comparison of the profiles of several important plasma parameters as calculated by the SNAP analysis code for different aiming of the neutral beams in TFTR. The base case (solid) uses the present aiming and the measured conditions of shot 83546 while the projected case (dashed) uses the "tangential" beam aiming with the same inferred transport coefficients.

were increased to exactly match the maximum pressure gradient of the reference shot. Somewhat larger improvements are expected for plasmas operated at smaller major radius (R = 2.45 m), because the effect of beam re-aiming on the beam deposition profile is larger for smaller major-radius plasmas.

Another important benefit of re-aiming the beams more tangentially would be the capability to study heat and particle confinement in supershot plasmas in the absence of strong core heating and fueling by the neutral beams. As we have seen in Sec. 2.2, a fundamental issue for extrapolating supershot plasmas to a larger tokamak is whether one needs core-localized particle and heat sources to sustain the favorable energy confinement, which would require high-voltage, high-power beams, making it difficult to achieve high Q. By contrast, if the favorable confinement in supershots is governed primarily by high ratios of T_i/T_e, as suggested by the theory of electrostatic micro-turbulence, it may prove feasible to achieve supershot confinement by generating gradients of temperature and pressure in the outer 1 – 1.5 m of an ITER plasma with conventional beam technology. The proposed beam re-aiming on TFTR would allow us to explore this possibility.

2.5 Improved limiter conditioning schemes

The success of the TFTR D-T program has been due in part to the development of methods for conditioning the carbon limiter. The ability to reduce the recycling of deuterium and tritium at the limiter surface and to suppress influxes of carbon and residual hydrogen from the limiter material are crucial to obtaining the peaked profiles, enhanced confinement and high D-T reactivity of the supershot regime in TFTR. In particular, lithium coating has extended the plasma current at which supershot characteristics are obtained to 2.7 MA, thereby increasing the   -limit and allowing us to make use of the enhanced confinement at the full neutral beam power available in D-T operation. At present the lithium is introduced by injection of small solid lithium pellets, either into the ohmically heated phase of a discharge immediately before neutral beam heating, or into a preceding discharge. The injected lithium rapidly leaves the plasma and appears to be deposited non-uniformly onto the carbon limiter through the plasma scrape-off layer. The evidence from a series of experiments in TFTR suggests that the beneficial effects of lithium coating could be increased if more lithium could be deposited. This can be seen in Fig. 2.2 which shows the peak D-T fusion power as a function of heating power for various levels of lithium conditioning. Furthermore, it appears to be beneficial to deposit lithium in the regions of the limiter contacted by the scrape-off plasma during the neutral beam heating (these regions are not the same as those contacted during the ohmic phase due to changes in the plasma shape as its energy increases). The recent success in producing a global confinement time above 0.3s in a supershot is a result of developing pre-conditioning sequences of ohmically heated discharges which contacted the limiter in different regions.

The lithium pellet injector currently in use was originally developed as a diagnostic tool and is not ideal for this coating process. In particular, it is limited to injecting a maximum of four pellets into a single

plasma discharge and its repetition rate, coupled with restrictions on the discharge length, is too low to allow more than two pellets to be injected into the highest current plasmas. Modifications to the injector can be made to increase its repetition rate and capacity. Preliminary designs have also been made for an injector tailored to this purpose.

New ways of depositing lithium, for example by evaporation from a probe introduced into the edge plasma, are also being considered and developed. In PBX-M [43] and the Tokamak de Varennes [44], coating of the first wall by boron evaporated from a solid target by the plasma has proved successful in improving discharge performance. A modification of this technique could be used for lithium coating in TFTR. Another potentially powerful technique would be to use repetitive laser ablation of a thin lithium film to provide a controllable, quasi-continuous source of lithium at the plasma edge. A prototypical system has already been developed for the ASDEX-Upgrade tokamak at the Max-Planck Institut für Plasmaphysik, Germany.

The high level of control for the plasma-wall interaction necessary for the best performance in TFTR requires extensive cleanup after major disruptions. Since a part of the TFTR-AP project will be directed to operation at high   where disruptions are likely, schemes to assist in and shorten the disruption recovery process are being developed. These include the ability to perform glow discharge cleaning with a short turn-around time, and, possibly, the deposition of a coating material such as boron which is known to assist in removal of oxygen impurities, a major plasma contaminant following disruptions.

2.6 Studies of MHD activity and disruptions in reactor-like conditions

In order to forecast confinement characteristics in future tokamak experiments, a major issue is how MHD behavior is likely to scale with key plasma parameters such as collisionality. In particular, the properties of the fundamental modes, generally those with low toroidal and poloidal mode numbers, will be influenced by whether the "collisionless" layer width, δ_C, exceeds the resistive layer width, δ_R. Taking δ_C to be the acoustic gyroradius $\left(\rho_s\right)$ and the usual estimate for the resistive layer width [45] the "collisionless MHD" criterion can be expressed as

$$\nu_{*e} < \frac{q\hat{s}n}{\varepsilon^{3/2}} \sqrt{\frac{M_i}{m_e}} \beta_e^{1/2} \left(\frac{\rho_S}{r_S}\right)^\alpha \tag{5}$$

where n is the toroidal mode number, $\alpha = 1$ for $n = 1$ and $\alpha = 1/2$ for $n \geq 1$, r_s is the radial location of the reference rational surface, β_e is the electron beta, $\hat{s} \equiv rq'/q$ is the magnetic shear parameter, ε is the local inverse aspect ratio, and $\nu_{*e} \equiv \nu_{ei} qR/\varepsilon^{3/2} \upsilon_{Te}$ is the banana regime collisionality parameter.

For typical parameters in TFTR and in reactors such as ITER, $n = 1$ modes will be "collisionless" according to Eq. (5). In considering MHD phenomena, the normalized gyroradius, $\rho^* \equiv \sqrt{T}/aB$

where a is the minor radius, should also be considered, since some theories [46], which are supported by TFTR data, indicate that ω_* and FLR effects are important. Although the collisionality criterion of Eq. 5 can be satisfied in smaller, lower field devices, it would be in a plasma regime where ρ^* would be very far from that in a reactor.

For n 1 modes, collisional effects may still dominate, even in TFTR. This is especially true for reversed magnetic shear where $\hat{s}$ can be very small over a significant radial extent of the plasma. TFTR has demonstrated the capability to access these reversed-shear regimes and can generate valuable information on the associated MHD characteristics in the TFTR-AP experimental program.

In addition to its capability for operating in a wide range of plasma regimes, which will be further expanded by the proposed equipment modifications, TFTR has excellent diagnostics for MHD phenomena. For example, the two toroidally separated electron-cyclotron-emission polychromators for measuring perturbations in the radial profile of the electron temperature have provided unsurpassed resolution of the structures preceding high- disruptions and other more routinely occurring phenomena. Furthermore, the multichannel reflectometer and beam-emission spectroscopy diagnostics are providing extensive information both about micro-turbulence and its relationship to transport and about coherent MHD structures in the core of the plasma.

During the experiments to optimize the D-T fusion performance in TFTR, a substantial body of data has been gathered about MHD activity occurring in the core of high pressure plasmas and, particularly, about the precursors and mechanism of the disruptions that can terminate such plasmas [19]. These data and the operational experience concerning disruptions in TFTR are important to ITER, which will be operating in a very similar regime to TFTR in terms of central pressure and magnetic field and can tolerate very few disruptions at full parameters due to stresses on the structure and damage to plasma facing components. One interesting observation concerns disruptions in D-T H-mode plasmas in TFTR. In these plasmas, the ELM activity has been found to be much stronger than in equivalent D-only plasmas and disruptions have occurred when there was an apparent coupling of these large ELMs to internal "fishbone" activity [47]. This unusual phenomenon could have a major impact on the proposed ITER operating scenario.

The dependence of the characteristics of high- disruptions on toroidal field has been investigated in TFTR. In a controlled experiment, disruptions at the -limit were produced with NBI heating at toroidal fields of 2 T and 5 T with plasma currents, scaled to produce similar edge q, of 1 MA and 2.5 MA, respectively. The current profile was somewhat more peaked in the low field shot, possibly consistent with the slightly higher normalized- reached at low field. The thermal pressure was slightly broader at low field than at high field, but the fast ion pressure was more peaked, giving a similar pressure profile at high and low field.

The disruption at high field and current, which has been extensively studied in TFTR [19,48], occurs in three stages. In the first, low (m,n) global modes grow at rates $10^3 - 10^4 \, s^{-1}$. The global modes, in some cases, trigger moderate n $(10 - 20)$ ballooning modes. This first stage ends in a partial quench of ion energy and a quench of the electron temperature. During the second stage, locked modes, possibly generated during the initial thermal quench or growing out of the $n = 1$ precursor kink, often appear. Impurities, resulting from the heat deposition on the limiter, enter the plasma and begin to cool it. The second stage ends in a global reconnection of magnetic flux possibly involving an $(m,n) = (1,1)$ internal mode, as in the high density disruption. This leads to a complete electron and ion thermal quench, followed by the slower current decay, in the third stage.

At the low toroidal field (2 T) the approach to the -limit was characterized by the growth of locked modes. Above $_N = 2.3$ (higher than was obtained at high field) a locked mode would appear and grow through the beam phase. The plasma then typically disrupted after the end of NBI. Thus, there appear to be differences, both qualitative and quantitative (in particular, an apparently higher $_N$ limit) between the disruption characteristics observed at low and high magnetic fields in TFTR.

These studies would be continued during the proposed program to increase the fusion performance with the goals of characterizing reactor-relevant operational limits and, if possible, to identifying suitable precursors, either in terms of detectable MHD activity or possibly in terms of combinations of measurable parameters which will define the disruption boundaries. Some success in avoiding high- disruptions has already been achieved in TFTR by implementing a feedback system to reduce the neutral beam heating power in real-time when $_N$ approaches a preset limit. Recent analysis of the TFTR database [49] has shown that an improvement in the reliability of disruption avoidance afforded by this system could be achieved, without unduly lowering the $_N$ limit and thereby restricting the maximum performance, if a real-time measurement of the pressure profile peakedness could be provided to this feedback system. It is proposed to develop such a measurement and to upgrade this feedback system during the TFTR-AP project.

3. Alpha-particle Physics

3.1 Projections of alpha-particle parameters achievable in TFTR-AP

Table 3.1 compares the maximum parameters of the fusion alpha-particle population already achieved in the TFTR experiments with those projected for the TFTR-AP project and those expected in ITER. The TFTR parameters have been calculated by the TRANSP code in which the energetic alpha-particles are assumed to slow down classically on the thermal plasma species and to experience only classical losses on unconfined orbits. The projections to TFTR-AP assume that the tokamak is operated at its current maximum ratings and that the application of the techniques described in Sec. 2 is successful in raising the global -limit by about 50% over present supershot limits while maintaining the present level of confinement. We believe these to be realistic goals.

	TFTR achieved	**TFTR-AP** projected	**ITER** nominal
P_{DT} (MW)	7.5	20	1500
$\dfrac{n_\alpha(0)}{n_e(0)}$	0.3%	0.5%	0.2 %
$R\ \beta_\alpha$	0.02	0.04	0.06
$\dfrac{v_\alpha(0)}{v_{Alfvén}(0)}$	1.6	1.6	1.3

Table 3.1. Parameters of the energetic fusion alpha-particle population achieved in a quies-
cent TFTR supershot (shot 76770) and those projected for TFTR-AP during an
extension of D-T operation together with the nominal values for ITER.

3.2 Interactions of alpha-particles with MHD instabilities and magnetic ripple

Although the neoclassical confinement of alpha particles and other high energy particles is better understood than many aspects of tokamak physics, there remain several areas in which further research is necessary and in which TFTR could make valuable contributions. These include ripple-induced stochastic particle loss, modification of alpha-particle distributions due to repeated sawteeth, sawtooth stabilization, the possible excitation of toroidal Alfvén eigenmodes (TAEs), fishbones and other MHD modes by high energy particles, nonlinear saturation of the TAE, and MHD-induced ripple trapping. The physics of some of these processes is not well developed. These phenomena are sensitive to the q-profile, particle distributions and MHD amplitudes and frequencies, for which TFTR has comprehensive diagnostics.

The TFTR DT experiments have greatly stimulated the development and refinement of alpha particle theory, in the areas of both single-particle effects, *e.g.* magnetic ripple losses, and collective alpha instabilities, *e.g.* toroidal Alfvén eigenmodes. These developments have already been directly useful in the ITER design process. However, more benchmarking of the theory against experimental results clearly remains to be done. One of the major goals of the TFTR extension is to continue and extend this cross-checking of alpha particle theory and experiment.

A unique and crucial advantage of TFTR for studying alpha-particle physics is the availability of several specialized alpha-particle diagnostics [50]. These were developed over the past 10 years in anticipation of the TFTR DT run and include measurements of both confined alpha particles, through single and double charge-exchange reactions, and of the alpha particles escaping from the plasma on unconfined orbits which intercept detectors near the wall. These diagnostics, which have already produced groundbreaking results, will continue to be improved to provide critical tests of alpha particle theory. In particular, the effects of MHD activity and alpha-particle instabilities on alpha-particle transport and loss can be measured and checked against the theoretical models of these processes. Understanding of these transport processes will allow a more reliable calculation of the alpha heating for ITER, *e.g.* the effect of sawteeth on the radial distribution of fast alpha particles.

The losses of energetic fusion alpha-particles from DT plasmas have been measured by four energy and pitch-angle resolving particle detectors mounted near the vacuum vessel wall at 20°, 45°, 60° and 90° below the outboard mid-plane, *i.e.* in the direction of the ion- B drift. Scans of the plasma current have shown that in MHD-quiescent plasmas, the alpha loss rate and pitch angle distribution at the 90° detector scale as expected for the prompt loss of particles born on unconfined orbits. This is shown in Fig. 3.1. However, for the detectors nearer the mid-plane, the first-orbit loss model does not adequately fit the data. Collisional and stochastic orbit losses in the toroidal field ripple may provide an explanation of these data and specific experiments to test these theories have been proposed which would be carried in the TFTR extension.

Stochastic ripple loss of alpha particles is a concern for reactors and avoiding such loss leads to expensive design choices in ITER. Recent work with TFTR indicates that collisionality can also play an important role in augmenting stochastic ripple loss [51]. Refinement of the theory of ripple-induced stochastic transport and its testing against experimental data would facilitate the design of future machines.

The healthy and successful interaction between theory and experiment in alpha-particle physics can be seen in the development of TAE physics. In the early work of Fu and Van Dam [52] and Cheng [53] a simplified theory of local stability, including only electron Landau damping, suggested that TAEs would be highly unstable for the anticipated TFTR D-T alpha particle parameters. These theoretical analyses stimulated experiments in TFTR [54] and DIII-D [55] which showed that a TAE could indeed be destabilized by the energetic ion populations created either by NBI or ICRF heating. The initial D-T
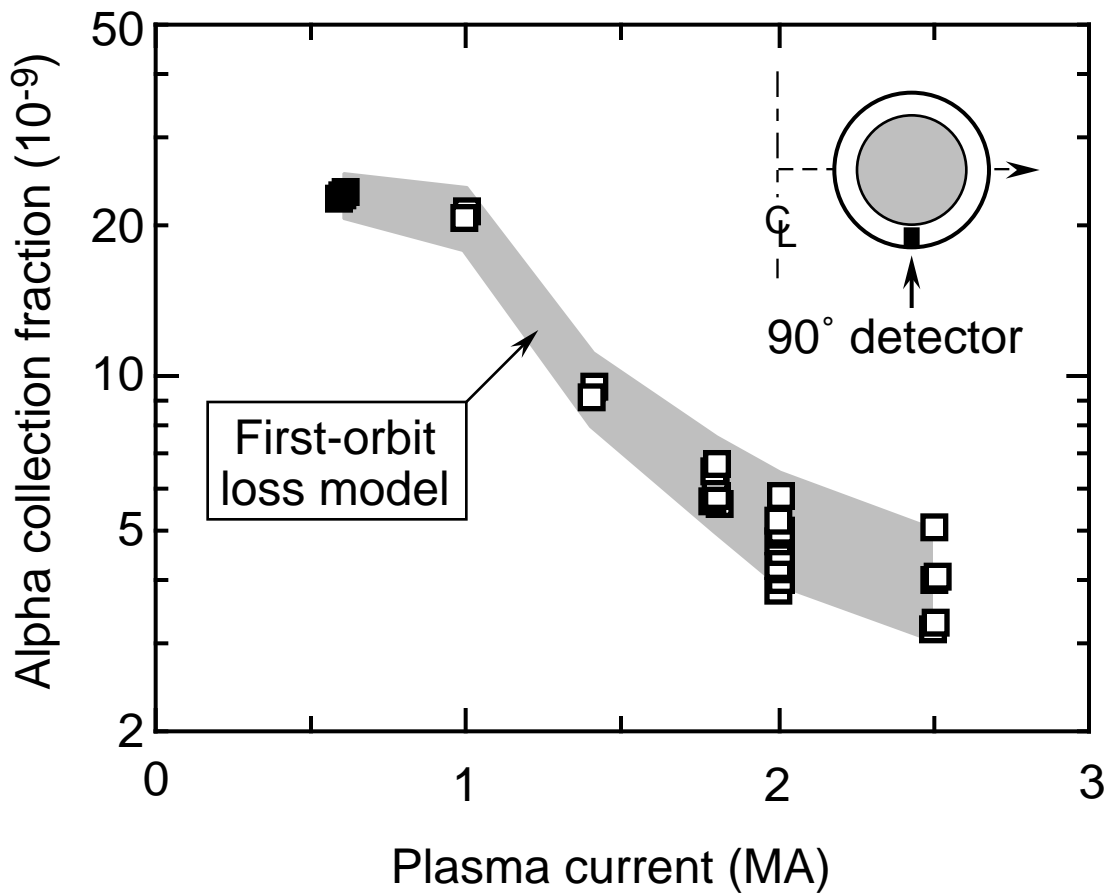
Fig. 3.1 Dependence of the loss rate of energetic alpha-particles on the plasma current. The location of the detector is indicated in the inset. The shaded region shows the loss rate calculated by an orbit-following code. The data were normalized to the calculation at 0.6MA (solid points) where all trapped alpha-particles are lost.

experiments in TFTR, however, showed no signs of instability in the TAE frequency range and the alpha-particle loss rate remained a constant fraction of the alpha production rate as the alpha pressure increased, suggesting that deleterious collective alpha instabilities were not being excited. The development of a more complete theory [56,57] has since shown that although TFTR achieves levels of the alpha-particle driving terms comparable to those of a reactor, the damping of the TAE in supershot conditions is generally stronger than the alpha-particle drive.

Bursts of alpha-particle loss are sometimes correlated with MHD activity in TFTR. In general, the losses are similar to those previously reported for energetic charged fusion products in D-only plasmas [58] and represent only a small fraction of the alpha population. However, at major disruptions, losses of energetic alphas estimated to be up to 10% of the alpha population have been observed to occur in ~2 ms during the thermal quench phase while the total current is still unperturbed. These pre-disruption losses are observed mainly on the 90° detector. It is important to identify the mechanism of these losses and to quantify their scaling and potential impact on first-wall components in a reactor so that appropriate design criteria and/or avoidance mechanisms can be developed.

The energy distribution of the alpha particles confined in the plasma has been measured for the first time in TFTR [59]. Using a diagnostic developed in collaboration with General Atomics and the Ioffe Institute, St. Petersburg, Russia, alphas in the range 0.5 – 3.5 MeV have been detected through conversion to neutral helium by double charge-exchange in the high-density neutral cloud surrounding ablating lithium and boron pellets. The pellets have been injected after the end of NBI, to improve their penetration, but before the alpha population had decayed. An example of a measured spectrum is compared with the TRANSP calculation in Fig. 3.2. In this MHD-quiescent plasma, the calculated and measured spectra show good agreement. This diagnostic has also detected a significant spatial redistribution of intermediate-energy alpha particles following a sawtooth, as shown in Fig. 3.3.

The alpha population in the lower energy range 0.1 – 0.6 MeV has also been detected by absolutely calibrated spectrometry of charge-exchange recombination emission [60]. In quiescent plasmas, the intensities of the detected signals are within a factor 2 of calculations by TRANSP, as illustrated in Fig. 3.4. This figure also shows that, following a sawtooth crash, the low-energy alpha-particle distribution becomes quite distorted. These effects of sawtooth relaxations on the spatial and energy distributions of the alphas are not well described by applying the Kadomtsev interchange prescription which has successfully modelled the thermal response to a sawtooth. Since alpha-particle orbits average over field perturbations, a fluid approach cannot be expected to be adequate but no appropriate alternative theory exists at present. Currently the alpha-particle profiles used to calculate stochastic ripple loss in ITER assume that no mixing takes place. Improved understanding of the effects of sawteeth on the alpha particles could impact calculated ignition margins, as well as limits on the toroidal field ripple allowable for ITER.

Figure 3.2

Figure 3.3

Figure 3.3

Apart from its effects on the alpha particles, the sawtooth oscillation tends to flatten the density and temperature profiles of the fuel ions leading to lower fusion reactivity for a fixed total plasma energy content. Furthermore, the effects of the sawtooth generally extend over an increasing region of the plasma as the edge q is reduced, which is required for a high β-limit. Operation at low q without sawtooth oscillations would provide advantages for reaching ignition. TFTR already has the capability to operate in regimes, including supershots and ICRF-heated plasmas, where the sawtooth is suppressed. The $m = 1$ mode responsible for the sawtooth is believed to be stabilized by nonlinear diamagnetic effects [61] in supershots or by a population of trapped high-energy particles [62] in ICRF-heated plasmas. Stabilization of the sawtooth in plasmas with a significant alpha-particle population through a combination of these effects could be systematically explored in TFTR.

Recently in TFTR it was discovered that the TAE and, indeed, other high-frequency MHD modes, can induce ripple trapping of high energy particles [63]. This process can lead to intense local fluxes which could be damaging to the first wall of an ignited tokamak such as ITER. Detailed comparison with experiments could improve modelling to allow reliable predictions for future machines.

Ignition devices depend crucially on the behavior of alpha-particle excited TAE modes. If TAEs with multiple toroidal mode numbers of sufficient amplitude are excited, large scale stochastic loss of alpha-particles could result. Theory will soon be capable of modelling this process, and comparisons with experimental TAE results are essential to complete understanding. The critical question is whether saturation of the modes occurs below the threshold for stochastic alpha-particle loss. Data from TAE modes destabilized by a high-energy tail from ICRF or NBI heating would provide cases to test and improve theories. Other MHD modes near marginal stability can be excited by high energy particles and could be important in a reactor. These include the Kinetic Ballooning Mode and Ellipticity-Induced Alfvén Eigenmode, and probably others.

Although alpha-driven TAEs appear to be stable in TFTR D-T experiments so far, it is possible that these modes could be excited deliberately by external driving mechanisms to study the effect of the modes on the alpha particles at present levels of performance. It would be possible to modify the external circuitry of existing ICRF antennas to resonate in the Alfvén range of frequencies, typically 0.2 – 0.5 MHz in TFTR. The ability to excite these modes externally would allow detailed measurements of their damping mechanisms to be made.

3.3 Alpha-particle physics in advanced D-T plasma regimes

The advanced D-T plasma regimes available on TFTR include high-performance discharges with high q(0), reversed magnetic shear and high edge-shear. Each of these configurations appears to have advantages with respect to plasma confinement and the β-limit which are attractive for reactor design. However, each will also have a potentially different threshold for alpha-particle induced instabilities such as the TAE, which can depend sensitively on the q and pressure profiles. Thus a goal of the

extended D-T run will be to evaluate the alpha-particle stability in each of these advanced tokamak configurations, in order to insure that the potential advantages are not offset by decreased alpha-particle stability.

An example of decreased stability for an alpha-driven mode in an advanced tokamak configuration is the core-localized TAE discovered by Fu *et al.* [64]. This mode can exist for relatively broad pressure profiles if the magnetic shear is small or negative and is predicted to have stability thresholds much lower than the conventional global TAE because it is localized near the center of plasma where the destabilizing drive is largest. Recently, in deuterium plasmas with H-minority ICRF heating at low field, B ≈ 3T, and relatively low q, q = 4 – 4.5, such a core-localized TAE was detected by the microwave reflectometer, as shown in Fig. 3.5. It has been predicted that an alpha-driven version of this instability can appear in TFTR plasmas with broad pressure profiles and reversed shear. D-T experiments are needed in this regime to test the theory of this mode.

The stability of TAEs in ICRF-heated D-T plasmas is also an important area for investigation. It was recently observed [65] that the TAE activity in ICRF-heated D-T plasmas is stronger than in comparable D-only plasmas. This is shown in Fig. 3.6. These data provide the first experimental evidence for a collective effect of the alpha particles in a D-T plasma. The synergistic effect of alpha particles and ICRF-driven ions on the TAE may be important for ITER where ICRF heating may be the principal heating mechanism.

Another issue for advanced tokamaks concerns the need to control the plasma pressure profile to avoid low-frequency MHD instabilities [22]. However, the pressure profile which is optimum for plasma-driven MHD ballooning or kink stability may not be optimum for alpha-particle stability. The effect of alpha particles on the β-limit is also critical for advanced tokamak schemes. Experiments by collaborators from Columbia University have already begun to search for the effects of alphas in high-β_p D-T plasmas at values of the Troyon normalized β, β_N, up to 3.2 and fusion powers up to 7 MW. Separate experiments by the DIII-D/Irvine group have begun to search for the alpha-driven "Beta-induced Alfvén Eigenmode" (BAE) seen with NBI ions in DIII-D at high β [66].

In addition to these tests of alpha-particle stability in advanced tokamak regimes, there is also a need to examine the single-particle alpha confinement and loss in these discharges. For example, the effect of stochastic TF ripple diffusion is expected to depend sensitively on the q(r) profile, such that flatter q profiles characteristic of the high q(0) regime should have lower alpha ripple loss. Experiments to test this theory using the confined and lost-alpha diagnostics have just begun.

The radial profiles of thermalized alpha particles, the helium ash, have been measured in TFTR by comparing charge-exchange recombination line emission from helium in otherwise similar DT and D-only plasmas [67]. As shown in Fig 3.7, for supershots, the initial measurements have been found to be consistent with TRANSP modelling for the helium profile based on transport coefficients that had
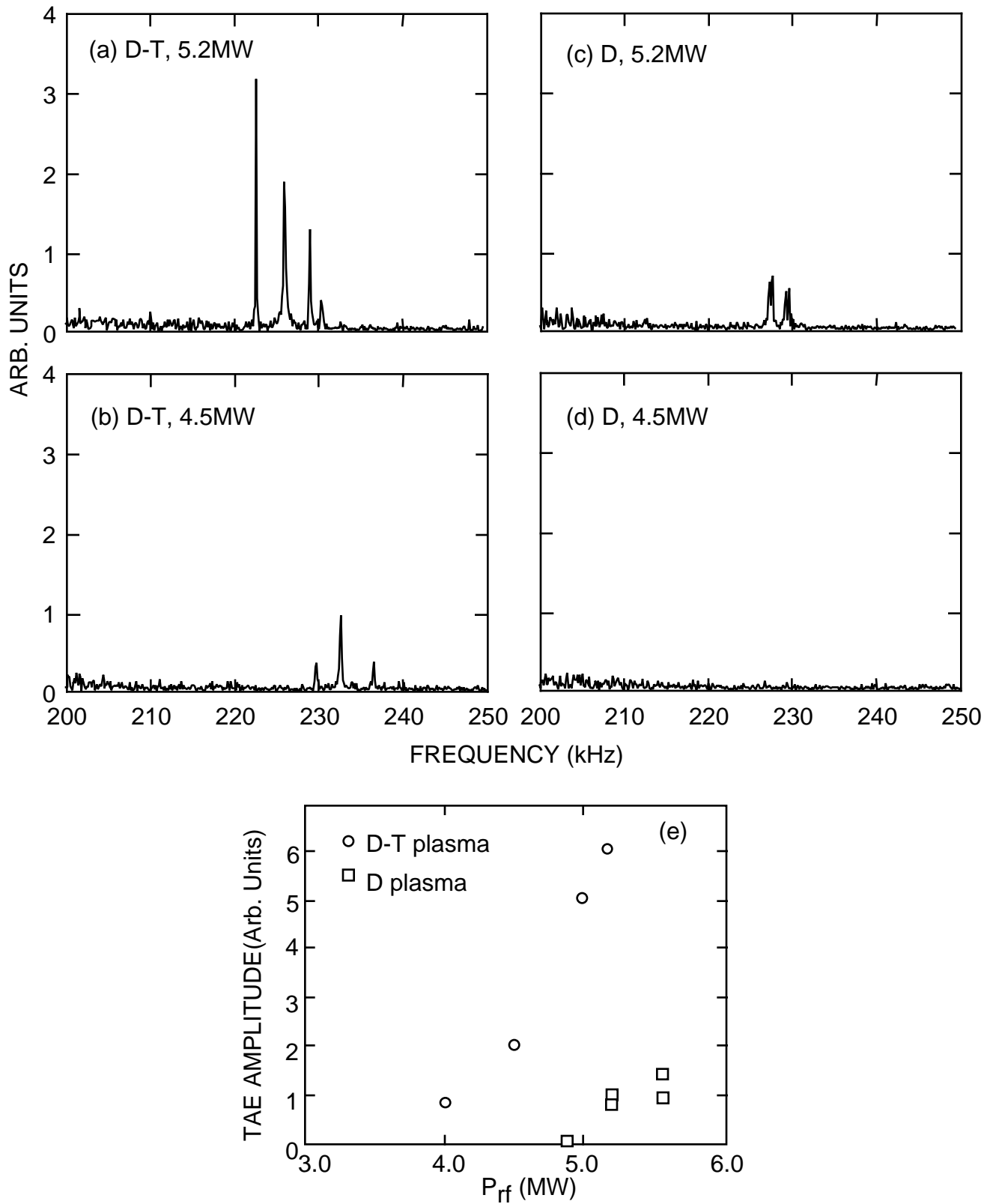
Fig. 3.6   Comparison of fluctuations detected by the Mirnov coils in the TAE range of
frequencies during combined ICRF and NBI heating of D-T and D-only
plasmas. The ICRF power threshold of the TAE is reduced and its amplitude
increased in the D-T plasmas.
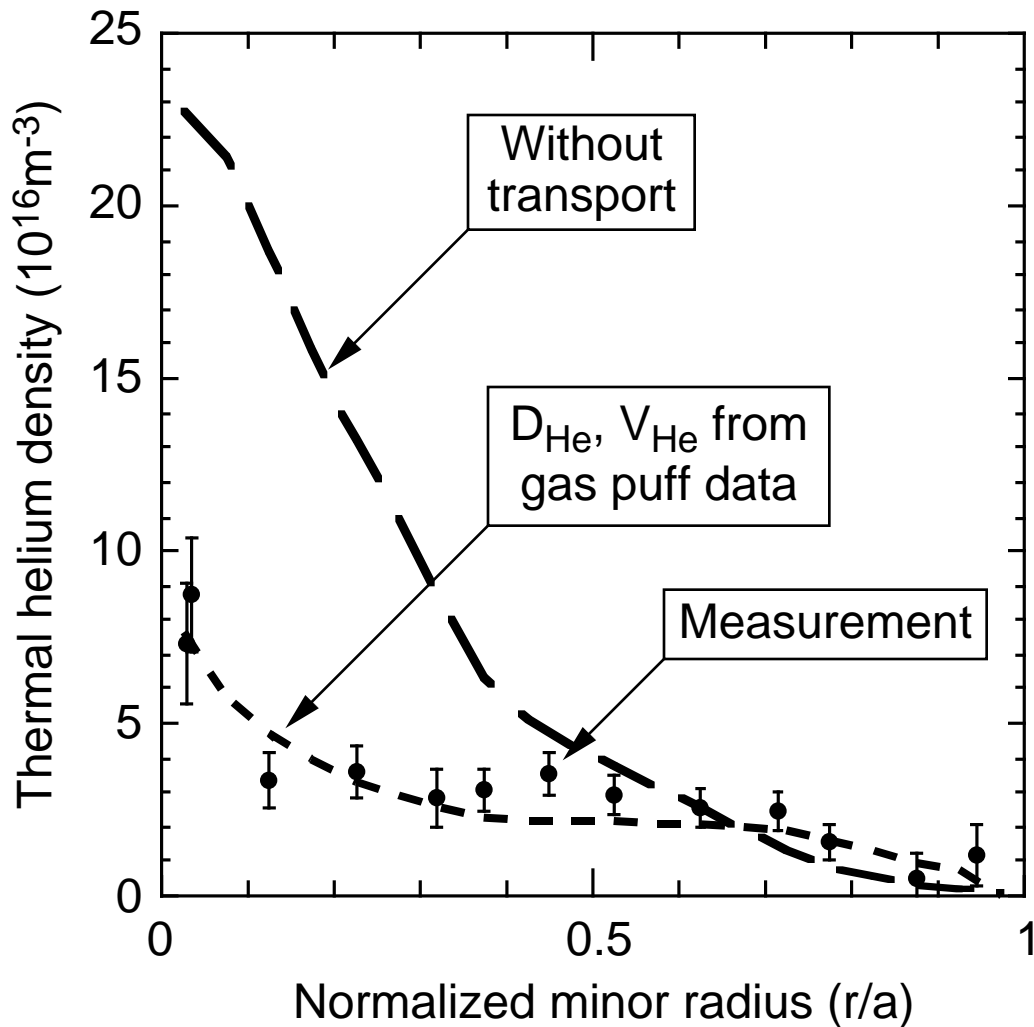
Fig. 3.7 Comparison of the radial profile of the thermal helium ash, measured by charge-exchange recombination spectroscopy, with calculated profiles for two different models of the helium transport. It was assumed either that there was no radial transport of the helium or that the helium diffusivity and radial pinch velocity were the same as had been deduced from measurements of the time evolution of the helium profile following small gas puffs.

been previously determined by using external helium gas puffs [68]. With these same transport coefficients, helium ash accumulation would not quench ignition in ITER provided the density of helium at the plasma edge can be controlled. However, the reversed-shear plasmas in TFTR have been found to have a significantly reduced particle diffusivity in the core region. It is important to extend the helium-ash transport measurements to these plasmas to ensure that the benefits of this reduced transport, in terms of fueling and heating requirements, are not outweighed by an unacceptable level of helium-ash accumulation in an ignited plasma.

3.4 Alpha-particle heating experiments

Evidence for heating of the electrons by the energetic alpha particles has been gained from the TFTR D-T experiments. In the plasmas with the highest fusion power, the potential alpha-particle heating of the electrons has so far amounted to about 5% of the total power flow through the electrons, although, in the core of the plasma, r/a ⪍ 0.25, the fraction has reached 15%. Thus, very careful measurements have been necessary to detect this heating. The situation is complicated by the apparent dependence of the energy confinement on the average mass of the hydrogen isotopes in the plasma. This dependence, which was observed in the first D-T experiments [7] and has since been studied in dedicated experiments [69,70], is manifested as an increase in both the ion and electron temperatures as tritium is substituted for deuterium NBI at constant total heating power, regardless of the fusion alpha-particle population produced. The evidence for alpha-particle heating has been found by comparing the electron temperature for D-only and mixed D-T NBI in ensembles of discharges closely matched in heating power and global confinement time, making use of the intrinsic variability of the confinement time with the limiter conditions. When the electron temperature profiles, measured by electron cyclotron emission spectrometry, are averaged over such ensembles, the profile of the temperature difference between the D-T and D plasmas matches that expected for alpha-particle heating. This is shown in Fig. 3.8

The possibility of measuring the effects and efficiency of alpha-particle heating in TFTR would be improved substantially if the fusion power density could be increased relative to the external heating power density at the plasma center and maintained for a longer period. As we have seen in Sec. 2, there are several promising techniques for improving both plasma confinement and stability in TFTR and the production of $15 - 20\,\mathrm{MW}$ of D-T fusion power is possible with the available NBI power if present levels of confinement can be achieved in regimes in which the β-limit can be increased by about 40%.

3.5 Controlling alpha-particle thermalization

In a D-T tokamak reactor, one fifth of the fusion power is produced in the form of energetic alpha-particles which can be confined in the plasma and their energy used to heat the fusion fuel. In present reactor designs, it is expected that the alpha-particles will collisionally slow down on the electron
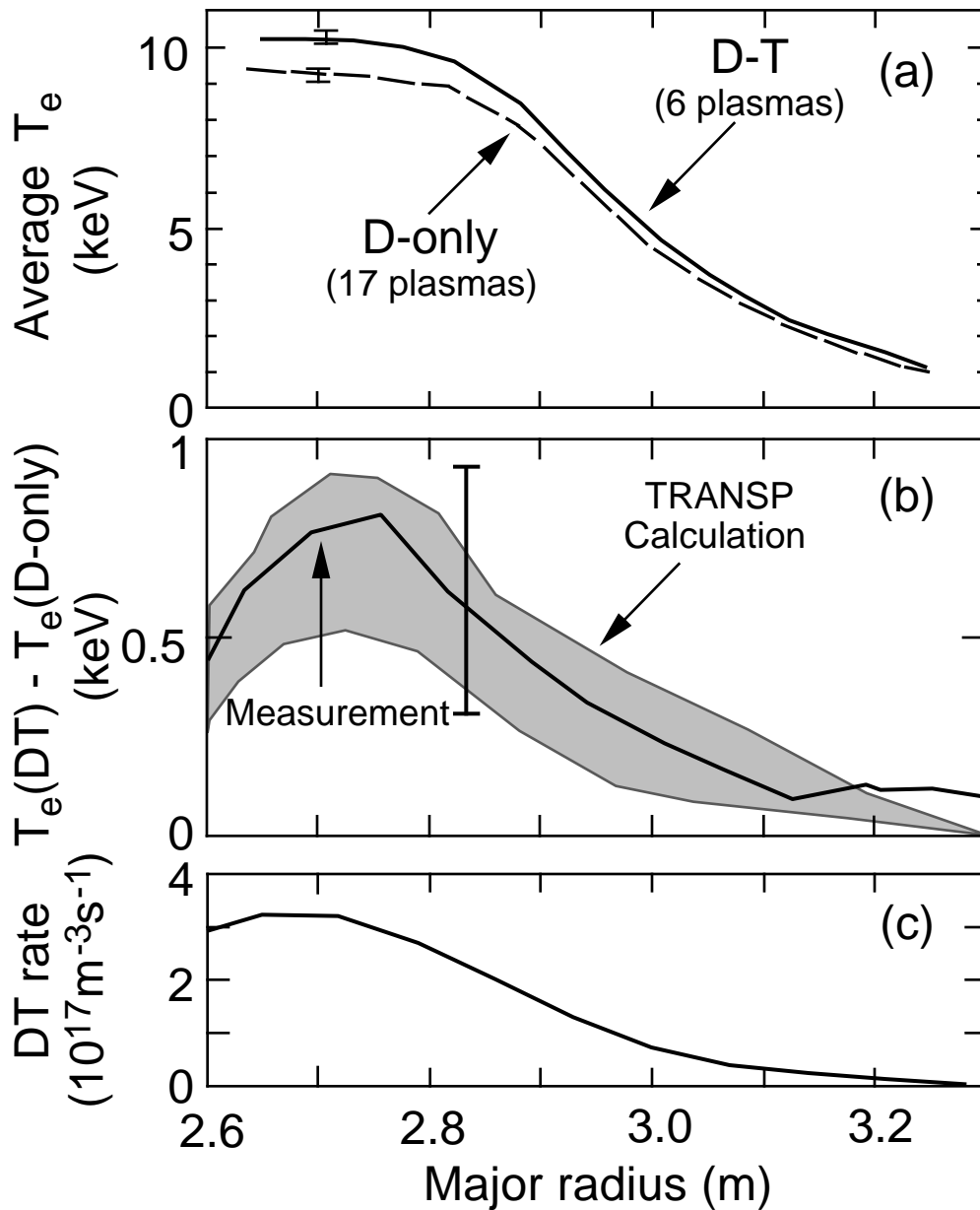
Fig. 3.8 Evidence for alpha-particle heating of the electrons in TFTR D-T plasmas.

(a) Measured electron temperature profiles 0.6s after the start of NBI heating averaged over ensembles of 17 D-only and 6 D-T plasmas. The discharges were matched for similar average heating powers (24.2MW D-only, 24.7MW D-T) an confinement times (0.15s D-only, 0.155s D-T).

(b) Measured difference in the averaged electron temperature profiles between D-T and D-only plasmas compared with the range of TRANSP calculations of the expected difference for these conditions in the D-T plasmas.

(c) Radial profile across the outer midplane of the D-T reaction rate per unit volume obtained by Abel inversion of data from the 10-channel array of collimated neutron detectors.

population, which will subsequently thermalize with the ion population. If this coupling of the alpha-particle power to the background plasma can instead be mediated with the aid of wave-particle interactions so that alpha-particle power is coupled *directly* to ion heating instead, then a higher fusion power density and hence more economically attractive reactor concept would result. Such *control* over the alpha-particle power is the aim of recent proposals for alpha-particle channeling by Fisch and coworkers [71], and could form the basis for a hot ion mode in a tokamak reactor driven by alpha power rather than auxiliary heating power. The physics basis of alpha-particle channeling has already undergone preliminary investigation in TFTR, and can be further tested in a high-reactivity D-T plasma with suitable modifications of the ICRF antennas and transmitters.

The mechanism of alpha-channeling relies upon the amplification of a wave at the expense of the alpha-particle energy. Amplification of the wave would occur if there is a population inversion in the alpha-particles along the wave diffusion path, where the diffusion path points from high energy alpha-particles in the plasma center to low energy alpha-particles at the plasma periphery. The wave need not be absolutely unstable. Instead, it could act as a catalyst, with growth due to the alpha-particles offset entirely by damping on the ions, or it might be convectively amplified by the alpha-particles and then heavily damped by the ions. Such a wave would have to be excited in the tokamak, since growth of the wave from noise would be limited. If a significant fraction of the alpha-particle energy is extracted, then the alpha-particle is displaced radially many gyroradii from its birthplace in the plasma core. Therefore alpha-particle ash removal is a byproduct of alpha-particle channeling.

The required wave characteristics are low poloidal phase velocity ω/k_θ, the Doppler cyclotron resonance condition $\omega - k_\parallel v_{Ti} = n\Omega_i$, and sufficiently high n, where k_θ, $k_\parallel$ are the poloidal and parallel wavenumber, ω is the wave frequency, v_{Ti} is the alpha-particle parallel velocity, Ω_i is the alpha-particle cyclotron frequency, and n is the toroidal mode number. These requirements may be fulfilled by an ion Bernstein wave propagating somewhat off the plasma midplane, near the major radius of the plasma axis [72].

Experimental observations of a strong interaction between fusion products and the IBW in TFTR have already been made. The IBW was excited by mode conversion with ~70% efficiency from the fast magnetosonic wave at the ion-ion hybrid layer [29,73] in D-^{3}He plasmas; at present, this is the only viable scheme for generating an IBW in TFTR with the currently available source frequencies (> 40 MHz). The large fraction of ^{3}He in these plasmas degraded fusion performance both by dilution of the reacting species and by ensuring that the discharge remained L-mode. In the initial experiments, the dominant observable wave interaction was believed to be with D-D fusion products (tritons) rather than with D-T fusion alpha particles whose population was extremely small in these plasmas.

A strong enhancement of the fusion product losses detected by the probes outside the plasma was observed when the IBW was generated near the plasma axis. The loss mechanism appears to be pitch angle scattering across the passing/trapped boundary. The detectors provide some energy resolution of

the escaping particles and show evidence that the fusion products are heated to approximately $1.5 \times$ their birth energy, as shown in Fig. 3.9. The effect is further dependent on the phasing of the RF antennas, *i.e.* the direction of toroidal wave launch. For 180° phasing (symmetric or non-directional launch) the effect is observed at power levels in the $3 - 4\,MW$ range. For 90° phasing (launch counter to the conventional current) the effect is observed with a threshold of $2 - 3\,MW$. For 270° (co-parallel to the conventional current) no RF driven losses have been observed up to the power limit of $4\,MW$. These observations are consistent with the alpha-channeling model, which further predicts that with the correct choice of toroidal propagation and wavenumber the fusion product energy would *decrease* during the wave interaction while the wave gained energy [71,72]. However, in this case the effect on the fusion product is not presently observable, because such a decrease would be unlikely to pitch angle scatter the fusion product onto a loss orbit, and in D-^{3}He plasmas the confined fusion product density in the plasma core is too low to be measured. Only fusion products on unconfined orbits, which may be detected by the escaping-particle probes, can be observed.

In a subsequent experiment, a small tritium gas puff was added to the D-^{3}He plasma with IBW heating. When the mode-conversion layer was close to the cyclotron resonance layer for alpha particles, there was a further increase in the measured fusion-product loss rate, suggesting that the D-T alpha particles were also interacting with the waves.

The limitations of the previous alpha-channeling experiments would be removed if sufficient ICRF power were available at $30 - 33\,MHz$. In this case mode conversion at the D-T ion-ion hybrid layer could be utilized to generate IBW in a plasma with no ^{3}He content and investigation of alpha-channeling in a high reactivity supershot would be possible. Ideally, these experiments require a unidirectional wave with a relatively high toroidal mode number (~50). The present two-strap antennas have poor toroidal directivity, especially for central plasma densities above about $4 \times 10^{19}\,m^{-3}$ and have also been found to increase edge recycling and produce impurity influx during operation at the 90° phasing which is required for a toroidally directed launch. The requirements for toroidal directivity and high mode number would be met by the upgraded four-strap antennas, described in Sec. 2.3.3, which would launch a fast wave with a toroidal mode number   40. An injected power of $5\,MW$ should be achievable from two four-strap antennas ($600\,kW$ of power per strap). This power level, which is routinely attained with the existing antennas during ICRH of supershot plasmas, is well above the observed threshold of $2 - 3\,MW$ for strong IBW interaction with D-D fusion products. Measurements could then be made in D-T plasmas of the effect of the IBW on the energy and spatial distributions of the confined alpha-particles with the alpha-CHERS and alpha-charge-exchange diagnostics. Calculations indicate that an IBW power of $5\,MW$ in TFTR should be sufficient to reduce the average alpha-particle energy by $>1\,MeV/\tau_s$, where τ_s is the alpha-particle slowing-down time. The existing TFTR experiments imply that the required energy diffusion rates have already been achieved for fusion tritons.
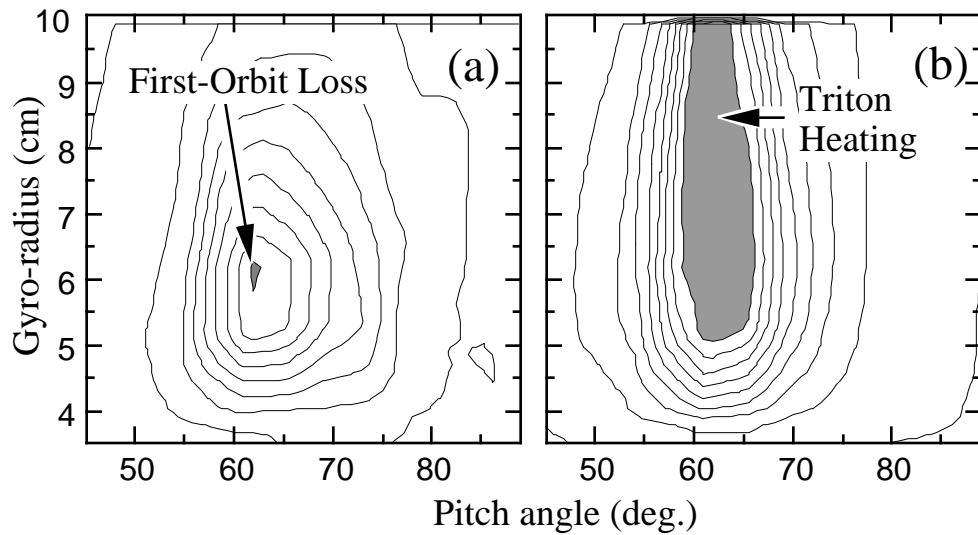
Fig. 3.9   Measurements of energetic fusion products from D-D fusion reactions escaping to the 90°
            particle detector. The contours show the flux of particles resolved in gyro-radius
            (equivalent to energy) and the pitch-angle of their orbits.

   (a) Spectra for a shot with deuterium NBI heating only. The peak (shaded) in the detected
       signal in this case corresponds to tritons near their birth energy which were born onto
       unconfined orbits.

   (b) Spectra for a shot with ICRF heating in which an IBW was produced near the plasma cente
       by mode conversion in the mixed D^3He plasma. In this case, the particle flux is increased
       substantially and a significant high energy "tail" (shaded) is produced on the triton energy
       spectrum as a result of their interaction with the IBW.

It is also planned to operate the direct-launch IBW antenna proposed for TFTR-AP at $30 - 33\,\mathrm{MHz}$ in a D-T plasma. This IBW would also satisfy the resonance condition $(\ \ -\ \ )/k_{\parallel} = v$ and interact with the alpha-particle population. Due to the high energy of the alpha-particles, the Doppler broadened resonance region for the alphas is wider by a factor of 10 than the region over which the IBW will interact with the thermal deuterons. The IBW will interact with the alpha-particles and then propagate further toward the deuterium resonance, where it will subsequently heat the deuterium. Again, energy spreading and radial transport of the alpha-particle population under the influence of the directly-launched IBW will be monitored with the confined-alpha diagnostics.

3.6 Controlling alpha transport with external magnetic perturbations

An alternative technique which would provide control over the alpha-particle pressure profile and helium ash removal is the frequency sweeping or "bucket transport" scheme proposed by Mynick and Pomphrey [74]. This technique for the energy-selective, non-diffusive transport of energetic ions would be useful in a tokamak reactor to remove helium ash, to modify the alpha pressure profile in order to avoid instabilities such as TAE, and to vary the alpha-heated thermal pressure profile. We propose to test this scheme in D-T supershots. Functionally, this is achieved by sweeping the frequency of an applied low frequency (~100 kHz) magnetic perturbation to transport particles with a selected velocity non-diffusively from one radius to another. The resonance condition for the particle interaction is $= n\ \ - m\ \ _b$, where n, m are the toroidal and poloidal mode numbers of the low frequency mode, is toroidal transit frequency and $_b$ is the poloidal transit frequency. For the particles which satisfy the resonance criterion, the magnetic perturbations induce an island in the particle drift surfaces having the same (m,n) symmetry. Sweeping the frequency of the perturbation moves the minor radius of this island, allowing the resonant particles to be adiabatically transported in minor radius.

Although the primary goal of frequency sweeping in TFTR-AP is to test the basic principles of "bucket transport", the capability of selectively driving low-frequency shear-Alfvén waves may also be useful for characterizing TAE damping in TFTR-AP. If the basic mechanism of bucket transport can demonstrated in TFTR-AP, there are a number of ways it could then be applied, making use of the fact that the wave properties determine which part of velocity space is affected. If the parameters are chosen to resonate with the 3.5 MeV alphas, the alpha pressure (and, therefore, heating) profile can be broadened or peaked (note that sweeping is a resonant rather than a diffusive process). This capability may be useful for investigating alpha driven instabilities such as the TAE. In testing the "bucket transport" for helium ash removal, it would be useful to compare the selective transport of particles with different pitch angles. If trapped particles are transported out in major radius they can become "ripple trapped" and are lost in a rather localized area of the vessel. An ash removal scheme which

ejects the helium in a localized area could benefit pumping schemes and minimize the recycling of the helium.

In TFTR-AP, the ICRF system would be used to generate the required low frequency wave. If two ICRF waves of slightly different frequency are launched simultaneously from a single antenna, the resulting beating of the waves can nonlinearly drive a wave at the difference frequency. Initial tests of this scheme at low power on TFTR have demonstrated that the ICRF system can launch fast waves with modulation frequencies swept through the range $10 - 300\,\text{kHz}$. These experiments must be extended to couple higher ICRF power into a D-T supershot with a substantial alpha particle population. During a high power supershot, the TFTR confined alpha diagnostics can be used to measure modifications in the radial distribution of alpha particles due to the frequency sweeping, and the lost ion probes can measure enhanced losses for alpha particles with energies $> 300\,\text{keV}$.

4. Transport Studies

TFTR has, in the past, made significant contributions to the study of transport in plasmas. This topic remains a significant programmatic element in the national program. Transport issues will be an important component in developing the advanced performance regimes which are a major focus of this proposal. Studies of the fundamental transport processes in tokamaks would be continued during the TFTR-AP project in support of the national Transport Task Force Initiative in areas in which TFTR can make a unique and significant contribution.

It is particularly important to understand and quantify the scaling of transport with isotopic mass through measurements in D-T plasmas over as wide a range of plasma regimes as possible, so that there is a solid basis for extrapolating the results obtained from those tokamaks operating only in deuterium to ITER and ignition devices. The availability in TFTR-AP of heating methods with different rates of fueling (NBI *vs*. RF heating) and momentum input (co- *vs*. counter- tangential NBI) and the good density control afforded by the large-area inner limiter, provide us with the capability to control independently several of the dimensionless variables which should be used to construct a general description of tokamak transport. It is important to note, in this regard, that TFTR is currently the only tokamak with balanced co- and counter- tangential NBI. This allows us to study both the effects of toroidal flow on transport and, perhaps more importantly for reactor relevance, transport in the *absence* of an imposed flow velocity.

TFTR is equipped with excellent diagnostics and powerful analysis tools for transport studies. Measurements of the radial profiles of important plasma quantities, including the q profile, are routine in most regimes. In addition, the TFTR diagnostics for the underlying plasma fluctuations are now maturing. A list of the diagnostics operating during the D-T experiments is presented in the Appendix. These diagnostics will be supplemented during the extension by some new and upgraded systems designed to provide additional real-time data for plasma control and to test transport theories. The diagnostic upgrades will be described in Sec. 6.

In the following subsections, we describe some of the specific transport experiments which can be performed during the TFTR-AP project. In addition, some transport-related experiments have already been described in Secs. 2.3 and 2.4, *e.g.* investigating the effects of IBW-driven flow shear and the CH-mode. In establishing priorities for these experiments, we would seek advice from the ITER physics group and the Transport Task Force.

4.1 Isotope scaling

In the first DT experiments in TFTR, it was immediately apparent that the overall energy confinement in supershots is significantly better in DT plasmas than in comparable D-only plasmas. The central ion

and electron temperatures also increased in the DT plasmas. Differences in the fast-ion thermalization are expected for tritium NBI and the fusion alpha particles can provide additional heating. The effect of the scaling of confinement with isotopic mass has been maximized and the alpha-particle heating minimized by comparing supershots with D-only and T-only NBI.

Analysis has shown that the improvement in confinement in supershots is primarily in the ion channel [69,70]. Figure 4.1 shows the variation of the global energy confinement time and the ion thermal diffusivity at the half minor radius for a set of plasmas with similar heating powers, currents and plasma geometry and varying fractions of T-NBI. The electron temperature rise is consistent with the combination of alpha-particle heating and scaling of the overall confinement with isotopic mass. Experiments comparing D- and T- NBI supershots at the same T_e and T_i but different neutral beam powers have established that the observed isotope scaling in supershots is *not* due to a scaling with temperature or T_i/T_e.

Following this work, a straightforward comparison of confinement in deuterium and tritium plasmas under high-recycling (L-mode) conditions with T_i T_e should be completed this year. Presuming that these studies follow the trend identified in previous isotopic comparisons (H *vs*. D) with TFTR L-mode plasmas, *i.e.* weak or non-existent isotope effect on $_i$ or   , an outstanding issue would then be what causes the "isotope effect" to vary in strength in the different regimes. This issue is important both for theoretical understanding and for empirically extrapolating present confinement results to ignition in ITER plasmas.

During the extension, it would be possible to determine whether the strength of the isotope effect is additionally influenced by the T_i/T_e ratio by comparing pure D and T supershots to those partially spoiled by helium. By puffing rather small amounts of helium into supershot comparisons of D versus T, it is possible to smoothly vary the T_i/T_e ratio from typical supershot values (~3) to L-mode (~1). Only a small amount of helium, insufficient to change the isotopic mix significantly, is required to make an appreciable difference in the T_i/T_e ratio, although a larger amount (~30% of the total density) is required to revert completely to L-mode.

4.2 Transport in reversed-shear plasmas

As with any new enhanced confinement regime, the reversed-shear plasmas present many important opportunities for study. In this case, the physics of the abrupt transition to reduced core transport as well as the resulting transport itself need to be clarified in order to understand the value of this regime to TFTR and future reactors. For both the transition threshold and transport, one of the initial steps will be to develop a parametric scaling database to compare with theoretical predictions. In particular, the scalings with q(r), r_{min}, gradient scale lengths, magnetic field, temperatures and heating power, NB applied torque and rotation velocity, and edge recycling need to be documented. If the plasma transport in this regime is governed by neoclassical processes,
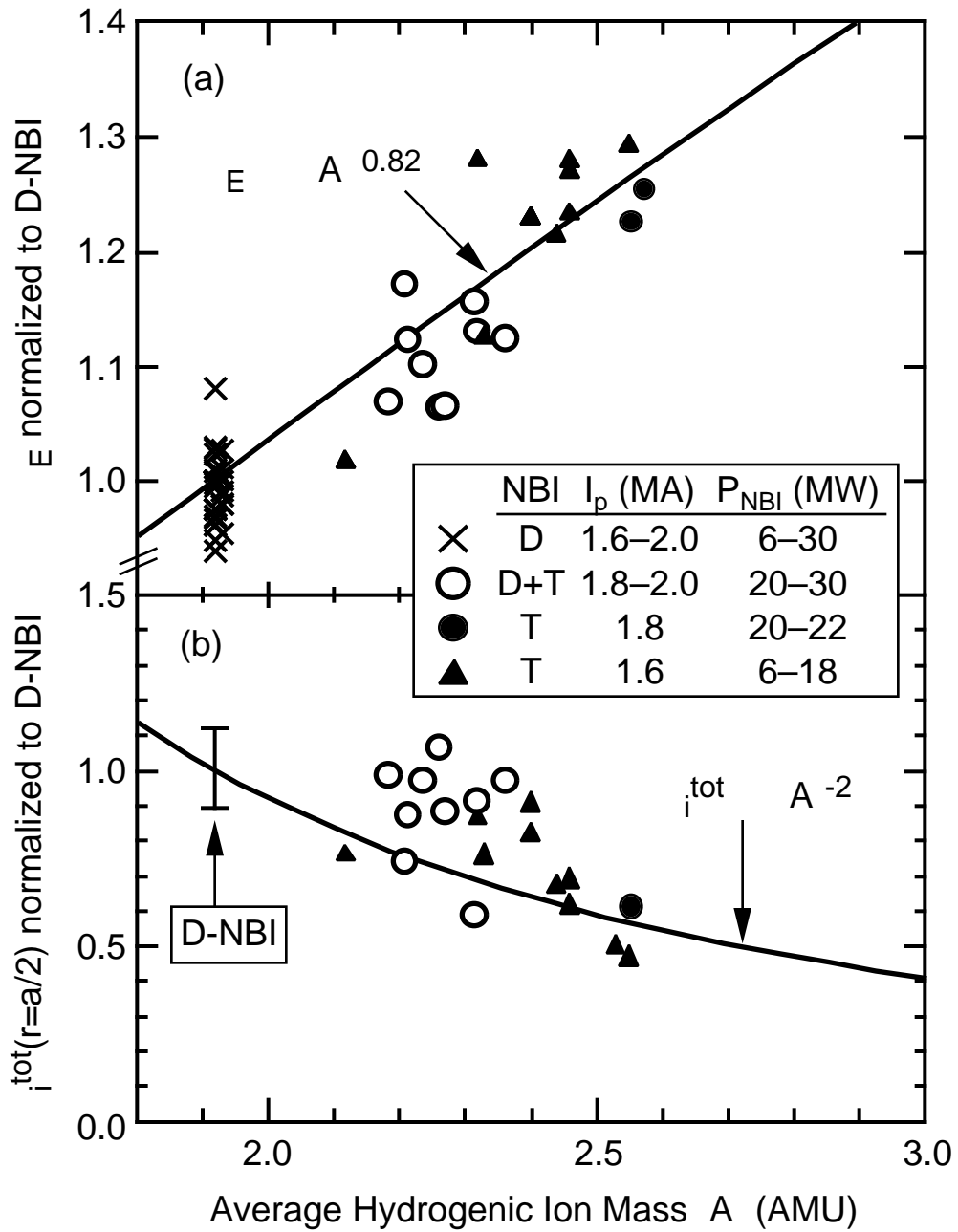
Fig. 4.1 Variation of (a) the global energy confinement and (b) the inferred total ion thermal diffusivity at half the minor radius with the average mass of the hydrogenic ions: $\langle A \rangle = \sum A_i n_i / \sum n_i$; $i = H,D,T$. Data are for supershots with varying fractions of T-NBI.

lowering q_{min} to increase the plasma stability should further reduce the transport. In addition, the issue that analysis of the ion energy balance indicates that the radial losses are significantly less than neoclassical could be resolved if the ion-electron equilibration energy exchange were significantly less than classical predictions. This would also drastically reduce the inferred electron transport. Alternately, the ion thermal transport might be reduced by orbit squeezing from the radial electric field due to the strong ion pressure gradient (and ion poloidal flow damping). To develop an understanding of the ion and electron thermal losses, perturbation experiments, *e.g.* using RF heating perturbations, will probably be required.

Preliminary measurements by the correlation reflectometer indicate that the density fluctuations may be substantially reduced in regions with reversed shear. The relationship between the reduced transport and the fluctuation levels needs to be documented over the full profile for both density and temperature fluctuations. The absence of coherent, low mode-number MHD activity in the core of reversed shear plasmas improves our ability to interpret the fluctuation measurements compared to both supershot and L-mode plasmas.

Due to the very low particle transport in these plasmas, it is important to measure the transport of the various ion species to see if they conform to neoclassical predictions, and to see if the diffusive and off-diagonal terms can be separated. In particular, it is important to determine whether these plasmas show impurity peaking and helium accumulation. TFTR-AP is well prepared for these studies through our well-established program of perturbative measurements of electron, helium, carbon, and hydrogenic (in particular, tritium) particle transport measurements. The time response of the ion densities to perturbative sources is measured directly by charge-exchange recombination spectroscopy for helium and carbon, and via neutron collimator measurements of the DT fusion profile for tritium. Preliminary analysis of the local carbon impurity density from charge-exchange recombination spectroscopy suggests that the carbon, as well as the electrons, experiences a dramatic improvement in confinement in the reversed-shear configuration. Control of impurity ion transport by injected NB torque, as predicted by neoclassical theory, and RF techniques also will be explored.

Finally, the reversed-shear plasmas have been prepared with low-recycling limiters in order to maximize T_e during the prelude phase (*i.e.* before the main NBI heating) to impede the current penetration. This has yielded plasmas with some supershot characteristics, including low edge-density and core $T_i \gg T_e$, although there are considerable differences in the profiles. It is important to study the effect of edge recycling on reversed-shear transport and the transition to reduced transport, and to study the effect of reversed shear on high-recycling plasmas (starting with L-mode profiles). This may be simple to achieve experimentally by introducing a helium puff at various times during a reversed-shear discharge. In supershot plasmas, helium puffs of ~10 Torr·l force a return to L-mode confinement within about 0.1 – 0.15 s. Introducing helium at the end of prelude should generate a reversed shear plasma with broad L-mode profiles for high power heating and transport studies.

Introducing helium after the transition to the reduced transport regime will test the sensitivity of this mode to the recycling.

4.3 Tests of IFS/PPPL transport model

A theoretically based transport model has recently been developed at the Institute for Fusion Studies, Texas, and PPPL (the IFS/PPPL model) [75] which predicts quantitatively the ion and electron temperature profiles in a variety of L-mode conditions. This model also describes qualitatively several of the features of the transition from L-mode to supershot confinement since the threshold for the ion-temperature-gradient (ITG) instability responsible for the dominant anomalous transport, increases with T_i/T_e. If this model correctly describes core transport in tokamaks, it might be possible to achieve substantial enhancements in confinement in an ITER-scale tokamak through control of the plasma profiles. Several important features of this model would be tested more thoroughly in TFTR-AP.

The gyro-fluid code, on which the numerical expression for χ_i in the IFS/PPPL transport model is based, calculates explicitly the amplitude of density and temperature fluctuations. These would be compared against diagnostic measurements in a number of parameter scans. For these experiments, L-mode plasmas would generally be used, because the ITG instability is robustly excited in the L-mode regime, whereas it is either below or near threshold in supershot plasmas. The potential experiments include: (a) plasma current scans, to explore the well-known scaling of χ_i and χ_e with current in steady-state; (b) current ramps, to investigate the previously-demonstrated shear dependence of χ_i; (c) toroidal field scans, to study why local transport is insensitive to toroidal field; and (d) systematic variations of the density-profile shape (controlled by helium puffing with a well-conditioned limiter), to study the effect of the density-gradient scale-length, L_n, and the ratio T_i/T_e on χ_i.

Expanded studies of the *transient* plasma response to perturbed temperature, density, impurity and gradient scale-lengths are also planned. The perturbations created by impurity pellet injection into both supershot and L-mode plasmas would provide powerful tests of the model. The use of boron pellets (a new capability in TFTR) offers significant advantages over the previously available carbon pellets because the important ion temperature diagnostic, which is based on carbon spectroscopy, is blinded for a period by the intense line radiation following carbon pellet injection.

These experiments, which would realize the full benefit of the diagnostic development on TFTR which was undertaken as part of the transport initiative over the past five years, would provide a unique opportunity to compare detailed theoretical predictions of microturbulence properties with actual plasma behavior. In particular, the very recent introduction of a diagnostic to measure the ion temperature fluctuations in TFTR may provide the most powerful means yet for such a comparison. The potential impact of such a theoretical and diagnostic comparison cannot be overemphasized.

4.4 Effect of the toroidal flow shear on transport

Steep gradients in toroidal velocity (v_ϕ) are often observed in during beam heating of TFTR supershot plasmas, particularly during partially or fully unbalanced injection [76]. The region where these large gradients occur is typically close to the region of steep gradients in the ion temperature (T_i) and total plasma pressure, *i.e.* the region of dramatically improved confinement. However, it has not been established whether the toroidal velocity gradient *causes* reduced transport, through shear in the radial electric field (E-field), as has been suggested as the underlying mechanism controlling VH-mode transport in DIII-D [77], or whether an independent mechanism simultaneously decreases both ion momentum and ion heat transport.

It should be possible to improve the spatial resolution of the T_i and v_ϕ measurements in the high-gradient region by using small major-radius "jogs" to sweep the plasma past the fixed channels of the charge-exchange spectrometer. This procedure improves the resolution approximately a factor of 3, from ~8 cm to 2– 3 cm. These experiments will clarify on what radial scale the regions of steep gradient in T_i and v_ϕ remain tightly coupled.

Simultaneous measurements should be made of the transport, velocity shear, and density fluctuations in supershot plasmas by microwave reflectometry. Such measurements would allow us to determine whether the confinement improvement is associated with a reduced amplitude and correlation length of the density fluctuations, as predicted for E-field shear-stabilization of transport. The experiment would consist of controlled variations in the co/counter mix of NBI sources at constant total heating power in supershot plasmas. A small scan in the TF at each condition would allow the reflectometer to obtain measurements across the entire region where the steep gradient in toroidal velocity is observed. The plasma conditions (beam power, plasma current, limiter conditioning) must be carefully selected to ensure the absence of both coherent MHD activity and sawteeth, which obscure the reflectometer measurement.

Additional experiments could possibly be carried out to measure the density and T_i fluctuations by beam-emission spectroscopy and high-frequency charge-exchange recombination spectrometry, although the diagnostic constraints and analysis difficulties are more severe. Typically, the signal/noise ratios for these diagnostics become small in the region of the steep velocity gradient ($R \approx 2.90$ m) because of attenuation of the neutral beams. An additional problem is that the Doppler shift imposed on the diagnostic signal will vary systematically as the co/counter mix of beam heating is changed. However, these measurements are potentially important to determine whether changes in T_i-fluctuation amplitude are correlated with the observed changes in transport.

4.5 H-mode confinement studies

Supershots with H-mode characteristics have been studied in both DT and D-only plasmas [78,47]. The DT H-mode plasmas have exhibited transient confinement times up to 0.24 s, which represents an enhancement by a factor of 4 relative to the ITER-89P scaling [10] while corresponding D plasmas had enhancements of ~3.2. The confinement was improved across the plasma during the H-mode phase. The ion heat conductivity was observed to decrease by a factor of 2 – 3 across the transition to H-mode. The edge localized modes (ELMs) are much larger during the D-T H-modes. This suggests that ITER D-T plasmas may be more susceptible to giant ELMs than inferred from D-only experiments or, alternatively, that ELM-free operation may be more easily obtained. The power threshold for the transition to an H-mode is similar in D and D-T discharges. These H-mode studies would be assisted by installation of additional diagnostics proposed for TFTR-AP, particularly the measurement of poloidal rotation.

4.6 Non-dimensional scaling of transport

Previous scans of the normalized gyro radius, $\rho*$, at constant beta and collisionality in TFTR indicated that the single-fluid thermal diffusivity obeys a Bohm scaling [79]. A two-fluid power balance analysis shows that χ_i obeys a "Goldston" scaling ($\chi_i \sim \chi_{Bohm} \rho*^{-1/2}$), *i.e.* "worse" than Bohm scaling, while the electrons appear best fit with a Bohm scaling. These results for χ_e scaling differ from measurements in DIII-D [80], where χ_e appears to be described by a gyro-reduced Bohm scaling ($\chi_e \sim \chi_{Bohm} \rho*$). However, the difference in predicted T_e between Bohm and gyro-Bohm scaling for χ_e in TFTR is relatively small, and the TFTR data have not been conclusively demonstrated to be inconsistent with gyro-Bohm scaling of χ_e. The projected performance in ITER is quite sensitive to whether heat transport obeys a Bohm versus a gyro-Bohm scaling.

Additional $\rho*$-scans will be carried out in deuterium L-mode plasmas to clarify the two-fluid $\rho*$ scaling of transport. In these scans, increased emphasis will be placed on maintaining constant T_i/T_e and rotation shear, and less emphasis on maintaining exactly constant collisionality, in accordance with recent theoretical guidance that T_i/T_e and rotation shear are more important than collisionality.

ICRF minority-ion heating offers the advantage over NBI heating of maintaining a constant heating profile shape as the plasma density is varied, and depositing power predominantly to thermal electrons, which should reduce the uncertainty in the inferred Bohm versus gyro-Bohm scaling of χ_e. Additional $\rho*$ experiments will be carried out using ICRF heating, spanning a range of approximately two in toroidal field.

Previous scans of plasma β at constant collisionality and constant $\rho*$ showed a large increase in transport up to a β of 0.25%, but then virtually no additional increase as β was increased an additional factor of two [81]. This parametric behavior is difficult to reconcile with microturbulence theory, since

electromagnetic effects are not expected to appear at such low . It is relatively straightforward to extend these studies to higher, more reactor-relevant values (increases of factors 2 – 3 are possible) by reducing the toroidal field and plasma current. These experiments would more clearly identify whether or not there is a dependence to local transport coefficients over the range of where theory predicts electromagnetic terms might be expected to modify the transport.

4.7 Density scaling of particle transport

Previous perturbative studies of electron particle transport using gas puffs in L-mode plasmas demonstrated that particle transport has an unfavorable temperature scaling (D_e $T^{(1.5–2.0)}$) at constant density [82]. The radial dependence of the inferred D_e profile could be fit with a dependence of the form D_e $T^{(1.5–2.0)} n_e^{-1} L_n^{-2}$. Predictive modelling studies of plasmas with multiple pellet injection, using a $D_e(r)$ of this form, reproduced the measured time response of the $n_e(r,t)$ profile reasonably well. However, a more direct approach would be to perform perturbative measurements of D_e in a L-mode density scan at constant temperature. This is a straightforward experiment which requires only run time.

It would be fruitful to carry out both the temperature scan (at constant density) and the density scan (at constant temperature) experiments. The difference in fusion cross sections for DT and DD reactions and the availability of collimated neutron measurements mean that minute tritium gas puffs can be used to measure tritium particle transport. For the electron transport, larger perturbations are required so helium gas puffs will be used. The plasma conditions of modest density and modest heating power are amenable to measurements of density and possible ion temperature fluctuations in the same plasmas using beam emission spectroscopy, high-frequency charge exchange recombination spectroscopy (HF-CHERS), and correlation reflectometry.

4.8 Magnetic field scaling of transport

Typically, studies of the dependence of local transport on plasma current I_p and toroidal field B_T have been carried out by varying these parameters *at constant heating power,* with little control over the plasma density. Although these measurements have indicated a favorable dependence of $_i$, $_e$, and on I_p [83], it is probable that the *strength* of this dependence is underestimated, perhaps seriously so, because the plasmas at higher current are hotter. Studies of the temperature dependence of $_i$ and $_e$ at constant density have clearly demonstrated an unfavorable temperature scaling with both particle and heat transport coefficients scaling as $T^{(1.5-2.0)}$ [82]. Analysis of existing data suggests nearly a factor of ten difference in $_i$ at $r = a/3$ in L-mode plasmas between $I_p = 1.2\,MA$ and $1.8\,MA$ when the comparison is performed at constant ion temperature rather than at constant power [84].

By iteratively adjusting the beam power and limiter recycling (or gas puffing), it should be straightforward to conduct a plasma current scan which holds both temperature and density constant as

I_p and B_T are varied by about a factor of two. We propose to carry out I_p scans both at constant q and at constant B_T. A convincing demonstration of a strong magnetic-field dependence to local χ_i, when temperature is held constant, would be an important guide for theory.

5. Core Fueling and Power Handling

There are issues in the areas of fueling and particle control for a reactor which are largely determined by the plasma edge configuration and by scale parameters outside the range readily accessible in TFTR. However, there are also several issues critical for the ITER design which can be appropriately and, in some cases, uniquely studied in TFTR. In particular, TFTR can study the critical issues of the transport of tritium and helium ash in the core of reactor relevant plasmas in a range of regimes. In this section, we discuss these issues and the experiments which are planned for TFTR-AP to address them.

In addition to these dedicated experiments, several of the studies described in previous sections of this proposal also impinge on the areas of fueling and particle control. For example, in the reversed-shear regime in TFTR (Sec. 2.3), the particle diffusivities appear to be substantially reduced within the shear-reversal radius. The implications of reversed-shear operation for reactor fueling will be carefully assessed in the planned TFTR experiments: it may be possible both to heat and to fuel the core of a reversed-shear reactor with high-energy neutral beams. The use of IBW heating to create a transport barrier for modifying the pressure profile (Sec. 2.4) will also provide important data on whether this technique could be used to assist in fueling the core of ITER and whether such a barrier would interfere with the removal of helium ash. We have also seen in Sec. 3.5 that, in addition to modifying the energy flow from energetic alpha particles to the thermal plasma, the process of alpha-particle channeling causes radial transport of the alpha particles and would assist in removing them from the core. The resonant alpha-particle transport scheme described in Sec. 3.6 could be used directly for ash removal, possibly with the added benefit of spatially localizing the helium ash flux through the plasma boundary.

5.1 Simulation of ITER fueling with pellets at high density

Fueling of TFTR plasmas by deuterium and tritium pellet injection will address three issues important for ITER: 1) operation at densities above normal limits; 2) transport of tritium in the plasma core and the possibilities for tailoring the fuel profiles; 3) ICRF heating at very high density using both tritium second-harmonic and deuterium fundamental coupling.

As presently envisaged, achieving ignition in ITER requires operation with the plasma density at or above the limits presently believed to apply in tokamaks, namely the Greenwald [85] and Borrass [86] limits. Experiments in TFTR [87] have already produced stable discharges which exceeded the Greenwald limit for up to 1.6 s and by as much as a factor of 2 transiently, through multiple deuterium-pellet fueling during NBI heating. A *volume-average* density above 2×10^{20} m^{-3} has been sustained for 0.4 s and a central density above 2×10^{20} m^{-3} has been sustained for more than 1 s. Since no disruptions occurred in these experiments, these values do not appear to represent the density limit;

they are simply the highest values achieved. Also, even at the highest densities, there was *no* deterioration of the central particle confinement, as had previously been observed, for example in Alcator-C, as the Greenwald limit was approached.

These past TFTR experiments were intended to demonstrate the possibility of high density operation at high power but were not a detailed study of the limits to that operation. These limits and plasma behavior near these limits will be studied in detail by a series of experiments in TFTR-AP focused on ITER plasma scenarios.

Multiple deuterium pellet sequences will be used to produce the high density plasma. Lithium pellets are also available on TFTR to supplement the deuterium pellet fueling. Plasmas with q_a 3.5, designed to approximate the current profiles for ITER, will be employed at intermediate and high toroidal field and plasma current (3.0 T, 1.8 MA and 5.0 T, 2.6 MA). The scaling of the density limit with power at these two current levels will be studied to separate the effects of power flow and plasma current. With the present deuterium pellet injector, the Greenwald limit is most readily exceeded at the lower current and most development work would be done in this condition. In order to exceed the limit at the higher field, it may be necessary to use the lithium pellet injector to provide some initial cooling of the plasma so that the first deuterium pellets can penetrate to the core and achieve the maximum fueling efficiency. In both cases, combined ICRF and NBI heating will be used to provide a strong central power input. The ICRF heating will be coupled to either a hydrogen or ^{3}He minority initially. Ultimately, when tritium pellets become available for fueling, ICRF heating via the second harmonic tritium or the fundamental deuterium resonance will be studied at high density. These experiments will be carried out at fields, temperatures and power densities close to those of ITER. Furthermore, the ICRF heating can be used to simulate the heating profile of the alpha particles in an ignited D-T plasma.

Tailoring the deuterium and tritium density profiles in ITER could lead to reduced tritium inventory in plasma facing components and, therefore, improved safety and reduced fuel cost [88]. This isotopic tailoring concept consists of utilizing a tritium-rich pellet source for core plasma fueling and a deuterium-rich gas source for edge fueling. Because of the improved particle confinement associated with the deeper tritium core fueling component, comparable core densities of deuterium and tritium can be maintained even when the edge deuterium source is much larger than the core tritium source. The fuel composition of the edge and scrape-off plasmas reflects the total throughput of all makeup fuel and would therefore be deuterium-rich. Consequently, that part of the fuel retained in the plasma facing components would also be deuterium-rich. It is proposed to explore the ability to maintain isotopically tailored deuterium and tritium profiles with tritium pellet injection on TFTR to duplicate precisely this innovative ITER fueling scenario. Figure 5.1 summarizes calculations with the WHIST predictive transport code for ITER conditions, *viz.* a constant fusion power of about 1500 MW and a constant divertor exhaust (and fueling) rate of 1 bar·l/s. It indicates how central and edge tritium concentrations
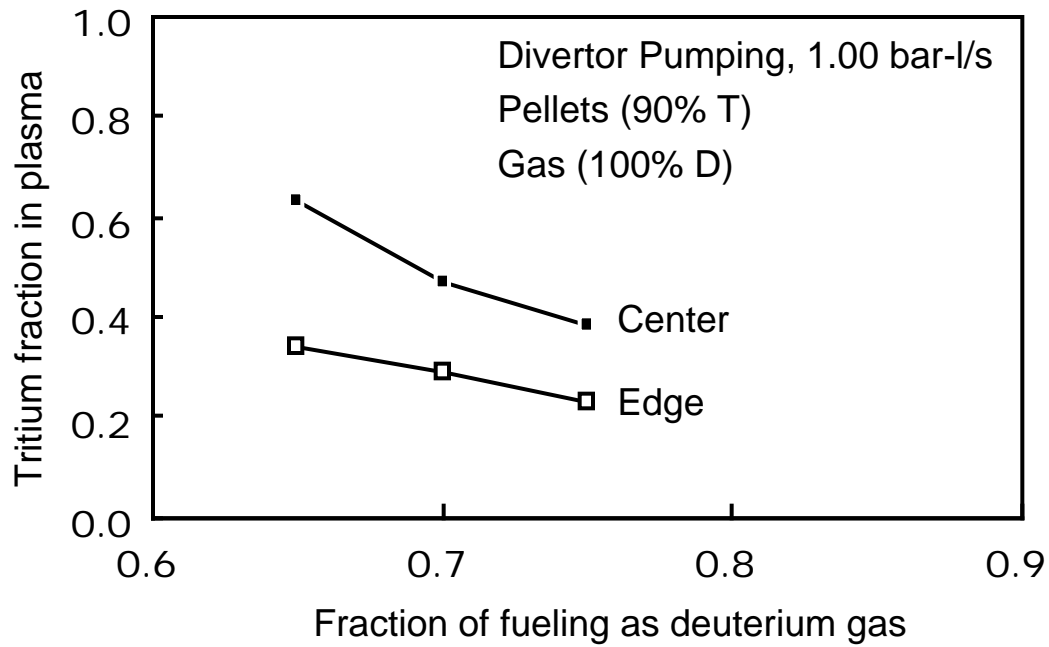
Fig. 5.1   Effect of type of fuelling on central and edge concentrations of tritium in ITER. Fuel is supplied as either deuterium gas or in the form of pellets with 90% T content. Modelling is with the WHIST code.

vary as the deuterium gas fueling is varied from 65% to 75% of the total fueling, with the balance of the fueling provided by 90% tritium pellets. The edge tritium fraction is directly proportional to the wall inventory and consequently inventory reductions on the order of 50% should be achievable.

Transport of tritium within the confined plasma will play a major role in this process of isotopic tailoring. The detailed measurement of tritium transport is a unique capability of TFTR. The vastly different cross-sections of the D-T and D-D fusion reactions and the availability of the collimated neutron detectors provides a powerful diagnostic technique for studying the diffusion of tritium from the edge. Both tritium gas puffing and tritium beam injection have been used in past studies.

In the experiments with pellet fueling designed to explore the density limit, these same techniques will be used to determine the tritium transport. Both edge and pellet tritium sources will be examined.

Tritium introduced by gas puffing at high density simulates the recycled tritium flux at the edge of the confined plasma. Although the efficiency of tritium fueling at the edge in ITER H-mode plasmas will not be determined by these experiments, the transport in the interior plasma, beyond the H-mode edge transport barrier and the region affected by ELMs, can be examined.

The pellet tritium source will be simulated initially using tritium introduced by NBI. The beam source profile is generally similar to that of pellet-deposited fuel in these high density plasmas. By using the tritium NBI in bursts concurrent with pellet injection, transport of pellet-deposited tritium will be approximated and can be studied in the same way as proposed for gas-fuelled tritium. Ultimately, tritium pellets will be used to duplicate the ITER fueling scenario more precisely. In these high density TFTR discharges strong edge deuterium sources duplicating ITER conditions will be present naturally due to deuterium wall recycling. Deuterium gas puffing can be used to increase deuterium wall sources further. Alternatively, lithium pellet injection is available to reduce wall recycling. Tritium enrichment within the plasma core will be studied over the range of edge conditions.

The extension of second harmonic tritium and fundamental deuterium ICRF heating studies in TFTR to plasmas simulating the high density phase in ITER will accompany these tritium pellet fueling experiments. Pellets with a tritium content varying from a trace to pure tritium can be prepared and will be used to vary the core tritium concentrations.

In all cases, the high fueling efficiency of tritium pellets will minimize the tritium throughput in TFTR. This operational advantage is also attractive for ITER due to economic, safety and machine duty cycle considerations.

5.2 Edge power flux control with a radiating mantle

Two major obstacles for the engineering design of ignited tokamaks, including ITER, are heat flux to the divertor plate and surface erosion caused by the particle flux. Both problems would be ameliorated significantly if the total power flux at the last closed plasma flux surface could be reduced by radiating

a significant fraction of the fusion power uniformly to the first wall. Deliberate introduction of low- to moderate- Z impurities to create an edge-localized highly radiating plasma "mantle" has been suggested as a means to increase the radiative losses [89,90,91,92], including application to ignited plasmas in ITER [93]. Experiments on several tokamaks including TFTR [94,95,96,97] have demonstrated that a significant fraction, 70 – 95 %, of the total input power can be radiated away in this fashion without suffering radiative collapse of the discharge. Most recently, ASDEX-U has achieved H-mode conditions with intense mantle and scrape-off-layer radiation, suffering only a 10% reduction in global τ_E and 10% addition dilution [98]. However, there are several important unresolved and intriguing physics issues relating to impurity-enhanced radiation, including:

1. Choice of the most appropriate element for reactor-like conditions;
2. Radiative and operational stability;
3. Effect on core energy confinement;
4. Impurity transport to the core causing fuel dilution;
5. Effect on T_e and T_i in a radiating edge mantle;
6. Effect on H-mode power threshold;
7. Effect on helium transport and pumping by the divertor.

Plasma geometry including the presence of a divertor geometry are critical to issues 6 and 7, and so they are most appropriately studied in tokamaks other than TFTR. However, plasma geometry is far less important for the other issues, and insights gained into the underlying physics mechanisms from studies on TFTR-AP would be valuable for the design and operation of ITER and reactors. The focus of radiating mantle studies proposed for TFTR-AP are measurements of radiative stability using more ITER-relevant, higher-Z impurities than can be studied on other tokamaks (making use of the higher electron temperatures and heating power densities available in TFTR), and the effect of enhanced core radiation on supershot plasmas, for use in TFTR and possibly in ignited reactors.

Radiating edge mantles have been studied extensively over the past several years with low-Z impurity puffing in a number of tokamaks, with generally encouraging results. TEXTOR [99] has radiated as much as 95 – 98% of the input power with neon injection and pumping by the ALT-II limiter. Tore Supra has transiently radiated ~80% of the input power in Ohmic plasmas [100] using nitrogen puffing and an ergodic limiter to control MARFE activity. ASDEX-U has radiated more than 90% of the input power using neon and argon puffing, and remained in the H-mode [98]. DIII-D has reduced the peak divertor heat flux by more a factor of ten using neon or argon [101], although this was achieved at the expense of somewhat reduced electron temperature. By contrast, JET [4] has been unable to sustain good H-mode confinement in detached plasmas having high radiated power.

The impurity concentration needed to radiate a significant fraction of alpha heating power in an ignited plasma such as that anticipated for ITER decreases with increasing impurity charge because impurity

radiation increases strongly with charge, *viz.* q_{rad} Z^3 [92]. Thus, fuel dilution is minimized if a high-Z impurity is used. An offsetting trend is the loss of radial localization of the "edge" radiating mantle. Studies for ITER [93,102,103] indicated that carbon could radiate only 30% of the alpha power, while argon could radiate 59%, and krypton up to 87%.

Plasmas with significant radiative losses are subject to instabilities which lead to Marfe activity [104] and disruption. These instabilities limit the maximum fraction of power which can be radiated, or alternately, limit the edge plasma density for a chosen radiated power fraction. A major driving term in these instabilities is the intrinsic temperature dependence of line emission from impurities, which is typically strongly negative for the plasma conditions prevalent in the plasma edge, *i.e.* line radiation increases strongly as temperature is reduced. Figure 5.2 shows the radiation cooling rate for selected impurities as a function of temperature at coronal equilibrium. As expected, the radiated power per ion increases strongly with impurity Z. Note that there is considerable structure in the temperature dependence, which is important in determining regimes of radiative stability. The temperature range over which the cooling rate decreases faster than $1/T_e$, an indicator of increasing thermal instability, varies strongly with impurity charge.

5.2.1 Fundamental edge mantle studies

Since there is little line radiation from fully-stripped impurities, schemes for highly-radiative edge mantle typically employ an impurity whose Z is chosen to be partially stripped at the edge, and fully stripped at the center. This minimizes radiative losses from the plasma center, while providing significant losses from the edge. The required impurity charge Z increases with electron temperature. Current experiments in DIII-D and TEXTOR use low-Z impurities such as neon and sometimes argon, consistent with their temperature profiles.

The electron temperatures for ignited operation in ITER will be larger, and therefore higher-Z impurities will be appropriate for the edge mantle. Line radiation is a complicated function of temperature for all impurities, so extrapolation of low-Z results to higher-Z, higher-temperature plasmas may be problematic. Therefore, experience at higher temperatures, using the impurities with the same or nearly the same Z as would be used on ITER would be extremely valuable. It is important to assess the radial transport of the higher-Z impurities in reactor-grade plasmas to determine whether preferential core accumulation could defeat the desired edge-localization of the radiation.

Figure 5.3 shows the parameter space (T_e *vs.* n_e) for some representative ignited plasmas in ITER versus the parameter space that can be explored in beam-heated TFTR discharges. Using high-power neutral beam heating, TFTR should be able to study the *same* impurities that would be used for a radiative edge mantle in ITER. The principal limitation of this study will be that ITER-relevant mantle plasma conditions can be obtained only in the core of TFTR, where the heating power density is considerably higher than the alpha-heating power density in ITER.

Figure 5.2

Figure 5.3

5.2.2 Improved supershot performance

The energy confinement time and fusion power yield in supershot plasmas varies with influx of carbon and deuterium from the limiter, with τ_E varying approximately as $H_\alpha^{-0.25}$ and $C_{II}^{-0.25}$ (where H_α and C_{II} are the average levels of those edge emission lines). Hydrogenic and carbon influx depends critically on the "conditioning" of the limiter surface, accomplished either by a sequence of low-density ohmic plasmas, or lithium pellets, or both. One important component of the TFTR-AP project would be to use and to extend the performance of high-confinement plasmas recently obtained with heavy lithium conditioning. For a given state of limiter conditioning, the magnitude of hydrogen and carbon influx during neutral beam injection is a nearly linear function of heating power to the limiter. Thus, it may also be possible to increase performance by reducing the power flux to the limiter by creating a radiative plasma mantle.

TFTR has already demonstrated reduced influx of carbon and hydrogen as a consequence of enhanced radiation. Argon puffing into NBI heated plasmas ($P_{NBI} = 12\,MW$) increased the radiated power fraction from 30% to 70% and decreased the influx of carbon and hydrogen $30 - 40\,\%$.

These experiments were designed to test the effect of reduced edge T_e on supershot performance, and so were not optimized to look for possible improvements in supershot performance. Argon was used, which radiates preferentially from the plasma edge. The edge density, which correlates inversely with supershot performance, increased ~20% during the argon puff, and no increase in τ_E was observed. Future experiments would use a higher-Z impurity (krypton, xenon) to radiate a comparable fraction of input power at a smaller concentration, thereby restraining the increase in edge density.

There is some experimental evidence that edge radiation might improve energy confinement in supershots: TEXTOR has demonstrated improved performance at high density in its I-mode regime, which closely resembles the supershot regime, when radiation was increased to 85% of the input power by adding neon or silicon to the discharge [105]. Improved energy confinement (up to $1.8 \times$ L-mode) was also obtained in the so-called Z-mode plasma regime in ISX-B by puffing neon into a beam-heated plasma.

Increasing energy confinement at fixed heating power by increasing radiative losses and thereby decreasing edge influx of hydrogen and carbon would provide new insights into the mechanism controlling heat transport in supershot plasmas, and may provide useful benchmark tests against the IFS/PPPL theoretical model. However, the principal use of a radiating mantle in TFTR would be to improve fusion performance in order to demonstrate alpha heating and to study alpha-driven TAE instabilities.

6. Control and Diagnostic System Upgrades

TFTR is equipped with a comprehensive diagnostic set, listed for reference in the Appendix. However, the program described for an extension of D-T operation in TFTR-AP, with its emphasis on developing advanced operating regimes for the study of alpha-particle and transport physics, would benefit substantially from upgrades to several of the existing plasma diagnostics and the installation of some new diagnostic systems. These are outlined in Table 6.1. The upgrades are shown in rough order of priority, with the highest priority items listed first.

Topic	Upgrade	Purpose/Strategy	Exposure
Poloidal Rotation	CHERS Poloidal Rotation Diagnostic	Investigation of regimes of improved confinement and effects of IBW	4
Current Profile	MSE Real Time Control	Provide current profile signal for use in feedback	1
	MSE scanning and mirror replacement	Obtain full spatial coverage; improve S/N ratio	5
	MSE Diamagnetic profile	Full equilibrium reconstruction with RF heating	1
Control System	Digital control system with additional inputs of J(r), p(r)	Disruption avoidance and control of advanced regimes	1
Alpha Studies	Extend infrared camera to lower temp.	Measure distribution of alpha loss to outer limiter	4
Fast Electrons	Oblique-view ECE	Measure fast electron distribution during LHCD	4

Table 6.1   List of proposed upgrades, modifications and repairs to the TFTR diagnostics for an extension of D-T operation. The column "Exposure" ranks the level of radiation exposure associated with the task: 1) all work outside test cell; 2) work outside central structure; 3) work near vacuum vessel; 4) vacuum vent and removal of small flange; 5) vent and removal of port cover (see Sec. 7 for operational implications).

6.1   Poloidal rotation

The poloidal rotation measurement is particularly important in view of the emphasis being placed on studying regimes in which the transport is radically modified over some region within the plasma, *e.g.* the reversed-shear regime or the CH-mode plasmas created by IBW heating. With a knowledge of the poloidal as well as the toroidal rotation, one may infer the local radial electric field which may be crucial in the transport processes.

The diagnostic would consist of vertical views of the same neutral beams (those in beamline 5) currently used by the charge-exchange recombination spectroscopy diagnostics (CHERS,   -CHERS) and the motional Stark effect (MSE) system, guaranteeing that most shots would have v measurements. Because of the port configuration, four small port covers would be replaced with windows. Two of these would be equipped with optics and fiber optic arrays to view the heating beam. Corresponding views at a toroidal location with identical views not intersecting a beam would be used for background determination.

The near circular flux surface cross-section and the large vertical extent of the heating beam results in components in the line-of-sight measurement from a range of values of minor radius, ranging from 5 cm at r/a = 0.9, to 30 cm at r/a = 0.25. This effective radial resolution can be improved through the use of an inversion technique. Expectations are that, given enough spatial channels, the effective radial resolution can be close to that (~3 cm) currently available in the toroidal rotation measurement.

6.2   Motional Stark Effect upgrade and modifications to the plasma control systems

Control of the current profile is an essential element of the TFTR extension. An important tool for effective j(r) control is the MSE (Motional Stark Effect) diagnostic, which would benefit greatly from an upgrade to provide scanning capability in the mirror which views the plasma. By scanning the 21 sightlines radially during the shot, one can compensate for many systematic effects. This is currently accomplished by "plasma jogs" [107]. At the same time, the aluminum mirror currently in use could be replaced with a dielectric mirror, which would result in a large reduction in background signal.

The mirror which would be modified is located in vacuum in a protective enclosure attached to a midplane port cover. The port cover would need to be replaced and a vacuum-tight reentrant enclosure added, with the mirror in air, avoiding the necessity of having moving parts in the vacuum. The scanning frequency would be in the range 10 – 20 Hz. There would be no other significant change in the optics.

The upgrades to the MSE diagnostic for the q profile are important to provide both added resolution and capability for a real-time measurement. With the latter capability coupled to the systems for controlling the current profile, in particular the LHCD system and, possibly, the plasma current control feedback loop, it should be possible to control the evolution of reversed-shear plasmas. At present, with only control of the gross plasma parameters possible, the evolution of these plasmas and their transport characteristics are quite interdependent, so reproducible conditions are hard to obtain. It is straightforward to provide MSE input to a digital control system. Analog fiber optics links are needed to bring 21 signals to the control system input. This would allow access to real-time pitch angle profiles for the control system.

With additional diagnostic inputs, we expect to improve the capability of the real-time feedback control for the neutral beam power to avoid high-   disruptions. Such a development would be extremely useful, not only for high-performance experiments in TFTR-AP, but for TPX and ITER which plan to operate near several limits simultaneously for extended pulses.

6.3   MSE measurement of the diamagnetic profile

Measurement of the diamagnetic profile would be a very attractive addition to the capability of TFTR. Particularly with the proposed additional ICRH and LHCD capability the ability to determine the pressure profile becomes more problematic. Also with the proposed enhancements for the MSE system

combined with a pressure measurement our ability to study MHD stability would be greatly enhanced. Recent tests of this technique on TFTR as well as some results from JET [108] suggest that a routine diamagnetic measurement can be developed. The JET data shows clear changes in the pressure profile due to ICRH heating or sawteeth.

TFTR has a larger toroidal field and higher beam energy compared to JET which would improve the sensitivity of the measurement. More importantly a substantial improvement can be obtained if the instrument is designed and optimized for this measurement. Since a typical diamagnetic change due to the change in pressure is ~1% of the toroidal field then a sensitivity of at least 0.1% is necessary.

The proposed design is a spectrometer with a resolution of about $0.5\,\text{Å}$. Since the Doppler broadened divergence will be about $0.5 - 1.0\,\text{Å}$ having higher resolution would not be of much use. The problem is determining the peak position to 1/50 of the width. With sufficient throughput this should be quite possible. The CHERS position to width ratio is better than 1/100. For a grating spectrometer with a focal length of ~$1.0\,\text{m}$, the dispersion will be ~$1.5\,\text{Å/mm}$ which translates into a slit width of ~$0.3\,\text{mm}$ for $0.5\,\text{Å}$ resolution. In order to get as high a throughput as possible a low f number spectrometer is needed. Typical off the shelf spectrometers of this size are $f/8$, limited by the grating size available from manufacturers. However with large astronomical gratings of $30 \times 40\,\text{cm}$ operated at higher order then $f/3\text{-}4$ may be possible. Another alternative is use a mosaic of smaller $12 \times 15\,\text{cm}$ gratings to give a similar f-number. This spectrometer would also be well suited for poloidal rotation measurements on TFTR or PBX-M in terms of resolution and throughput.

6.4 Detection of alpha-particle heat loads

The most important alpha particle physics issue for the ITER EDA is the prediction of the alpha particle heat loading of the first wall [109]. Even a few-percent loss of the $300\,\text{MW}$ of alpha particle heating could potentially lead to overheating or damage to the wall if this alpha loss is spatially localized, e.g. due to TF ripple trapping.

We propose to use the technique originally developed for JT-60U [110] to study the spatial distribution of alpha-particle loss at the first wall of TFTR, using an upgraded version of the existing IRTV system. The present IRTV system is capable of spatial coverage over most of the vessel wall, with a spatial resolution on the order of 1 cm. However, the quartz optics of the present system transmits only below about $2\,\mu\text{m}$, which limits the temperature to above $300\,^\circ\text{C}$. This is sufficient to study the heating of the wall due to plasma heat flow, but not sufficient to study the effects of alpha-particle heating.

For detecting the heating by alpha particles, the simplest, least expensive, and most flexible solution is to modify the existing periscope system. A necessary modification is to replace the quartz vacuum window and periscope optics with IR transmitting glass. This is preferably CaF, which transmits well up to $9\,\mu\text{m}$ and also transmits in the whole visible range. The neutron damage threshold for CaF is about 10^6 rad, not as high as fused silica, but high enough to take at least 10^{21} DT neutrons.

With only this change in optical material, keeping the periscope optics at a relatively slow f/8, the minimum detectable temperature using the existing detector is estimated to be ~80˚C. If the optics were improved to f/4, the minimum detectable temperature using the present detector would be reduced to 30˚C so that alpha-particle heating of about 10˚C could be observed. The expected temperature rise due to alpha particle heating over a 1 s high-powered DT pulse is at least $\Delta T \approx 40$˚C.

6.5   Oblique-view measurement of ECE

In order to measure the current produced by LHCD on TFTR, we propose installing an oblique-view ECE radiometer. This type of instrument, which has been developed at PPPL and has been used on PBX-M during LHCD experiments [111], measures the radial distribution, magnitude, and energy of the fast electron distribution from the extraordinary mode emission spectrum just above the second harmonic at an oblique angle to the magnetic field. The LH energy spectrum and location on PBX-M was scanned by slightly varying the magnetic field. Because of the relatively high T_e and low ordinary-mode optical depth, significant areas of the interior had to be covered with a viewing dump.

On TFTR the same type of measurement could be made in a much simpler way. The energy and position would be scanned by changing the angle rather than the field and the $2f_{ce}$ resonance layer would act as a dump for both O and X-modes eliminating the need for installing viewing dumps [112]. In TFTR, the rays travel in nearly straight lines, even in supershots, thereby reducing the need for ray tracing analyses. In order to cover the energy range expected for LH current drive and to obtain spatial resolution for $R > R_0$ where $B_T = 5.0$ T, the frequency range will be $200 - 400$ GHz and the angle between the ray direction and the field will be between 45˚ and 90˚ counter to the plasma current for the $v_{\parallel}$ range expected for LH current drive of 100 ± 30 keV. Radial localization is obtained from modelling the emissivity and from constraints imposed by the second harmonic resonance itself on the inside and the second harmonic resonance condition, $n_{\parallel}^2 + (2f_{ce}/f)^2 \geq 1$, on the outside. Fully relativistic emission codes coupled with ray tracing have been developed to analyze this measurement.

This instrument can be used to study the radial distribution of LH current and the diffusion of fast electrons and will provide additional information for the interpretation of the "normal - 90˚" Michelson interferometer data. If only equilibrium current information is needed, a scanning Michelson instrument, viewing at the angles described above, would be sufficient . However, measurements of fast electron diffusion and MHD effects require a fast scanning heterodyne receiver.

7. Operational Issues for the TFTR-AP Project

7.1 Review of D-T operational history

Experiments with D-T plasmas began in TFTR on 12 November 1993. In the first series of D-T experiments one or more of the neutral beam sources was operated in a mixture of approximately 2% tritium in deuterium. Injection of pure tritium began on 9 December 1993. To date (June 1995), more than 400 plasma shots have been run in which pure tritium was injected by at least one neutral beam source. In addition on some 63 shots, tritium gas has been injected into the plasma. During this period, more than 12,000 total plasma shots have been run, including more than 5,000 shots with NBI heating and 2400 shots with ICRF heating. The neutral beam power has reached a maximum of 39.5 MW and the ICRF power 8.5 MW during D-T operation.

This excellent record of experimental productivity has been achieved under the Conduct of Operations requirements of the Department of Energy Order 5480.19 applicable to a low-hazard nuclear facility.

Following extensive analysis and reviews of the design and present status of the TFTR magnetic field coils, the maximum toroidal field in TFTR was increased during 1994 by 8% (from 73kA to 79kA maximum coil current) for a small number of shots. This was done to take advantage of the improved energy confinement which was achieved in D-T operation through a combination of an apparent favorable scaling of the confinement with hydrogen isotopic mass and developments in lithium conditioning techniques. Raising the magnetic field contributed to the success of the campaign to produce more than 10 MW of D-T fusion power in November 1994.

The TFTR diagnostic set (see Appendix) has continued to perform extremely well in the D-T experiments. A few systems, previously identified as vulnerable, have been adversely affected by the high neutron fluxes during D-T operation but corrections for the effects or alternative sources of the data were generally available. The data from D-T experiments is receiving intensive analysis. All D-T shots have been analyzed by the TRANSP and SNAP codes.

There has been widespread interest in the D-T experiments by the scientific community and the general public. The results have been widely disseminated through articles in refereed scientific journals, in conference proceedings and through invited lectures and colloquia at many scientific institutions.

7.2 Tritium handling

The TFTR Tritium Facility has matured into a safe, dependable system [113]. As of June 1995 more than 550 kCi of tritium have successfully been processed in support of D-T operations. Typically during TFTR D-T runs, up to 20 kCi of tritium are processed per week.

During 1994, there were about 500 "line breaks" (the decontamination and opening to air of a tritium-exposed component or system) performed within the tritium system for maintenance and repair. The total release of tritium up the stack for 1994 was only 139 Curies (Ci), 28% of the 500 Ci established by the TFTR Environmental Assessment (EA) for routine operations and maintenance. The maximum measured annual dose at the site boundary from tritium release was only 1.65×10^{-2} mrem, 0.17% of the limit of 10 mrem per year. The total release of tritium from the Liquid Effluent Collection Tanks during 1994 was 0.29 Ci, 29% of the limit of 1 Ci/year. The site-boundary dose in CY'94 from all sources (direct dose as well as that due to tritium and activated air release) was less than 0.3 mrem, compared with the design limit of 10 mrem per year. A significant portion of the line breaks during CY 94 were the result of infant mortality in newly commissioned equipment, and for incorporation of design improvements. During the first six months of operation this year (CY 95), only 21 Ci of tritium has been released, confirming that as the tritium systems mature during extended TFTR operation, it would be reasonable to expect smaller releases.

7.3 Neutron activation

The neutron-induced radioactivity of the TFTR vacuum vessel and central tokamak structure affects the maintenance and repair of existing equipment and would affect the installation of the new equipment proposed for the TFTR-AP project. The existing D-T operations have provided data on the levels of radioactivity resulting from specific neutron doses and of the distribution of that activity so that plans to minimize personnel exposure can be made for work near the tokamak. Since the start of D-T operations, the yearly radiation exposure for personnel involved in maintenance and repair within the TFTR Test Cell has not increased significantly over the level in the preceding D-only phase due to careful planning of work. The experience gained since November 1993 in planning and executing D-T experiments also allows us to make reasonable projections of the likely production rates for both D-D and D-T fusion neutrons during experimental campaigns. Table 7.1 below shows the projected total fusion neutron production from all TFTR plasma operation planned through September 1998. Note that the dose rates are quoted for contact with the vacuum vessel; the rates drop off very rapidly with distance from the vessel so that even work which requires vessel contact for some operations usually involves much lower average dose rates.

	D-D Neutrons	D-T Neutrons	Contact dose rate at vessel (mrem/hr)	
	(10^{20})	(10^{20})	1-Week Cooldown	2-Year Cooldown
28 February 1995	0.95	2.4	75	n/a
30 September 95	1.0	3.3	125	30
30 September 96	1.2	6.3	162	39
30 September 97	1.4	9.3	183	44
30 September 98	1.6	12.3	200	48

Table 7.1   TFTR fusion neutron production and induced radioactivity at the vacuum vessel. Data are shown to February 1995, projected to the end of FY'95 and through an extension of D-T operation by up to three years at the yearly rate shown.

7.4 Reliability and maintenance of the facility

Throughout the lifetime of TFTR, including D-T operations, availability has steadily improved. The excellent availability results from an effective preventive maintenance program that incorporates experience-driven improvements. There is reason to expect this trend to continue if operation is extended.

Key technical personnel from the TFTR project were requested to survey their areas of responsibility for potential reliability problems, different from current experience, that might surface during extended operation. They were asked to categorize results of projected failure modes into the four risk-associated topics listed below:

(1)   A new scenario for an accidental tritium release not covered in the TFTR Final Safety Analysis Report (FSAR) [114];

(2)   An increased probability of an accidental tritium release scenario described in the FSAR;

(3)   An increased probability of a long (>1-month) downtime for repair;

(4)   An increased rate of "normal" failures that would result in a significant reduction of TFTR availability.

The general results of the survey are summarized below:

- New preventive maintenance (PM), including equipment replacement, is recommended for aging systems in the computer and facility-infrastructure areas. Projected problems with the equipment identified by respondents would result in reduced TFTR availability, but would not involve tritium releases or other ES&H concerns. The costs of the recommended PM can be accommodated within a reasonable operating budget.

- Risks associated with the tokamak structure and coils have been analyzed extensively to support current operations. The risks are essentially the same for extended operation as for current operation, and new analyses are not required.

The specific issues discussed below have been highlighted because neutron activation or tritium contamination would make repairs difficult, or the systems would be difficult to replace.

Coil Coolant Leaks

There are 16 coolant fittings for each of the 20 toroidal field (TF) coil assemblies. Prior to D-T operations, 6 of the TF coil assemblies developed cooling water leaks, associated with the fittings, that prevented operation until repairs were made. The leaking water provided a conductive path (electrical leakage) that reduced coil resistance to ground. Although leak repairs were successful, a reliability upgrade, incorporated prior to D-T operation, has prevented the problem from recurring. For cooling the TF coil water has been replaced with an inert fluid, Fluorinert™ (perfluoro-heptane) whose increased electrical resistivity prevents the deleterious effects of water leaks. While TFTR could operate indefinitely with small Fluorinert™ leaks, it is prudent to repair an unstable leak that grows to a significant loss of fluid per day. Such behavior may be a symptom of worsening mechanical degradation to a coil fitting that could result in a more serious failure. Recently, it has been demonstrated that it is possible to perform a local repair on a cooling connector with approximately two weeks of downtime. The effectiveness of this repair is now being assessed.

Shim Blocks

Shim blocks are associated with the clips that attach the TF coils to the internal support structure (ISS). The set of 40 shim blocks (2 per coil, 10 per quadrant) provide pre-load for the ISS to offset coil forces. The shim blocks are wedged into place and held with small bolts.

In 1985, inspection showed 13 "loose" shim blocks. When they become loose the blocks become displaced and may eventually fall out. The inspection showed that 5 blocks had fallen out and 8 were displaced. Regular inspection and maintenance was initiated. Blocks that had fallen out completely and the displaced blocks were replaced with a new design that appears to be successful. Since 1990, only two shim blocks have fallen-out completely. However, because of their location, repair of a lost shim block now would involve personnel exposure to the high radiation field directly under the activated TFTR structure.

Analysis shows that operation within design margins is possible with 7 (of 10) shim blocks per quadrant, providing no more than 2 contiguous shim blocks are missing in any quadrant and no more than 1 (of 2) missing on any TF coil. The design review process for 6-Tesla operation considered operation with less than a full complement of shim-blocks. It is unlikely that an unacceptable configuration of missing shim blocks would occur for three years of extended operation, based on experience since 1990 with the current shim block design.

Loose TF Coil Case Bolts

During the years of TFTR operation, a number of the bolts holding together the TF coil cases became loose. Some of these bolts are difficult to access. An analysis of the TF coil, case and support structure was performed considering a severe worst case scenario of loose bolts, *i.e.*, more than had been identified. The analysis determined that TFTR could operate at 5.2 T toroidal field. As part of the preparation for D-T operations, special remotely operated tooling was developed, and the bolts were tightened. After 6 months of D-T operation, the bolts were inspected and a small number were found to have loosened.

Machine stresses were analyzed as part of the investigation to increase the TF field from 5.2 to 6 T. The analysis, which assumed a severe loose-bolts condition, *i.e.* more loose bolts than has actually occurred, showed that 6-Tesla operation for 1000 pulses was allowable within design margins.

Machine activation during D-T operation makes the use of the existing bolt tightening tools undesirable because personnel using the tools must be on the activated structure. If, during extended operation, the worst-case condition was reached, then operations would be constrained to a lower stress level. It is unlikely that new tooling, which allowed operators to be further from the activated structure, could be developed because of cost and the long development time. However, extrapolation of actual experience, from the time the bolts were tightened to the inspection after 6 months D-T operations, indicates that the worst case will probably not be reached during three years of extended operations.

In-Vessel Components

TFTR has operated at record power levels during D-T operations. The quality of the plasma remains high, an indication that there is no significant damage to plasma facing components. This is verified by inspection through port windows.

If TFTR operation is extended, it would be possible to enter the vacuum vessel for an inspection and for minor repairs. A plan for entry into the vacuum vessel, with minimal equipment removal, has been formulated. Entry is possible through a neutral beam duct after removal of the calorimeter or by removing an ICRF antenna. A specially designed platform would assist personnel wearing bubble suits. Radiation exposure for the entry crew could be kept within DOE limits.

Vacuum Vessel Integrity

There is no trend of degradation in TFTR leak tightness. A trend of increasing numbers of small leaks should happen long before the structural integrity of the vacuum vessel is threatened. The vessel has now been under vacuum for more than two years continuously with only two leaks, one of which was minor. Last September, a significant leak caused by damage to an internal weld by energetic plasma particles excited by ICRF heating was successfully repaired. The design of the vacuum vessel was based upon 300,000 full-power pulses including 4,000 full-power D-T pulses. At the end of FY'95

the number of full-power D-T pulses will reach about 450. After three years of extended operation, the number of full-power D-T pulses will be approximately 1200. Extended operation will, therefore, not challenge the vacuum vessel design life. Materials degradation is discussed below. The margin for cumulative neutron exposure for the Vacuum Vessel is 50,000 times the February 1995 level, far better than needed.

Neutral Beam Heating System

Neutral Beam availability during D-T operations improved over the non-tritium availability performance. Some sub-systems have failed, but personnel were able to make repairs or substitute spares quickly even with the constraints of handling tritium contaminated equipment. Because essentially all of the neutral beam source and supporting systems are maintainable, it is planned to use them on TPX after TFTR. It is reasonable to expect continuation of the current availability performance during extended operations.

Motor-Generator Sets

The two motor-generator (MG) sets have achieved an availability of 99% for the last three years. Through FY'94, the sets used only 6% of their life expectancy for number of pulses and 19% for number of start/stop cycles.

An increase in MG output voltage is required to support 6-Tesla operation. An analysis estimated that 8% of the MG lifetime would be expended to support each 1000 pulses at 6 T. MG reliability is not considered to be an issue for extending TFTR operation for three years.

Materials Exposure to Neutrons

The TFTR vacuum vessel assembly has been designed to withstand a total integrated radiation dose of 5×10^7 Rad, equivalent to about 1.5×10^{22} D-T neutrons. That dose will not be exceeded for three years of extended operation.

An estimate has been made of the neutron irradiation levels through February 1995 for some of the critical components of TFTR, and those levels have been compared those at which noticeable radiation damage occurs. A noticeable effect may not, necessarily, be detrimental to the function performed by the material. For each component analyzed, the ratio of the noticeable effect level (called the "significance level") to the February 1995 level was calculated. That ratio, called the "margin", indicates how many times the February 1995 total neutron exposure level would be necessary before that component would experience a noticeable effect. Table 7.2 shows the components analyzed and the resulting margins.

Component	Margin at Feb. 95
First Wall (graphite)	5×10^3
Vacuum Vessel (SS 304L)	5×10^4
Coil Conductor	5×10^2
Coil Insulation	25
Coil Insulation (epoxy)	1×10^2

Table 7.2   Margins for potential effects of irradiation by fusion neutrons on several critical components in the TFTR structure. The margins are calculated for the neutron irradiation produced through February 1995.

Extended operation for 3 years after FY95 will increase the neutron total exposure to less than 4 times the February 1995 level. Since the lowest critical component margin is 25 (for coil insulation), a 4-times increase in total exposure after 3 years of extended operation will not cause noticeable induced irradiation effects. Note that the coil insulation margin of 25 is derived from test data that is questionable because there was no control sample, and the margin of 100 for epoxy may be more accurate.

7.5 Installation of new systems

The installation of the LHCD and new ICRF couplers proposed for the TFTR-AP project would require a vacuum vessel vent and the removal of several of the large port flanges. Some of the important diagnostic upgrades being considered also require removal of smaller vacuum flanges. However, entry to the vacuum vessel, while feasible, would not be required for the extension as presently envisaged. Use of appropriate tools, careful planning of the work and training of the personnel involved would all be used to minimize radiation exposure and the possibility of tritium contamination. Much of the work would be in areas well away from the central structure where the radiation field is much lower.

7.6 New Contributions of TFTR-AP to reactor technology

7.6.1 Tritium technology

TFTR has pioneered techniques for routinely handling tritium in the environment of a research tokamak and valuable experience continues to be gained. Solutions to problems in handling tritium in this environment, including tritium monitoring, tritium accountability and plasma exhaust processing, continue to be developed. Real-time tritium monitoring in a mixed ionizing radiation field, accompanied by magnetic fields (>100 Gauss) has been successfully achieved. A comprehensive

tritium inventory control program has been developed. Plasma exhaust and neutral beam regeneration gases are routinely processed.

The Tritium Systems Division is currently commissioning the Tritium Purification System (TPS) which will recycle tritium back to the uranium storage beds in the Tritium Storage and Delivery System for reuse in TFTR, thus significantly reducing tritium shipments to PPPL. The TPS will also reduce the number of disposable molecular-sieve beds, on which the tritium is currently absorbed after passing through the plant, which will be shipped off site for final disposal.

A current issue for the ITER-EDA concerns the possibility of using carbon for plasma facing components. The critical issue is tritium retention in and the removal of co-deposited layers that will inevitably form in a device like ITER, even if a small area of carbon is used. TFTR offers a unique opportunity examine this in a reactor-like environment. For example, the influx to the plasma of tritium deposited in the toroidal carbon limiter has now been measured spectroscopically in TFTR [115]. The D-T neutron flux may alter the trapping sites in carbon, making TFTR uniquely suited to experiments on the retention of tritium by carbon in a reactor environment. Studies of tritium removal techniques will be particularly relevant to operation of ITER with carbon plasma facing materials.

7.6.2 Tritium pellet injector

During the TFTR-AP project, it is proposed to install the tritium pellet injector (TPI). This project would be developed in collaboration with the Oak Ridge National Laboratory. The use of tritium pellets for fueling could lead to a substantial reduction in the total tritium inventory for ITER [88]. The experimental plan for using the TPI has been described in Sec. 5.1.

7.6.3 Folded Waveguide ICRF antenna

The folded waveguide antenna is under development at ORNL and PPPL as an advanced ICRF launcher that has several potential advantages for reactor relevant applications such as ITER and can also provide significant additional capabilities to the TFTR ICRF heating system. A key advantage of the FWG is the ability to operate at very high power density, in principle five times higher than conventional loop-type antennas. The FWG antenna is a fixed-frequency resonant waveguide structure that places very high RF magnetic fields at the plasma edge while keeping high internal electric field regions well removed form the plasma. The resulting all-metal structure is quite strong, has excellent array properties, operates at very high power, and is expected to provide superior RF-plasma coupling for both Fast Wave (FW) and Ion-Bernstein wave (IBW) launch. FWG tests at ORNL have achieved 1.1 MW operation into a low density plasma under conditions which typically limit loop antenna of similar cross section to five times lower power. This capability can be exploited on ITER where the plasma-wall separation must be much greater which results in very low plasma antenna loading and consequently low coupled power density. A shift to in-port type ICRF antenna designs for ITER

coupled with the requirement of high delivered power has made a high-power density antenna design, such as the FWG, very attractive. Calculations indicate that an array of 8 FWG launchers installed into a single port on ITER is capable of delivering 50 MW of ICRF power to the plasma. The FWG has been shown to provide excellent array performance due to very low mutual coupling between adjacent units. An array of FWG antennas can also be phased to launch nearly any spectrum including a low $k_{||}$ $0-\pi/2-\pi-3\pi/2$ current drive spectrum. Alternatively, the FWG can provide a $0-\pi$ (dipole) launch spectrum from a single antenna by substitution of a alternate face plate design.

The need for a particularly large port for the FWG at lower frequencies and acceptable performance from existing loop antenna designs (which also offer variable frequency operation) has so far limited testing of the FWG to low density plasmas on the RF Test Facility at ORNL. To gain further acceptance of the FWG for ITER, a high power test on a high density tokamak plasma is required. TFTR provides an outstanding opportunity to further develop the FWG due to the large ports available, the high power ICRF systems installed and the advanced diagnostic support available. The FWG can also benefit TFTR operation significantly by providing higher power density, an improved IBW launcher, and possibly an improved in-port FW current drive launch capability.

A 58 MHz, 0.31×0.31 m folded waveguide antenna and associated vacuum enclosure suitable for installation on TFTR is being designed and fabricated at ORNL and will be available for installation in January 1996. This waveguide is also compatible with PBX-M and can be installed and operated on either device. This FWG is capable of operating at >4 MW and can be installed as either a FW or IBW launcher by 90° rotation. Hardware for retraction and vacuum isolation of the antenna has been incorporated into the design to facilitate this rotation as well as maintenance tasks. Several experimental scenarios have been proposed for this antenna on TFTR. At 58 MHz, 5 MW of power is currently available on TFTR by combining the power from 2 transmitters. With TFTR operating at 5.6 T, $2\Omega_T$ (second-harmonic tritium) and Ω_{He3} (fundamental helium-3) minority ion heating modes are available as well as $2\Omega_T$ IBW launch for heating and transport control experiments. Additionally, $2\Omega_D$ and $2\Omega_{He4}$ heating modes are available at 3.74 T as well as direct electron heating at other field values.

In FY96, the 58 MHz FWG will be installed on TFTR and both FW and IBW heating experiments carried out as well as demonstration of the FWG capabilities for ITER such as high power coupling studies with large plasma edge separation. The FWG will be installed with a vacuum isolation valve and will be retractable for rotation, modification or upgrading without breaking TFTR vacuum. To reach the full power capability of this antenna, the power from two transmitters will be combined into one feed.

During the first year of operation, an improved 1×2 or 1×4 FWG array which utilizes the entire available Bay K port area will be scoped out as a collaboration between ORNL and PPPL. This upgraded FWG design could provide the option of fabricating an ITER relevant configuration with the desired launch spectral control needed for a wide range of ICRF experiments on TFTR including FW

current drive and IBW pressure profile control. Using the entire port area with multiple FWGs could potentially increase the power capability to >25 MW and the improved launch spectrum available from a phased toroidal array of FWGs would enhance the ICRF performance significantly. An additional 5 MW of ICRF power could be provided by retuning two fixed-frequency transmitters to match the FWG making a total of 10 MW available.

8. Cost

While this proposal is being submitted to the Department of Energy, Congress is debating the FY'96 fusion budget. There are strong pressures to decrease government spending and in particular to decrease the funding for fusion research. In response to the uncertainty in the budgets, two proposed budgets have been developed. The first is to continue operating TFTR two full shifts with supporting activities on third shift and weekends. The requested budget for FY'96 for Confinement Systems is $63M compared with a projected spending of $66.9M this year as shown in Table 8.1. The budget requests for both FY'97 and FY'98 are also less than this years as shown in Table 8.2. The second budget corresponds to a reduced level of operations. The run day, including startup and beam conditioning, would be reduced from 16 to 12 hours, and the time allocated to maintenance activities increased from 1 week per four run weeks to 1 week per three run weeks. Furthermore, supporting activities on weekends and third shift such as beamline regenerations and tritium processing would be nearly eliminated. The impact of this budget option is to reduce the number of shots by about 30% relative to the base case as shown in Table 8.3. In this option, the funding for operations and maintenance in FY'96 is reduced from $59.3 to $50M and the overall budget is reduced from $66.9M to $56.M as shown in Tables 8.1 and 8.4. This option is consistent with the intent of the PCAST recommendations. Both budget options are aggressive and assume increases in productivity based on the experience with tritium operation during the past two years. Neither option has funds for management reserve consistent with operations of other tokamaks in the U.S. If problems were to develop, operations would stop and the personnel would be reassigned from operations to address the problem. The costs for various upgrades are explicitly identified. The values quoted are the incremental costs of fabricating and purchasing the upgrade. Labor, which is covered during run periods under operations and maintenance, is used to design, install and test the upgrade; these labor costs are not included in the upgrade costs. By decreasing the number of run weeks relative to this year's operation, labor was made available to develop the upgrades listed in a cost effective manner.

In response to the request by the Department of Energy, a schedule and cost estimate for a one year extension have also been developed as shown in Fig. 8.1 and Table 8.5. Since this would be the last year of operations on TFTR, the request is for full operations to make maximum use of the facility.

In these analysis, the G&A rate was assumed to be same as that used in the Field Work Proposal submissions. Due to the lack of a comprehensive funding profile for the entire Laboratory, it is not meaningful to refine the indirect cost distribution further at this time. In addition in the weeks ahead, the Laboratory will discuss with the Department of Energy proposals to decrease the indirect costs through regulatory relief.

Table 8.6 shows the allocation of experimental time amongst the topics discussed in this proposal.

Table 8.1

TFTR Three-Year Extension, FY-96

Funding: Oper & Eqpt $(M) as spent

		FY-94	FY-95	FY-96 Baseline	FY-96 Alternate
TFTR Ops & Maint					
Diagnostics					
1301	Diagnostics	8.5	6.8	6.8	6.0
Physics Program					
1310	Physics	7.4	7.7	7.7	6.8
Tokamak Operations					
1335	Computer Facility	4.4	4.5	4.5	3.9
1350	Tokamak Operations	13.0	9.5	9.5	8.6
	Energy	9.6	4.5	3.6	2.9
1361	ICRF Physics Ops & Dev	1.0	1.1	1.1	.8
Tritium Systems Division					
1392	Tritium Systems Ops	9.6	8.7	8.6	7.8
	Savannah River Plant	.0	1.6	.7	.6
Heating Systems					
1345	Neutral Beams	9.8	9.1	8.1	7.9
1349	Power Systems	6.9	5.8	5.7	4.7
TFTR Ops & Maint Subtotal		**70.2**	**59.3**	**56.3**	**50.0**
TFTR Upgrades					
Current Profile Modification					
LH Antenna UG (to 1.3 MW)				2.0	1.5
Extend NB Pulse Length				.1	.1
MSE Upgrade				.2	.2
Digital Control System				.1	.1
	Subtotal			2.4	1.9
Pressure Profile Modification					
Ion Bernstein Wave				.3	.3
Poloidal Rotation Diagnostic				.3	.3
Laser Ablation of Li				.1	.1
LPI Upgrade (8 pellets)				.2	.0
	Subtotal			.9	.7
Alpha-Particle Physics Studies					
ICRF Frequency Change				.4	.4
ICRF Antenna Modifications				.6	.6
	Subtotal			1.0	1.0
Fusion Technology					
Folded Wave Guide Port				.2	.2
Tritium Pellet Injector				.2	.2
Tritium Purification System		1.0	3.0	.0	.0
	Subtotal	1.0	3.0	.4	.4
TFTR Upgrades Total		**1.0**	**3.0**	**4.7**	**4.0**
S&R		**5.1**	**2.7**	**.0**	**.0**
PPPL Subtotal		**76.3**	**65.0**	**61.0**	**54.0**
Other Labs and Univ Subtotal		**2.6**	**1.9**	**2.0**	**2.0**
TOTAL CONFINEMENT SYS. FUNDING		**78.9**	**66.9**	**63.0**	**56.0**
TOTAL ERWM FUNDING (CONTAINERS)		**1.1**	**.6**	**.6**	**.6**
TOTAL		**80.0**	**67.5**	**63.6**	**56.6**

TFTR-AP Proposal

Table 8.2
TFTR Three-Year Extension FY-95 through FY-98, Baseline

Funding: Oper & Eqpt $(M) as spent

TFTR Ops & Maint	FY-95	FY-96	FY-97	FY-98
Diagnostics				
1301 Diagnostics	6.8	6.8	7.1	7.4
Physics Program				
1310 Physics	7.7	7.7	8.0	8.3
Tokamak Operations				
1335 Computer Facility	4.5	4.5	4.7	4.9
1350 Tokamak Operations	9.5	9.5	9.9	10.3
Energy	4.5	3.6	4.0	3.9
1361 ICRF Physics Ops & Dev	1.1	1.1	1.1	1.2
Tritium Systems Division				
1392 Tritium Systems Ops	8.7	8.6	8.9	9.3
Savannah River Plant	1.6	.7	.7	.8
Heating Systems				
1345 Neutral Beams	9.1	8.1	8.4	8.8
1349 Power Systems	5.8	5.7	5.9	6.2
TFTR Ops & Maint Subtotal	**59.3**	**56.3**	**58.8**	**60.9**
TFTR Upgrades				
Current Profile Modification				
LH Antenna UG (to 1.3 MW)		2.0	.8	.0
LH Antenna UG (to 2.6 MW)		.0	1.8	.2
Extend NB Pulse Length		.1	.0	.0
NB Reconfiguration		.0	.6	1.4
MSE Upgrade		.2	.0	.0
Oblique ECE		.0	.3	.0
Digital Control System		.1	.1	.0
Subtotal		2.4	3.6	1.6
Pressure Profile Modification				
Ion Bernstein Wave		.3	.0	.0
Poloidal Rotation Diagnostic		.3	.0	.0
Laser Ablation of Li		.1	.0	.0
NB Reaiming		.0	.1	.0
LPI Upgrade (8 pellets)		.2	.0	.0
Subtotal		.9	.1	.0
Alpha-Particle Physics Studies				
IR Periscope		.0	.3	.0
ICRF Frequency Change		.4	.0	.0
ICRF Antenna Modifications		.6	.0	.0
Subtotal		1.0	.3	.0
Fusion Technology				
Folded Wave Guide Port		.2	.0	.0
Tritium Pellet Injector		.2	.4	.0
Tritium Purification System	3.0	.0	.0	.0
Subtotal	3.0	.4	.4	.0
TFTR Upgrades Total	**3.0**	**4.7**	**4.4**	**1.6**
S&R	**2.7**	**.0**	**.0**	**1.0**
PPPL Subtotal	**65.0**	**61.0**	**63.2**	**63.5**
Other Labs and Univ Subtotal	**1.9**	**2.0**	**2.0**	**2.0**
TOTAL CONFINEMENT SYS. FUNDING	**66.9**	**63.0**	**65.2**	**65.5**
TOTAL ERWM FUNDING (CONTAINERS)	**.6**	**.6**	**.6**	**.6**
TOTAL	**67.5**	**63.6**	**65.8**	**66.1**

Table 8.3

Planned Plasma Shots

	FY-96	FY-97	FY-98
Baseline	5600	6400	5600
Alternate	3800	4200	3800

Table 8.4
TFTR Three-Year Extension FY-95 through FY-98, Alternate

Funding: Oper & Eqpt $(M) as spent

TFTR Ops & Maint		FY-95	FY-96	FY-97	FY-98
Diagnostics					
1301 Diagnostics		6.8	6.0	6.2	6.5
Physics Program					
1310 Physics		7.7	6.8	7.1	7.4
Tokamak Operations					
1335 Computer Facility		4.5	3.9	4.1	4.2
1350 Tokamak Operations		9.5	8.6	8.9	9.3
Energy		4.5	2.9	3.2	3.1
1361 ICRF Physics Ops & Dev		1.1	.8	.8	.9
Tritium Systems Division					
1392 Tritium Systems Ops		8.7	7.8	8.1	8.4
Savannah River Plant		1.6	.6	.6	.6
Heating Systems					
1345 Neutral Beams		9.1	7.9	8.2	8.5
1349 Power Systems		5.8	4.7	4.9	5.1
TFTR Ops & Maint Subtotal		**59.3**	**50.0**	**52.2**	**54.0**
TFTR Upgrades					
Current Profile Modification					
LH Antenna UG (to 1.3 MW)			1.5	1.3	.0
LH Antenna UG (to 2.6 MW)			.0	1.8	.2
Extend NB Pulse Length			.1	.0	.0
NB Reconfiguration			.0	.6	1.4
MSE Upgrade			.2	.0	.0
Oblique ECE			.0	.3	.0
Digital Control System			.1	.1	.0
	Subtotal		1.9	4.1	1.6
Pressure Profile Modification					
Ion Bernstein Wave			.3	.0	.0
Poloidal Rotation Diagnostic			.3	.0	.0
Laser Ablation of Li			.1	.0	.0
NB Reaiming			.0	.1	.0
LPI Upgrade (8 pellets)			.0	.2	.0
	Subtotal		.7	.3	.0
Alpha-Particle Physics Studies					
IR Periscope			.0	.3	.0
ICRF Frequency Change			.4	.0	.0
ICRF Antenna Modifications			.6	.0	.0
	Subtotal		1.0	.3	.0
Fusion Technology					
Folded Wave Guide Port			.2	.0	.0
Tritium Pellet Injector			.2	.4	.0
Tritium Purification System		3.0	.0	.0	.0
	Subtotal	3.0	.4	.4	.0
TFTR Upgrades Total		**3.0**	**4.0**	**5.1**	**1.6**
S&R		**2.7**	**.0**	**.0**	**1.0**
PPPL Subtotal		**65.0**	**54.0**	**57.3**	**56.6**
Other Labs and Univ Subtotal		**1.9**	**2.0**	**2.0**	**2.0**
TOTAL CONFINEMENT SYS. FUNDING		**66.9**	**56.0**	**59.3**	**58.6**
TOTAL ERWM FUNDING (CONTAINERS)		**.6**	**.6**	**.6**	**.6**
TOTAL		**67.5**	**56.6**	**59.9**	**59.2**

Figure 8.1

Table 8.5
TFTR One-Year Extension FY-96

Funding: Oper & Eqpt $(M) as spent

	FY-94	FY-95	FY-96 Baseline
TFTR Ops & Maint			
Diagnostics			
1301　Diagnostics	8.5	6.8	6.8
Physics Program			
1310　Physics	7.4	7.7	7.7
Tokamak Operations			
1335　Computer Facility	4.4	4.5	4.5
1350　Tokamak Operations	13.0	9.5	9.5
Energy	9.6	4.5	3.6
1361　ICRF Physics Ops & Dev	1.0	1.1	1.1
Tritium Systems Division			
1392　Tritium Systems Ops	9.6	8.7	8.6
Savannah River Plant	.0	1.6	.7
Heating Systems			
1345　Neutral Beams	9.8	9.1	8.1
1349　Power Systems	6.9	5.8	5.7
TFTR Ops & Maint Subtotal	**70.2**	**59.3**	**56.3**
TFTR Upgrades			
Current Profile Modification			
Extend NB Pulse Length			.1
MSE Upgrade			.2
Digital Control System			.1
Subtotal			.4
Pressure Profile Modification			
Ion Bernstein Wave			.3
Poloidal Rotation Diagnostic			.3
Laser Ablation of Li			.1
LPI Upgrade (8 pellets)			.2
Subtotal			.9
Alpha-Particle Physics Studies			
ICRF Frequency Change			.3
ICRF Antenna Modifications			.6
Subtotal			.9
Fusion Technology			
Folded Wave Guide Port			.2
Tritium Pellet Injector			.2
Tritium Purification System	1.0	3.0	.0
Subtotal	1.0	3.0	.4
TFTR Upgrades Total	**1.0**	**3.0**	**2.6**
S&R	**5.1**	**2.7**	**.0**
PPPL Subtotal	**76.3**	**65.0**	**58.9**
Other Labs and Univ Subtotal	**2.6**	**1.9**	**2.0**
TOTAL CONFINEMENT SYS. FUNDING	**78.9**	**66.9**	**60.9**
TOTAL ERWM FUNDING (CONTAINERS)	**1.1**	**.6**	**.6**
TOTAL	**80.0**	**67.5**	**61.5**

Table 8.6

Allocation of run time

	FY'96 21 weeks	FY'97 24 weeks	FY'98 21 weeks
High reactivity and MHD stability	35%	40%	45%
Pressure profile modification techniques(CH-mode)			
Current profile modification techniques			
Improved limiter conditioning schemes			
MHD activity and disruptions in reactor-like conditions			
20MW of fusion power			
Alpha-particles in reactor-like conditions	25%	25%	30%
Interactions of alpha-particles with MHD and ripple			
Alpha-particle physics in advanced D-T plasma regimes			
Alpha-particle heating experiments			
Controlling alpha-particle thermalization			
Controlling alpha transport with magnetic perturbations			
IBW interaction with alpha particles			
Heating and thermal transport of the plasma	20%	15%	15%
Isotope scaling			
Transport in reversed-shear plasmas			
Tests of IFS/PPPL transport model			
Effect of the electric field shear on transport			
H-mode confinement studies			
Non-dimensional scaling of transport			
Density scaling of particle transport			
Magnetic field scaling of transport			
Core fueling and power handling	20%	15%	10%
Simulation of ITER fueling with pellets at high density			
Edge power flux control with a radiating mantle			
Folded waveguide			

9. Collaborator Participation

A strength of the TFTR D-T program has been the strong participation of collaborators from other Institutions both within the U.S.A. and abroad. Scientists from nineteen different institutions have participated in the D-T experiments. Collaborating scientists have taken a lead role in many of the experiments. It is most important that this participation be continued and extended.

Personnel from Oak Ridge National Laboratory have participated in the experimental program, particularly in evaluating the profiles of edge density important to the matching of ICRF to the plasma, in measurement of alpha-ash transport, in leading the studies of H-mode plasmas and also in providing hardware for the experiments. These activities should continue, while, in addition, ORNL provides new hardware for the pellet injector reconfiguration to handle tritium and the development of the folded wave-guide antenna as described in Sections 5.1 and 7.6.3 respectively. The pellet injector program relates closely to ITER R&D needs, and using it to test isotopic tailoring of the pellet constituents as a method of inventory control will be very valuable. The folded wave-guide antenna relates to the development of a high power density ICRF launcher for ITER.

The measurements of alpha-particles and neutrons have been strongly enhanced by the groups from General Atomics and the Ioffe Institute in Russia providing the first measurements of the high-energy confined alpha-particles using a neutral particle analyzer in conjunction with lithium-pellet injection. (This pellet-injector was provided by MIT). Recent exciting results using boron pellets have allowed measurements further in to the plasma core where the alpha-particles are born. This work will be extended to develop an understanding of the confinement of these high energy particles, particularly in the presence of sawteeth and other MHD activity. As the alpha-particles slow down to the energy range below about 600 keV, a spectrometer developed at the University of Wisconsin has been used to examine the confinement properties and this physics study by Wisconsin staff will be continued. They have proposed techniques for improving the signal-to-noise ratio of the instrument and this enhancement will provide a valuable test of a measurement capability for ITER. A group from MIT has been working with people at Lodestar and at JET on a low-power collective scattering system for measuring a large fraction of the alpha-particle energy spectrum and are now evaluating initial results. This experiment, related as it is to the much higher power capability recently applied at JET, is an important measurement of the confined alphas but also should provide an important validation of the theoretical basis. A small time-of-flight 14 MeV neutron spectrometer has been used by a group from NIFS in Japan and its capabilities are only just being demonstrated; it will complement the other neutron measurements. This detector and a diamond detector, recently demonstrated by the TRINITI (Russia) group, are both candidates for doing spatially-resolved ion-temperature measurements in ITER.

In addition to very significant operational leadership on the neutron activation system on TFTR, people from Los Alamos National Laboratory have been very instrumental in doing component testing in the reactor-relevant nuclear environment. They have exposed material samples for the UCLA group evaluating activation for ITER and are examining "radiation-hard" Hall-probes, to determine their capability for measuring "steady-state" magnetic fields. This groups is interested in expanding on their neutron-detector development (they trouble-shot and calibrated their scintillating-fiber detector on TFTR) and magnetic measurement techniques heading to systems capable of operating on ITER or TPX. The UCLA group is interested in continuing their neutronic studies on TFTR studying different materials as well as benchmarking their codes.

TFTR's D-T transport physics results, due to the strong combination of transport and fluctuation diagnostics and analysis codes, have led to the participation of many theorists in the experimental program. The IFS/PPPL model has so far successfully described the performance of L-mode TFTR plasmas, and its capability is being extended to incorporate electron dynamics to address particle transport and the role of convection in the core of supershot plasmas. The University of Wisconsin group has developed the beam emission spectroscopy diagnostics which are a very important element of the proposed transport studies and are interested in continuing to participate in these experiments. MHD studies at Wisconsin and Kurchatov have been extremely supportive and should continue. The improvement of performance without terminating in a disruption is a goal in which theory and experiment must be combined. The General Atomics group and the UCI group have conducted experiments on the effects of alpha particles on MHD stability and this valuable work should be encouraged. One potential experimental area is feedback control of external kinks and kink-ballooning modes using modulated ICRF, where a collaboration with Columbia University is proposed.

A group from Columbia has already led the pioneering studies of high-β_p plasmas in TFTR with very high energy confinement enhancement factors. This series of experiments has provided very encouraging results in D-T and should extrapolate to even better performance.

There have been strong contributions to the TFTR program in experimental planning, physics analysis and diagnostic operation from the teams at the JET and JT-60U devices. The JET collaboration will be especially significant as they prepare for their own D-T program at the end of 1996, for which TFTR's results and operational methods will provide significant guidance. Detailed studies of radiation effects on fiber optics have already been done on TFTR for the JET program. The alpha-particle studies will be of importance to the JT-60U group preparing for their experiments with a high energy, negative-ion based, neutral beam.

In the cost summary in the previous section, an allocation based on this year's funding was made to continue the participation of collaborations on TFTR.

10.   Summary

The TFTR Advanced Performance project planned for the fiscal years 1996 – 1998 will provide a wealth of data on issues for the next generation of experiments being planned to investigate ignited D-T plasmas. The existing capabilities of TFTR for producing highly reactive D-T plasmas in conditions prototypical of a reactor will be extended by a set of modest upgrades and additional equipment to explore regimes of advanced tokamak performance as yet only glimpsed. In these regimes it will be possible to study the behavior of D-T fusion alpha particles, particularly their loss, thermalization and transport, upon which the achievement of ignition ultimately depends. The possibilities for using hot-ion D-T plasmas to achieve substantial self-heating as a route to ignition in a reactor will be investigated, as will means of controlling alpha-particle heating and transport through wave interactions of the plasma. Fundamental studies of plasma transport and stability in a wide range of plasma regimes will continue using the unsurpassed TFTR diagnostic set, modified or upgraded, where appropriate, for the new regimes. Issues of fueling and density limits will be investigated in support of ITER. Finally, there will be substantial technological benefits from continuing to run a major tokamak facility with D-T fuel. Table 9.1 summarizes the upgrades proposed for the TFTR-AP project and their impact on the major issues for tokamak research which were identified in Sec. 1.

This program will be accomplished within a tightly constrained budget which makes maximal use of the existing facilities and of the experience already gained in D-T operation. Collaboration with a range of institutions will continue to ensure the most effective use of expertise in the fusion community, the widest participation in the experiments and rapid dissemination of the results.

Table 9.1

Relationship of Proposed Upgrades to Program Elements

D indicates a direct and **I** an indirect contribution to the program element

	Stability and Reactivity		Alpha physics	Transport	Core fueling	Technology
	J(r) control	p(r) control				
LHCD	**D**		**I**	**I**	**I**	
Extend NB Pulse	**D**		**I**	**I**	**I**	
IBW		**D**	**I**	**D**	**D**	
ICRF Frequency Change	**D**		**D**	**I**		
ICRF 4-Strap Antennas	**D**		**D**			
Folded Waveguide		**I**	**I**			**D**
Tritium Pellet Injector		**I**	**I**		**D**	**D**
Laser Lithium Ablation		**D**	**I**	**D**	**I**	**D**
LPI Upgrade		**D**	**I**	**D**	**I**	
NB re-aiming		**D**	**I**	**D**	**I**	
NB re-configuration	**D**		**I**	**I**		
Poloidal Rotation		**D**		**D**		
MSE Upgrade	**D**		**D**	**D**		
Control System Upgrade	**D**	**D**	**I**			**D**
IR Periscope Upgrade			**D**			**I**

Appendix

Plasma Diagnostics for D-T Operation

| **Diagnostic System**
(listed for its primary use) | **Configuration for D-T Operation** |

Electron Temperature and Density

TV Thomson Scattering (TVTS)	two midplane, 76 point radial points,
ECE Heterodyne Radiometer	horizontal midplane scan, 4 ms scan, 4 – 10 cm res.
ECE Fourier Transform Spectrometer	15 ms scan, 2 – 6 cm res.
ECE Grating Polychromator	20 point horizontal midplane radial profile
Multichannel Far Infra-Red Interferometer (MIRI)	10 vertical chords

Ion Temperature

X-ray Crystal spectrometer	horizontal chord (point)
Charge Exchange Recombination Spectroscopy (CHERS)	18 channel array

Impurity Concentration

Visible Bremsstrahlung Array	16 chord tangential horizontal array, 18 chord (HAIFA) poloidal array. 4 toroidal locations
VUV Survey Spectrometer (SPRED)	radial view in horizontal midplane
Multichannel Visible Spectrometer	4 views with fiber optics
Pellet polychromator	1 vertical location, 1 horizontal view
X-ray Pulse Height Analysis (PHA)	horizontal chord

Radiated Power

Tangential Bolometers	16 chord counter-viewing, 2 chord co-viewing array
Bolometer Arrays	19 horizontal radial view, 19 vertical. chords
Wide-Angle Bolometers	6 toroidal locations

Neutrons and Alpha-particles

Epithermal Neutrons	6 toroidal locations with different sensitivities
Neutron Activation Detector	7 toroidal locations, with 1 reentrant top location
14 MeV Neutron Detectors	1 toroidal location
Neutron Fluctuation Detector	6 locations
Collimated Neutron Spectrometer	1 toroidal location
Multichannel Neutron Collimator	10 vertical channels; D-D and D-T sets of detectors
Lost Alpha/Triton Array	3 poloidal detectors, 1 movable near-midplane probe
Fast Neutron Scintillation Counters	Horizontal midplane
Gamma Spectrometer	Horizontal view
Alpha-Charge-Exchange Analyzer	Horizontal midplane view (with Lithium Pellet Injector)
Alpha-Charge-Exchange Recombination Spectroscopy (-CHERS)	5 Horizontal radial channels, 5 vertical sightlines
Gyrotron Scattering System	Small angle scattering, single mid-plane position, moveable between shots.

Alpha-Charge-Exchange spectroscopy	Horizontal midplane view (with Lithium Pellet)

Magnetic Properties

Rogowski Loops	2 toroidal locations
Voltage Loops	6 poloidal locations and various saddle coil
B ,B Loops	2*26 pairs external to the vacuum vessel
Diamagnetic Loops	2 toroidal locations
Locked mode Coils	4 Toroidal locations

Plasma Edge/Wall

Plasma TV	periscopes at 2 locations
IR Camera	periscopes at 2 locations
Filtered Diodes (H-alpha)	5 telescopes in poloidal array
Filtered Diodes (C-II)	5 telescopes in poloidal array
Sample Exposure Probe	1 edge location, moveable radially between shots
Disruption Monitor (IR Detector)	1 toroidal location
Edge density reflectometer	1 channel which is scannable to get edge n_e profile

Fluctuations/Wave Activities

Microwave Scattering	Scannable antenna and receiver
X-mode Microwave Reflectometer	4 variable frequency system at 1 toroidal location
Beam Emission Spectroscopy	25 channel variable radial and poloidal profile at 1 toroidal location
X-ray Imaging System	20 vertical chords, 64 horizontal chords at 1 toroidal location
ECE Grating Polychromator	2 toroidal locations with 20 point radial profile
Mirnov Coils	40 locations inside vacuum vessel
Neutron Fluctuation Detector	6 toroidal locations
RF Probes	7 toroidal locations

Plasma Current/Safety Factor Profiles

Motional Stark Effect Polarimeter	10-channel radial profile at 1 toroidal location

Miscellaneous

Hard X-ray Monitors	5 wall locations
Torus Pressure Gauges	2 toroidal locations
Residual Gas Analyzers	2 toroidal locations on pump ducts
Vacuum Vessel Illumination	3 top toroidal locations

References

[1]   ITER DESIGN TEAM, "Physics Design Description Document for the ITER Plasma", March 1995.

[2]   HAWRYLUK, R.J. *et al.*, *to appear in* Plasma Physics and Controlled Nuclear Fusion Research 1994 (Proc. 15th Int. Conf., Sevilla, Spain, Sep.1994) Paper A-1-I-1

[3]   KIKUCHI, M. *et al.*, *to appear in* Plasma Physics and Controlled Nuclear Fusion Research 1994 (Proc. 15th Int. Conf., Sevilla, Spain, Sep.1994) Paper A-1-I-2

[4]   STORK, D. *et al.*, *to appear in* Plasma Physics and Controlled Nuclear Fusion Research 1994 (Proc. 15th Int. Conf., Sevilla, Spain, Sep.1994) Paper A-1-I-3

[5]   STRACHAN, J.D. *et al.*, Phys. Rev. Lett. **58** (1987) 1004

[6]   STRACHAN, J.D. et al., Phys. Rev. Lett. **72** (1994) 3526

[7]   HAWRYLUK, R.J. *et al.*, Phys. Rev. Lett. **72** (1994) 3530

[8]   BELL, M.G. *et al.*, *to appear in* Plasma Physics and Controlled Nuclear Fusion Research 1994 (Proc. 15th Int. Conf., Sevilla, Spain, Sep. 1994) Paper A-2-I-1

[9]   McGUIRE, K.M. *et al.*, Physics of Plasmas **2** (1995) 2176.

[10]   YUSHMANOV, P. *et al.*, Nucl. Fusion **30** (1990) 1999

[11]   JET TEAM, Nucl. Fusion **32** (1992) 187

[12]   BATHKE, C.G. and KRAKOWSKI, R.A. "STARLITE Systems Studies", Project Meeting, Argonne National Lab., May 11-12, 1995.

[13]   TROYON, F. *et al.*, Plasma Phys. Control. Fusion **26** (1984) 209

[14]   SNIPES, J.A. *et al.,* J. Nucl. Materials **196−198** (1992) 686

[15]   MANSFIELD, D., *et al.*, "Enhanced D-T Supershot Performance at High Current Using Extensive Lithium Conditioning in TFTR", *in preparation*

[16]   BELL, M.G. *et al.*, Plasma Physics and Controlled Nuclear Fusion Research 1988 (Proc. 12th Int. Conf., Nice, France) Vol. 1, p. 27

[17]   SABBAGH, S.A. *et al., to appear in* Plasma Physics and Controlled Nuclear Fusion Research 1994 (Proc. 15th Int. Conf., Sevilla, Spain, Sep. 1994) Paper A-5-I-6

[18]   BUDNY, R.V., "A Standard DT Supershot Simulation", Nucl. Fusion, *to appear;*

[19]   FREDRICKSON, E.D. *et al., to appear in* Plasma Physics and Controlled Nuclear Fusion Research 1994 (Proc. 15th Int. Conf., Sevilla, Spain, Sep. 1994) Paper A-2-II-5

[20]   LEVINTON, F.M. *et al.,* "Improved Confinement with Reversed Magnetic Shear in TFTR", *submitted to* Phys. Rev. Lett.

[21]   SCHMIDT, G.L. *et al.*, Plasma Physics and Controlled Nuclear Fusion Research 1988 (Proc. 12th Int. Conf., Nice, France) Vol. 1, p. 215.

[22]   MANICKAM, J. *et al.*, Physics of Plasmas **1** (1994) 1601.

[23] STALLARD, B.W., *to appear in* Plasma Physics and Controlled Nuclear Fusion Research 1994 (Proc. 15th Int. Conf., Sevilla, Spain, Sep. 1994) Paper IAEA-CN-60/A3/5-P-11.

[24] SOLDNER, F.X. The JET Team, *et al., to appear in* Plasma Physics and Controlled Nuclear Fusion Research 1994 (Proc. 15th Int. Conf., Sevilla, Spain, Sep. 1994), Paper IAEA-CN-60/A-3-I-2.

[25] MANICKHAM, J. , POMPHREY, N. and TODD, A.M.M. Nuclear Fusion **27** (1987) 1461.

[26] GREENOUGH, N. *et al.,* Proc. 14th IEEE/NPSS Symp. on Fusion Engineering (San Diego, Sep. 1991) Vol. 1, p 126.

[27] SÖLDNER, F.X. *et al.,* Nucl. Fusion **34** (1994) 985

[28] IGNAT, D.W., VALEO, E.J., JARDIN, S.C., Nucl. Fusion **34** (1994) 837

[29] MAJESKI, R., PHILLIPS, C. K., WILSON, J. R., Phys. Rev. Lett. **73**, 2204 (1994).

[30] MAJESKI, R. *et al.*, *submitted to* Phys. Rev. Lett.

[31] MAJESKI, R. *et al.*, *to appear in* Plasma Physics and Controlled Nuclear Fusion Research 1994 (Proc. 15th Int. Conf., Sevilla, Spain, Sep. 1994) Paper IAEA-CN-60/A-3-I-4.

[32] NOTERDAEME, J.M., in Radiofrequency Power in Plasmas, AIP Conf. Proc. **244** (1992) 71.

[33] ONO, M. *et al.*, *to appear in* Plasma Physics and Controlled Nuclear Fusion Research 1994 (Proc. 15th Int. Conf., Sevilla, Spain, Sep. 1994) Paper IAEA-CN-60/A-3-I-7.

[34] WILSON, J.R. et al. J. Nucl. Mater. **145-147** (1987) 616.

[35] MOODY, J.D. et al, Phys Rev Lett **62** (1988) 298.

[36] SESNIC, S. *et al.*, *to appear in* Plasma Physics and Controlled Nuclear Fusion Research 1994 (Proc. 15th Int. Conf., Sevilla, Spain, Sep. 1994) Paper IAEA-CN-60/A3/5-P-12.

[37] LEBLANC, B. *et al.*, Phys. Plasmas, **3**, 741 (1995).

[38] ONO, M., Phys. Fluids B **5** (1993) 241.

[39] CRADDOCK, G.G. and DIAMOND, P.H., Phys. Rev. Lett. **67** (1991) 1535.

[40] BIGLARI, H., ONO, M., DIAMOND, P. H. and CRADDOCK, G. G. in proceedings of Ninth Topical Conference on Radio-Frequency Power in Plasmas (Charleston, 1991), AIP Conference Proceedings 244 (New York, 1992) 376.

[41] CRADDOCK, G.G., DIAMOND, P.H., ONO, M.,. BIGLARI, H, Phys. Plasmas **1** (1994) 1944.

[42] BIGLARI, H., DIAMOND, P., TERRY, P., Phys. Fluids B **2** (1990) 1.

[43] KUGEL, H.W., J. Nucl. Mater. **220-222** (1995) 636.

[44] BOUCHER, C. et al, J. Nucl. Mater. **196-198** (1992) 587.

[45] WHITE, R. B., in Theory of Tokamak Plasmas, p. 176ff (1989).

[46] ZAKHAROV, L. *et al.*, *to appear in* Plasma Physics and Controlled Nuclear Fusion Research 1994 (Proc. 15th Int. Conf., Sevilla, Spain, Sep. 1994) Paper D-3-III-4.

[47] BUSH, C.E. *et al.*, Physics of Plasmas **2** (1995) 2366.

[48] FREDRICKSON, E.D. *et al.,* " Limit Disruptions in the Tokamak Fusion Test Reactor", *to be presented at* IEA Workshop W29 "Disruptions and Termination of High-Performance Plasmas", JET Laboratory, July 1995.

[49] MUELLER, D., BELL, M.G., FREDRICKSON, E. *et al.,* "Disruption Avoidance on TFTR", *submitted to* Fusion Technology

[50] TFTR alpha-particle diagnostics are described in several papers in the Proceedings of the Tenth Topical Conference on High-Temperature Plasma Diagnostics (Rochester, N.Y.; May, 1994), Rev. Sci. Inst. **66**(1) Part II (Jan. 1995).

[51] REDI, M. *et al.,* "Collisional Stochastic Ripple Diffusion of Alpha Particles and Beam Ions on TFTR", Report PPPL-3011, *to be published in* Nucl. Fusion.

[52] FU, G.Y. and VAN DAM, Phys. Fluids B**1** (1989) 1949.

[53] CHENG, C.Z., Phys. Fluids B **3** (1991) 2463.

[54] WONG, K.-L., FONCK, R.J., PAUL, S.F., Phys. Rev. Lett. **66** (1994) 1874

[55] HEIDBRINK, W.W., STRAIT, E.J., DOYLE, E., SAGER, G. and SNIDER, R.T., Nucl. Fusion **31** (1991) 1635

[56] CHENG, C.Z. *et al., to appear in* Plasma Physics and Controlled Nuclear Fusion Research 1994 (Proc. 15th Int. Conf., Sevilla, Spain, Sep. 1994) Paper D-3-III-2

[57] SPONG, D. *et al., to appear in* Plasma Physics and Controlled Nuclear Fusion Research 1994 (Proc. 15th Int. Conf., Sevilla, Spain, Sep. 1994) Paper D-P-II-3

[58] ZWEBEN, S.J. *et al.,* Physics of Plasmas **1** (1994) 1469

[59] FISHER, R.K. *et al.*, "Results of Confined Alpha Particle Measurements in TFTR" *to appear in* Physics of Plasmas

[60] McKEE, G.R. *et al.*, "Confined Alpha Distribution Measurements in a Deuterium-Tritium Tokamak Plasma", *submitted to* Phys. Rev. Lett.

[61] LEVINTON, F.M., *et al.*, Phys. Rev. Lett. **72** (1994) 2895.

[62] WHITE, R. *et al.*, Phys. Rev. Lett. **62** (1989) 539.

[63] WHITE, R. *et al.* PPPL-3090, *submitted to* Physics of Plasmas.

[64] FU, G.Y. *et al.*, *submitted to* Phys. Rev. Lett.

[65] WONG, K.L., *et al.,* "First Evidence of Collective Alpha Particle Effect in the TFTR D-T Experiment", *in preparation*

[66] HEIDBRINK, W.W., STRAIT, E.J., DOYLE, E., SAGER, G. and SNIDER, R.T., Nucl. Fusion **31** (1991) 1635.

[67] SYNAKOWSKI, E. *et al.*, "Measurements of the Production and Transport of Helium Ash on the TFTR Tokamak", *submitted to* Phys. Rev. Lett.

[68] EFTHIMION, P.C. *et al.*, *to appear in* Plasma Physics and Controlled Nuclear Fusion Research 1994 (Proc. 15th Int. Conf., Sevilla, Spain, Sep. 1994) Paper A-2-II-6

[69] ZARNSTORFF, M.C. *et al.,* "Heating and Transport in D-T Plasmas", *to appear in* Plasma Physics and Controlled Nuclear Fusion Research 1994 (Proc. 15th Int. Conf., Sevilla, Spain, Sep. 1994) Paper A-2-I-2.

[70] SCOTT, S.D. *et al.*, Physics of Plasmas **2** (1995) 2299.

[71] FISCH, N.J. and RAX, J.M., Phys. Rev. Lett. **69** (1992) 612

[72] FISCH, N., Physics of Plasmas **2** (1995) 2375.

[73] PHILLIPS, C. K. *et al.*, Physics of Plasmas **2** (1995) 2427.

[74] MYNICK, H.E. and POMPHREY, N., Nucl. Fusion **34** (1994) 1277

[75] KOTSCHENREUTHER, M. , DORLAND, W. BEER, M.A., and HAMMETT, G.W., Phys. Plasmas **2** (1995) 2381.

[76] BUSH, C.E. *et al.*, (Sherwood, 1995)

[77] BURRELL, K.H. *et al., to appear in* Plasma Physics and Controlled Nuclear Fusion Research 1994 (Proc. 15th Int. Conf., Sevilla, Spain, Sep. 1994) Paper A-2-I-5

[78] BUSH, C.E. *et al.*, Proc. 21st EPS Conference On Controlled Fusion And Plasma Physics, 1994.

[79] PERKINS, F.W. *et al.*, Phys Fluids B **5** (1993) 472

[80] PETTY, C.C. *et al.*, Phys. Rev. Lett. **74** (1995) 1763

[81] SCOTT, S.D. *et al.*, in Plasma Physics and Controlled Nuclear Fusion Research, 1992 (Proc. 14th Int. Conf., Würzburg, 1992; IAEA, Vienna, 1993), Vol. 3, p. 427

[82] EFTHIMION, P.C. *et al.*, Phys. Rev. Lett. **66** (1991) 421

[83] SCOTT, S.D. *et al.*, Phys. Fluids B **2** (1990) 1300

[84] MEADE, D.M., Plasma Physics and Controlled Nuclear Fusion Research, 1990 (Proc. 13th Int. Conf., Washington, 1990; IAEA, Vienna, 1991), Vol. 1, pp. 9–24.

[85] GREENWALD, M., TERRY, J.L., WOLFE, S.M. *et al.*, Nucl. Fusion **28**, (1988) 2199

[86] BORRASS, K., Nucl. Fusion **31** (1991) 1035

[87] BELL, M.G., SCHMIDT, G.L., EFTHIMION, P.C. *et al.*, Nucl. Fusion **32**, (1992) 1585

[88] GOUGE, M.J., HOULBERG, W.A., ATTENBERGER, S.E., MILORA, S.L., "Fuel Source Isotopic Tailoring and Its Impact on ITER Design, Operation and Safety", *to be published in* Fusion Technology

[89] MILLS, R.G., Report MATT-1050, Princeton Plasma Physics Laboratory (1974).

[90] GIBSON, A. and WATKINS, M.L., Controlled Fusion and Plasma Physics **1** (1977) 31.

[91] LACKNER, K., CHODURA, R., KAUFMANN, M., NEUHAUSER, J., RAUH, K.G. *et al.*, Plasma Phys. Controlled Fusion **26** (1984) 105.

[92] CUMMINGS, J., COHEN, S.A., HULSE, R., POST, D.E., REDI, M.H. *et al.*, J. Nucl. Mater. **176–177** (1990) 916.

[93]   MANDREKAS, J. and STACEY, W.M., "An Impurity-Seeded Radiative Mantle for ITER", Technical Report GTFR-114, Georgia Institute of Technology, 1994, *submitted to* Nuclear Fusion.

[94]   BUSH, C.E., SCHIVELL, J., MEDLEY, S.S., and ULRICKSON, M., Rev. Sci. Instrum. **57** (1986) 2078.

[95]   STRACHAN, J.D., BOODY, F.P., BUSH, C.E., COHEN, S.A., GREK, B. *et al.*, J. Nucl. Mater. **145–147** (1987) 186.

[96]   BUSH, C.E., STRACHAN, J.D., SCHIVELL, J., MANSFIELD, D.K., TAYLOR, G. *et al.*, "Neutral Beam Heating of Detached Plasmas in TFTR", Report PPPL-2616, Princeton Plasma Physics Laboratory (1989).

[97]   SCHIVELL, J., BUSH, C.E., COHEN, S.A., JANOS, A., MUELLER, D. *et al.*, "Marfes at 21MW Heating Power in TFTR", Presented at the Workshop on Edge Plasma Physics for BPX and ITER, Princeton University, 15–17 January 1991.

[98]   KALLENBACH, A., MERTENS, V., DUX, R., ALEXANDER, M., BEHRINGER, K. *et al.*, "Radiating Boundary in ASDEX Upgrade Divertor Discharges", *to appear in* Plasma Physics and Controlled Nuclear Fusion Research 1994 (Proc. 15th Int. Conf., Sevilla, Spain, Sep. 1994) paper IAEA-CN-60/A2/4-P-13.

[99]   SAMM, U., BERTSCHINGER, G., BOGEN, P., CLAASSEN, H.A., GERHAUSER, H. *et al.*, "Plasma Edge Cooling by Impurity Radiation in a Tokamak", in Plasma Physics and Controlled Nuclear Fusion Research, 1992 (Proc. 14th Int. Conf., Würzburg, 1992; IAEA, Vienna, 1993), Vol. 1, pp. 309–315.

[100]   MONIER-GARBET, P., DEMICHELIS, C., GHENDRIH, P., GRISOLIA, C., GROSMAN, A. *et al.*, "Active Impurity Control in Tore Supra", in Plasma Physics and Controlled Nuclear Fusion Research, 1992 (Proc. 14th Int. Conf., Würzburg, 1992; IAEA, Vienna, 1993), Vol. 1, p. 317

[101]   HILL, D.N., ALLEN, S.L., BROOKS, N.H., BUCHENAUER, D., CUTHBERTSON, J.W., "Divertor Research on the DIII-D Tokamak", *to appear in* Plasma Physics and Controlled Nuclear Fusion Research 1994 (Proc. 15th Int. Conf., Sevilla, Spain, Sep. 1994) paper IAEA-CN-60/A-4-I-2.

[102]   HE, H., MANDREKAS, J., and STACEY, W.M., Bulletin of the American Physical Society **38** (1993) 2051, *(abstract only)*.

[103]   MANDREKAS, J., STACEY, W.M., and KELLY, F., "Impurity Seeded Radiative Mantle Simulations for ITER", ITER document, 1995.

[104]   LIPSCHULTZ, B., LABOMBARD, B., MARMAR, E.S., PICKRELL, M.M., TERRY, J.L. *et al.*, Nucl. Fusion **24** (1984) 977.

[105]   MESSIAEN, A.M., ONGENA, J., SAMM, U., UNTERBERG, B., VANDENPLAS, P.E. *et al.*, Nucl. Fusion **34** (1994) 825.

[106]   POST, D.E., JENSEN, R.V., TARTER, C.B., GRASBERGER, W.H., LOKKE, W.A., Atomic Data and Nuclear Data Tables **20** (1977) 397.

[107]   LEVINTON, F.M., BATHA, S.H., YAMADA, Y., and ZARNSTORFF, M.C., Phys. Fluids B **5** (1993) 2554.

[108]   WOLF, R.C., ERIKSSON, L.-G., VON HELLERMANN, M., KONIG, R., MANDL, W. and PORCELLI, F., Nuclear Fusion **33** (1993) 1835.

[109]   PUTVINSKI, S. *appear in* Plasma Physics and Controlled Nuclear Fusion Research 1994 (Proc. 15th Int. Conf., Sevilla, Spain, Sep. 1994) Paper IAEA-CN-60/E-P-4.

[110]   TOBITA, K. *et al.,* Rev. Sci. Instruments **66** (1995) 594.

[111]   PREISCHE, S. Ph.D. Thesis, "Radially Localized Measurement of Superthermal Electrons using Oblique ECE", Princeton University (June 1995).

[112]   PREISCHE, S., EPS Meeting, Bournemouth, UK July 1995, *and*

TRIBALDOS, V. et al, 8th Workshop on ECE and ECRH, Gut Ising (1992).

[113]   ANDERSON, J.L. *et al.*, *to appear in* Plasma Physics and Controlled Nuclear Fusion Research 1994 (Proc. 15th Int. Conf., Sevilla, Spain, Sep. 1994) Paper F-2-II-1

[114]   Final Safety Analysis Report, Tokamak Fusion Test Reactor, Amendment No.3, Vol. No. 1, October 4, 1994, PPPL Document DTSD-FSAR-17.

[115]   SKINNER, C.H., ADLER, H., BUDNY, R.V., KAMPERSCHROER, J., JOHNSON, L.C., RAMSEY, A.T., STOTLER, D.P. "First Measurements of Tritium Recycling in TFTR", Nucl. Fusion **35** (1995) 143.

The TFTR Advanced Performance Project
Table of Contents